Extraction of fetal ECG and its characteristics using multi-modality

Saman Noorzadeh

Communauté
UNIVERSITÉ Grenoble Alpes

THÈSE

Pour obtenir le grade de

DOCTEUR DE LA COMMUNAUTÉ UNIVERSITÉ GRENOBLE ALPES

Spécialité : **Signal, Image, Parole, Télécommunication (SIPT)**

Arrêté ministériel : 7 août, 2006

Présentée par

Saman Noorzadeh

Thèse dirigée par **Pierre-Yves Guméry**
et codirigée par **Bertrand Rivet**

préparée au sein du **Laboratoires Grenoble Images Parole Signal Automatique (GIPSA) et Techniques de l'Ingénierie Médicale et de la Complexité (TIMC)**
et de **l'Ecole Doctorale d'Electronique, Electrotechnique, Automatique, Traitement du Signal (EEATS)**

Extraction de l'ECG du fœtus et de ses caractéristiques grâce à la multi-modalité

Extraction of Fetal ECG using Multi-Modality

Thèse soutenue publiquement le **2 Novembre, 2015**,
devant le jury composé de :

M. Christian Jutten
Professeur, Université Joseph Fourier, Président
M. Mohammad Bagher Shamsollahi
Professeur, Université de technologie de Sharif, Rapporteur
M. Philippe Ravier
Maître de conférences, Université d'Orléans, Rapporteur
M. Reza Sameni
Maître de conférences, Université de Shiraz, Examinateur
M. Pierre-Yves Guméry
Professeur, Université Joseph Fourier, Directeur de thèse
M. Bertrand Rivet
Maître de conférences, Grenoble INP, Co-Encadrant de thèse
Mme. Véronique Equy
Gynécologue-Obstétricien, CHU de Grenoble, Invité

Acknowledgments

I would like to thank the supervisors of this research Prof. Pierre-Yves Guméry and Dr. Bertrand Rivet without whom the thesis would not be accomplished. Pierre-Yves has thought me a lot, through this research, with his endless patience, understanding and knowledge. I thank Bertrand for his kind support, expertise, and his vast knowledge and guidance which gave direction to the work.

I would like to thank the other members of my thesis committee: Prof. Christian Jutten, to whom I owe my special gratitude for what he has thought me in research, and what I have learned from his special character, Prof. Mohammad Bagher Shamsollahi, Dr. Philippe Ravier, Dr. Reza Sameni, and Dr. Véronique Equy. I appreciate their encouragement, and their insightful comments.

A special thanks goes to Dr. Julie Fontecave-Jallon, without her support the data recording experiments were not possible.

I would also like to thank my friends and colleagues. They were fundamental in supporting me during thesis stress and difficult moments, and I also thank them for contributing to the development of my research.

Finally, my gratitude goes to my family: my parents and my two sisters for all their love and support throughout my life and my study.

Abstract

Fetal health must be carefully monitored during pregnancy to detect early fetal cardiac diseases, and provide appropriate treatment. Technological development aims at monitoring during pregnancy using the noninvasive fetal electrocardiogram (ECG). This method allows not only to detect fetal heart rate, but also to analyze the morphology of fetal ECG, which is now limited to analysis of the invasive ECG during delivery. However, the noninvasive fetal ECG recorded from the mother's abdomen is contaminated with several noise sources among which the maternal ECG is the most prominent. That is why this problem is still a challenge in the research which is handled by uni-modal approaches, up to now.

In the present study, the problem of noninvasive fetal ECG extraction is tackled using multi-modality. In the multi-modal concept, beside ECG signal, this approach benefits from the phonocardiogram (PCG) signal as another signal modality, which can provide complementary information about the fetal ECG. These signals are introduced and their characteristics and relationships are explained. Then, a general method for quasi-periodic signal analysis and modeling is described, and its application to ECG denoising and fetal ECG extraction is explained. Considering the difficulties caused by the synchronization of the two modalities, the event detection in the quasi-periodic signals is also studied, which can be specified to the detection of the R-peaks in the ECG signal. Multi-modality is based on the Gaussian process modeling, in this study, in order to provide the possibility of flexible models and nonlinear estimations.

Both signal processing and experimental aspects of this application are studied, here. The method is tested on synthetic data and also on preliminary real data that is recorded to provide a synchronous multi-modal data set. The method is also tested on the 1-bit reference signals instead of the full-bit ones, as an alternative to reduce the implementation cost of the device. The first results show that the proposed approach is efficient in the detection of R-peaks and, thus, in the extraction of fetal heart rate, and it also provides the results about the morphology of the fetal ECG.

Résumé

La surveillance de la santé fœtale permet aux cliniciens d'évaluer le bien-être du fœtus, de faire une détection précoce des anomalies cardiaques fœtales et de fournir les traitements appropriés. Les développements technologies actuels visent à permettre la mesure de l'électrocardiogramme (ECG) fœtal de façon non-invasive afin d'extraire non seulement le rythme cardiaque mais également la forme d'onde du signal. Cet objectif est rendu difficile par le faible rapport signal sur bruit des signaux mesurés sur l'abdomen maternel. Cette mesure est donc toujours un challenge auquel se confrontent beaucoup d'études qui proposent des solutions de traitement de signal basées sur la seule modalité ECG.

Le but de cette thèse est d'utiliser la modélisation des processus Gaussiens pour améliorer l'extraction des signaux cardiaques fœtaux, dans une base multi-modale. L'ECG est utilisé conjointement avec le signal Phonocardiogramme (PCG) qui peut apporter une information complémentaire à l'ECG. Une méthode générale pour la modélisation des signaux quasi-périodiques est présentée avec l'application au débruitage de l'ECG et à l'extraction de l'ECG du fœtus. Différents aspects de la multi-modalité (synchronisation, $\cdots$) proposée sont étudiées afin de détecter avec plus de robustesse les battements cardiaques fœtaux. La méthode considère l'application sur les signaux ECG et PCG à travers deux aspects: l'aspect du traitement du signal et l'expérimental. La modélisation des processus Gaussien, avec le signal PCG pris comme la référence, est utilisée pour extraire des modèles flexibles et des estimations non linéaires de l'information. La méthode cherche également à faciliter la mise en œuvre pratique en utilisant un codage 1-bit des signaux de référence.

Le modèle proposé est validé sur des signaux synthétiques et également sur des données préliminaires réelles qui ont été enregistrées afin d'amorcer la constitution d'une base de données multi-modale synchronisée. Les premiers résultats montrent que la méthode permettra à terme aux cliniciens d'étudier les battements cardiaques ainsi que la morphologie de l'ECG. Ce dernier aspect était jusqu'à présent limité à l'analyse d'enregistrements ECG invasifs prélevés pendant l'accouchement par le biais d'électrodes posées sur le scalp du fœtus.

Contents

List of Figures

List of Tables

List of Abbreviations

AV atrio-ventricular

BSS blind source separation

BPM beat per minute

CTG cardiotocography

ECG electrocardiogram

ePCG envelope of the PCG

fECG fetal ECG

fEcho fetal echocardiography

fHR fetal heart rate

fMCG fetal magnetocardiography

GP Gaussian process

ICA independent component analysis

IVA independent vector analysis

mECG maternal ECG

PCA principal component analysis

PCG phonocardiogram

PDF probability density function

SA sino-atrial

SNR signal to noise ratio

SVD singular value decomposition

1 Introduction

The well-being of the fetus must be carefully monitored during pregnancy and also during labor [Meathrel et al., 1995]. Indeed, the procedure of monitoring the fetus allows the clinicians to assess the health of the fetus, detect early fetal problems, and provide appropriate treatment [Patterns, 1999, Meathrel et al., 1995]. Effective monitoring of a fetus requires continuous assessment and is commonly performed using electronic technology. However, the number of babies born with congenital heart defects has called into question the validity of present monitoring techniques in identifying the fetus at risk. One of the main intentions in healthcare is to reduce the number of babies born with an illness, and the technology can provide best in this regard by developing tools for monitoring.

What the clinicians are interested in today, is the precise monitoring of the fetal heart rate (fHR). Technology has been developed to allow some existing clinical tools like cardiotocography (CTG). CTG, which is an external (noninvasive) monitoring technique, is widely used in hospitals to measure the fHR and is believed to have a reliable output. However, it is not suitable for long-term monitoring, and it can also lead to error in the detection of fHR or the loss of this information. For example, in [Bakker et al., 2004] it has been shown that, in average, the ultrasound technology has about 40% failure in fHR detection between 30 and 40 weeks. In a patient with an at-risk fetus, this loss of signal can be dangerous. In addition, fetal heart monitoring may be more difficult with CTG in some categories of patients, such as very obese mothers or those with fetal arrhythmias [Ross and Beall, 2014]. These difficulties may require the clinicians to use internal (invasive) monitoring when CTG is unsatisfactory in a laboring patient. The internal ECG monitoring involves a fetal scalp electrode to give not only a measure of fHR but also some of the characteristics regarding the morphology of the fetal ECG (fECG). The use of internal monitors may also increase the risk for the mother [Ross and Beall, 2014], as well as for the fetus [Miyashiro and Mintz-Hittner, 1999] e.g. it may lacerate the fetal scalp.

Fetal monitoring using noninvasive fECG is completely safe, and aims at estimating both fHR and the fECG morphology during pregnancy and during delivery. The processing of the noninvasive ECG, which is recorded from the surface of the abdomen, has already been tackled by a lot of researches. The main problem is that the electrical signal obtained

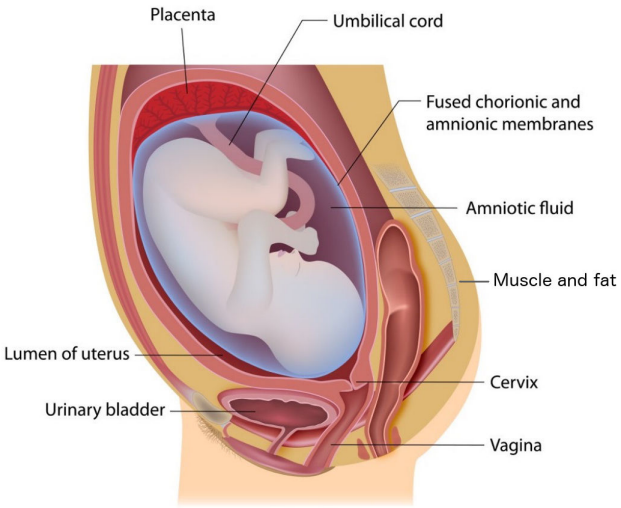

Figure 1.1: The anatomy of maternal womb layers where the fetus is placed.

through the abdominal surface electrodes does not only contain fECG signals, i.e. the Signal to Noise Ratio (SNR) of the fetal abdominal signal, appearing in the abdomen, is usually very low. The reasons behind the fact that fECG on the abdomen is noisy can be of different kinds:

- Maternal ECG which is recorded through abdominal surface electrodes, and has much larger amplitude than fECG.
- Electrical noise from electromyographic (EMG) maternal muscle activities, either from the abdominal wall, or other muscular activities like the abdominal contractions or movements, can cause high amplitude noise in the abdominal ECG recordings.
- The fetal heart is very small and the fetus is surrounded by the amnion and amniotic fluids which makes the examination of the fetus very difficult. [Greenberg et al., 2004]. A simplified anatomy of the fetomaternal compartments can be seen in Fig. 1.1. These layers have low-conductivity; therefore, the fetal signal captured through surface electrodes would be weak and of low amplitude.
- The position of the fetus within the womb, and the movements of the fetus can make noises in the signal.
- Proper placement of the abdominal electrodes is one of the critical points in this regard [Vigneron et al., 2005].

Considering all the limitations, noninvasive fECG extraction is a challenging problem which needs complex signal processing techniques. Previous studies have employed different approaches which are based on uni-modal techniques. However, up to now, there is not a unique reliable solution to the problem.

In this thesis, the signal processing and the experimental aspects of the extraction of noninvasive fECG are investigated. The main contribution of the signal processing aspect, is using a multi-modal framework in this context. Multi-modality is employed to benefit from the complementary and redundant information that two different signal modalities can provide. These two modalities, which will be used in this study, are Electrocardiogram (ECG) and Phonocardiogram (PCG). Multi-modality is proposed not only to increase the robustness of the method, but also to solve the problem of finding beat indexes, which have been assumed to be known in advance, in some of the previous studies. The main focus is thus to extend the existing methods in a multi-modal context. Multi-modality is based on Gaussian process modeling in this study, since this model considers few assumptions about the data (e.g. about the temporal shape of the signal).

The method is then tested on the synthetic data to estimate the fHR and also the morphology of fECG beats. It is also necessary to apply it on the real data so that the functionality of the method is assessed. The lack of an existing database of synchronous ECG and PCG data requires us to record our own data set. From an experimental point of view, the factors that can affect the data registration are studied, and the difficulties of fetal signal registrations are listed. The method can finally be examined on this real data, and its efficiency is tested on the signals recorded in the last month of pregnancy, which is the best period adapted for the proposed multi-modal method using the least number of sensors.

Thesis Overview

As mentioned above, the extraction of noninvasive fECG extraction concerns signal processing and experimental difficulties which are already described along with the main contributions. In the following, the chapters of this document are briefly described.

Chapter 2

In Chapter 2 the state of the art in fECG and QRS detection is presented. The previous studies are classified into the existing clinical tools and the signal processing methods. To better clarify the need for fECG, we first introduce the existing clinical tools, the devices used nowadays in the hospitals and the technologies which are being developed, and discuss their advantages and limitations in order to illustrate the motivation of this study. Second, the signal processing methods which are developed are presented. These methods exist in a very large number, and the effort is to present the principal of the most efficient techniques in this regard. After presenting the approaches concerning fECG, the

fetal PCG methods are briefly presented. Next, at the end of Chapter 2, the remaining challenges are investigated.

Chapter 3

In order to shed light on the data modalities which are employed in the following chapters, the two ECG and PCG signals are investigated in this chapter from two angles: physiological and mathematical. From the physiological point of view, the origin of the two modalities, heart, is studied and how ECG and PCG signals are generated from this organ is briefly explained. Consequently, the differences between the fetal and adult heart in generating these two signals are presented. Afterwards, the two signals are analyzed mathematically; first, their separate temporal and frequency characteristics are shown and then the complexities of the multi-modal approach using these two signals are presented. The presented models of the two signals are beneficial in understanding the multi-modal approach presented in Chapter 4.

Chapter 4

This chapter presents the models which are used to model the quasi-periodic signals. This model is based on Gaussian Process (GP) and considers the general properties of the quasi-periodic signals. Therefore, first the basics of modeling and signal denoising using GP is described in Section 4.1 and then according to the properties of the quasi-periodic signals two uni-modal GP models are described named as time-varying and periodic, and their limitations are investigated (Section 4.2). To solve these problems, the multi-modal approaches are presented in Sections 4.3 and 4.4. These methods handle also the problem of synchronization which might be existing between different modalities. Finally, the model is applied on synthetic ECG and PCG signals as the quasi-periodic biomedical signals. PCG is referred to as the reference modality and is used to denoise an ECG signal channel. The results show the ability of the multi-modal method to detect the R-peak instants. This information is assumed to be known in advance in previous methods.

Chapter 5

In this chapter, the method explained in the previous chapter is used in the extraction of fetal ECG from the maternal abdominal channel. So using this method, both maternal and fetal ECGs are modeled by suitable reference modalities and the results are shown on synthetic data. These results also show that the fHR and R-peaks of the fetus can be detected precisely.

Chapter 6

Previous chapters focused more on the signal processing aspect. Now, this chapter tries to consider the problem from an experimental point of view. As explained before, the acquisition of the data is a complicated task which requires the definition of many parameters. These parameters can affect the quality of the captured data. The recording of one modality is itself complicated, therefore the acquisition of multi-modal signals should be defined in a suitable framework. After presenting the factors which affect the data recording and explaining the difficulties of experiments that we had on pregnant subjects, we test the proposed method on the preliminary recorded signals from a pregnant woman in the 9^{th} gestational month, which can be a good generalization of the intrapartum period.

2 The State of the Art

L'état de l'art dans l'extraction de cardiaque fœtal peut être étudié sous deux aspects: Les outils cliniques existants, et les méthodes de traitement mathématique et de signaux qui sont développées pour l'analyse numérique des données.

2.1 Clinical Tools

Monitoring the conditions of the unborn child is a necessary task in the clinical aspects since it can avoid the fetal death or permanent damages to the fetus. Therefore, in most of the countries, all pregnant women take the tests to check the well-being of the fetus. These tests are done to check the fetal growth patterns, the availability of oxygen and the well-being of cardiac functions [Ruffo et al., 2011]. The first device to examine the health of the fetal cardiac function was the fetal stethoscope (Pinard) [Steer, 2008]. However, the development of technology has brought the electronic systems to monitor the fetal cardiac health.

Cardiotocography

The most widely used clinical technique to monitor the fetal heart rate (fHR) is the cardiotocography (CTG) [Alfirevic et al., 2006]. This method is used to monitor the fetal heart beat (cardio) and also the maternal uterine contractions (toco). CTG is an external noninvasive method, meaning that the equipment is placed on the maternal abdominal surface. This device works based on the ultrasound, so the ultrasound beam in frequency of 1 or 2 MHz is emitted from the transducer, placed on the maternal abdomen, and reaches the beating heart. Then, it is reflected with a frequency shift in accordance with doppler effect [Jezewski et al., 2011]. An algorithm in the device calculates the time interval between these reflections and displays a heart rate. Doppler fetal monitor [Freeman et al., 2012] is also a hand-held device which works based the same technology to monitor the fHR. CTG is the most common method used nowadays; however, it may sometimes leads to the superposition of maternal and fetal heart rates in the intrapartum period; and in this case, the analysis of the variability of the fHR would be difficult for the special-

ists. Besides, it is not suitable for long-term monitoring since it is sentitive to movements. Moreover, the exposure of the fetus to ultrasound waves is not yet proven to be completely harmless [Ibrahimy et al., 2003, Kieler et al., 2002, Barnett and Maulik, 2001].

Echocardiography

Fetal echocardiography (fEcho) is a diagnostic sonography also based on ultrasound [Fetal et al., 2011].

Magnetocardiography

Fetal magnetocardiography (fMCG) is another noninvasive tool which measures the magnetic field caused by the electrical activity of the fetal heart [Janjarasjitt, 2006]. The recording uses the SQUID (superconducting quantum interference device) biomagnetometry technique [Kariniemi et al., 1974]. This device is mainly used as a research tool and is not in clinical practice. fMCG and fetal magnetic resonance imaging (MRI) are two areas which are being developed technologically. However, they require high cost and fixed equipment which are not suitable for routine antepartum or intrapartum use.

Phonocardiography

Another noninvasive method uses the fetal Phonocardiogram (fPCG) which can provide significant clinical information from the normal growth of the fetal heart. This method is widely being studied to be used as a clinical tool for the automatic analysis of the fPCG [Tan and Moghavvemi, 2000]. This signal can be captured by placing a small and low cost acoustic sensor on mother's abdomen [Varady et al., 2003, Kovács et al., 2000].

Electrocardiography

Fetal electrocardiogram (fECG) is another signal which can be recorded in two different ways: **invasive**, by placing the electrodes inside the mother's uterus, or **noninvasive** [Holls and Horner, 1994]. The invasive electrodes, which are actually invasive to the mother, are of two types: scalp electrodes which are also invasive to the fetus; or intrauterine catheter electrodes which are noninvasive to the fetus [Randall et al., 1988] but are not used by commercial known monitors. The invasive ECG is only captured in the intrapartum period and usually during delivery [Hasan et al., 2009] when there is a risk in the process of delivery. All of the mentioned tools has their own specific problems which makes the fetal heart monitoring a challenging task. The clinical tools with their advantages and limitations are summarized in Table 2.1.

Method	Advantages	Limitations
CTG	Noninvasive fHR recording	Needs precise location of transducer Requires skilled specialist Not suitable for long term monitoring Sensitive to maternal movements Ultrasound irradiation may be harmful
fEcho	Noninvasive Info. on heart size and shape	Cost of device Ultrasound irradiation
fMCG	Noninvasive Morphologically simmilar to fECG	Size and complexity of instrumentation Cost of device Sensitive to maternal movements
fPCG	Noninvasive Cheap Info. on hurt murmurs	Low SNR Sensitive to the sensor placement
Invasive fECG	low SNR fECG Info. on ECG morphology	Infection risks Used only during delivery
Noninvasive fECG	Noninvasive Cheap Info. on ECG morphology	Low SNR

Table 2.1: The clinical tools for fetal heart monitoring.

Newer Technologies

The study of the fECG is not only limited to the study of fHR. The research has shown that an assessment of morphological and temporal characteristics of the fECG during gestation can also provide further information about the health of the fetus. Nowadays, the only way to monitor these characteristics is the **STAN** method [Welin et al., 2007]. This method uses the scalp electrodes to analyze the segment between S and T waves and also the ratio of QRS and T wave amplitudes. This information has been proved to be useful in detecting whether the fetus is suffering from oxygen deficiency. This method however does not provide the information, about the possible fetal problems, early enough. STAN provides information in the very last stages of pregnancy (because of the availability of the scalp ECG). This stage may be late for the doctors to provide treatments.

Today, there are only two noninvasive devices known: the Monica AN24 monitor (at Monica Healthcare, Nottingham, UK) [Graatsma et al., 2009] and the MERIDIAN monitor from MindChild Medical in North Andover, MA [Clifford et al., 2014, Adam, 2012]. An early work on extracting morphological information has also been published [Behar et al., 2014a, Clifford et al., 2011].

Future Technologies

There are also some technologies being developed like Lifewave, Inc. (Los Altos, CA) which is based on radiofrequency technology similar to radar. This technology emits a low-energy electromagnetic signal and analyzes the return waveform that has bounced off moving fetal structures for monitoring the fHR monitoring. This device is a portable and small device, but is not yet approved for use [Adam, 2012]. Beside medical devices, computer science is also playing an efficient role in analyzing the existing data from the classical devices to better help clinicians in identifying fetal abnormalities [Warrick et al., 2010].

To summarize, in most hospitals, there are two reliable technologies which are widely used for fetal heart monitoring: Doppler ultrasound and noninvasive scalp fECG. The other techniques are used either in research or in specific cases. New techniques, as in STAN, are also being used but are still under research. Beside these techniques, noninvasive fetal ECG analysis is potentially important to help clinicians for making more accurate decisions during pregnancy. However such a device requires an innovative combination of technology, algorithms, and human systems. The detection of fECG signals using advanced signal processing methodologies is becoming a very crucial requisite for clinical diagnosis.

2.2 Signal Processing Tools

2.2.1 Fetal ECG

The first recording of fetal ECG from the maternal abdominal surface was done by Cremer in 1906 [Cremer, 1906]. He could observe the fetal electrical impulses related to fetus among the high-voltage maternal signal. Despite the technological improvements, the extraction of fetal ECG from abdominal recordings is still a challenging problem which is tackled by a great number of studies. A review of the existing methods has been done in [Sameni and Clifford, 2010]. These studies are done for either the calculation of fHR or to extract the morphology of the fECG. Moreover, these techniques can be classified into single or multi channel methods.

The **classical filtering** techniques are the basic approaches to handle this problem [Van Bemmel and Van der Weide, 1966]. Since the fECG is superposed with the existing noise in the abdominal recording in the time and frequency domain, these methods cannot be very efficient. Fig. 2.1 shows the overlap of the two fetal and maternal ECGs in both time and frequency domains [Clifford et al., 2014]. It is seen that some of the fetal beats are overlapping with those of the mother's in the abdominal channel, and the frequency analysis shows that the main power of frequencies of maternal and fetal scalp

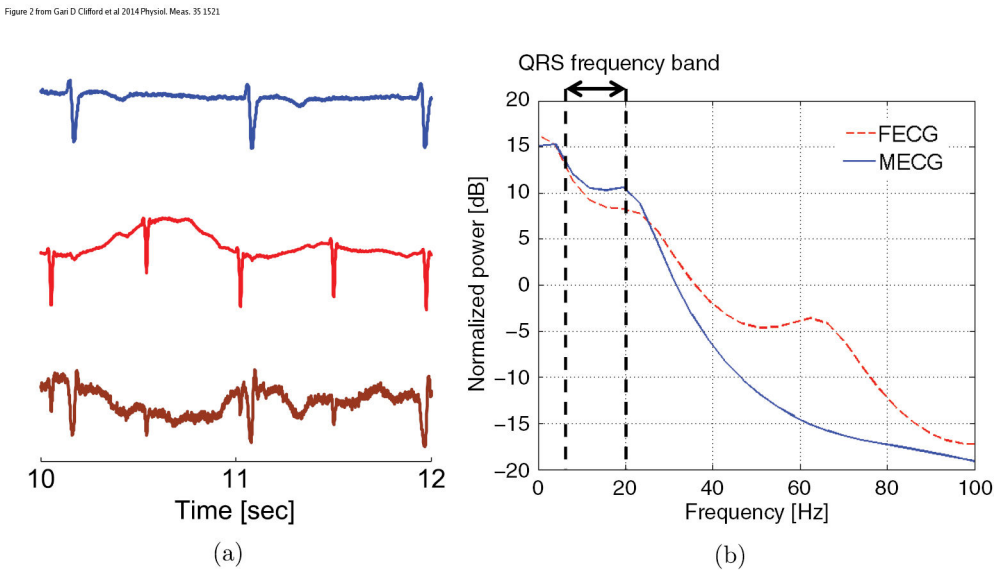

Figure 2.1: The overlap of maternal and fetal ECGs in time and frequency domains. (a) from top to bottom: fetal scalp ECG, maternal ECG, abdominal ECG in time domain (b) the maternal and fetal ECGs overlap in frequency domain. The Figure is taken from [Clifford et al., 2014].

ECGs are superposing in this domain.

Other researchers have used **spatial filters** based on the fact that the maternal and the fetal ECG sources are separated in space because of the differences in the source locations [Bergveld and Meijer, 1981, Vanderschoot et al., 1987, Chen et al., 2001]. They use a number of electrode signals, to find a linear combination between the observations, and determine the best coefficients to model a weighted sum of these observation signals. Assuming that the ECG is caused by a time-dependent dipole varying in amplitude and orientation, any of the observations $s(t)$, can be expressed as the linear combination of 3 other observations proposed by [van Oosterom, 1986]:

$$s(t) = a_1 s_1(t) + a_2 s_2(t) + a_3 s_3(t), \tag{2.1}$$

If a time segment $\boldsymbol{t}^* = [t_1^*, \cdots, t_n^*] \in \boldsymbol{t} = [t_1, \cdots, t_n]$ of the recording only corresponds to mECG: $s(t^*) = s_m(t^*)$, the coefficients a_j can be found to model the maternal activity, $s_m(t)$, according to equation (2.1). Considering that each observation is the summation of maternal and fetal ECG, $s(t) = s_m(t) + s_f(t)$, by replacing the estimated coefficients, the term indicated by this equation would contain only the fetal activity. In the same study, singular value decomposition is used to select the best weights which minimize the maternal ECG in the observation signals, and these weights are again filtered by selecting the ones which maximize the result of fetal ECG. With the same idea, [Bergveld and Meijer, 1981] tried to cancel the maternal ECG from the abdominal recordings, and the coefficients are estimated as $\hat{a}_1$, $\hat{a}_2$, and $\hat{a}_3$ by using the optimization procedure of Hildreth and d'Esopo [Künzi et al., 2013]. This optimization process is then repeated on windows of

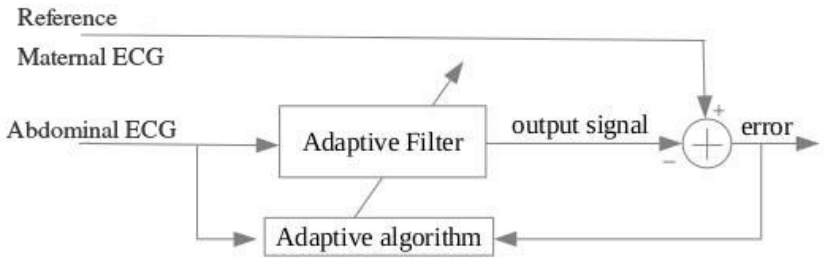

Figure 2.2: A schema of the adaptive filtering for fECG extraction.

4s. The drawback of these methods is that the variations in the mECG complexes caused by respiration or movements cannot be very well extracted.

The **template subtraction** is another technique which is used in this context. The maternal ECG template is generated by event synchronous averaging; in other words, before averaging, the mECG complexes are synchronized on the QRS complexes. This template is subsequently linearly scaled to minimize the mean square error (MSE) with respect to the mECG complex, and is then subtracted using an adaptive gain as done in [Cerutti et al., 1986]. Different techniques are presented in the literature to generate or improve this template by event synchronous interference canceler [Ungureanu and Wolf, 2006, Martens et al., 2007] or by linear prediction [Ungureanu et al., 2007, Comani et al., 2004]. For example, in linear prediction, after synchronization on the QRS complexes, the weights are calculated for a weighted average which minimizes the MSE. Using an N order model, the mECG complex $\vec{M}_i$ is estimated by the linear combination of preceding mECG complexes, with weights a_{i-n}:

$$\hat{\vec{M}}_i = \sum_{n=1}^{N} a_{i-n}\vec{M}_{i-n}. \tag{2.2}$$

Considering $\boldsymbol{M}_i = [\vec{M}_{i-1}, \cdots, \vec{M}_{i-N}]^\dagger$, where $\dagger$ denotes the transpose of a matrix, the MSE is then minimized between the estimate $\hat{\vec{M}}$ and the actual mECG complex, M_i, and hence the weights $\vec{a}_i = [a_{i-1}, \cdots, a_{i-K}]^\dagger$ are estimated [Ungureanu et al., 2007].

Beside the mentioned methods, **adaptive filter** has also been applied successfully on the problem of fetal ECG extraction [Widrow et al., 1975]. This filter is generally based on adapting the coefficients of a linear filter through several iterations in order to estimate the maternal ECG contribution in the abdomen, using reference signals, and remove it to obtain fetal ECG [Ferrara and Widraw, 1982, Thakor and Zhu, 1991]. The schema of this filter is depicted in Fig. 2.2. The adaptive filters may be sensitive to the temporal shape of the reference signal specially if only one reference is used; therefore, it normally requires multi reference signals [Sameni, 2008, Widrow et al., 1975]. By using an artificial reference created by the event-synchronized averaging of mECG complexes, problems coming from

the nonlinear propagation of the mECG can be overcome [Strobach et al., 1994].

The decomposition techniques are also among the popular techniques which are used in this regard. **Singular Value Decomposition** (SVD) is one of these methods which is used to extract the maternal and fetal components in the abdominal recordings [Vanderschoot et al., 1987, Callaerts et al., 1990, Ayat et al., 2008]. For instance, in [Kanjilal et al., 1997] a method is developed to be used on a single-channel abdominal signal by first detecting the maternal heart beats, and then configuring the beats in the rows of a $m \times n$ matrix, $\boldsymbol{A}$, such that the peaks are in the same column. Next, SVD is performed on this matrix:

$$\begin{aligned} &\boldsymbol{A} = \boldsymbol{U}\boldsymbol{\Sigma}\boldsymbol{V}^{\dagger}; \text{ with} \\ &\boldsymbol{U} = [\boldsymbol{u_1}, \cdots, \boldsymbol{u}_m], \boldsymbol{V} = [\boldsymbol{v_1}, \cdots, \boldsymbol{v}_n], \boldsymbol{\Sigma} = [diag\{\sigma_1, \cdots, \sigma_p\} : \boldsymbol{0}], \end{aligned} \tag{2.3}$$

where $p = min(m, n)$ and $\boldsymbol{u}_i$ and $\boldsymbol{v}_i$ are column vectors. $\boldsymbol{A}_M = \boldsymbol{u}_1\sigma_1\boldsymbol{v}_1^{\dagger}$ is calculated to contain most of the information which lies in the most dominant dyad associated with σ_1, and the residual $\boldsymbol{A}_R = \boldsymbol{A} - \boldsymbol{A}_M$ is calculated as the fECG component and the noise. The denoising of the estimated fECG is then done with the same procedure by computing the most dominant component $\boldsymbol{u^B}_1\sigma_1^B\boldsymbol{v^B}_1^{\dagger}$ of a matrix $\boldsymbol{B}$, which is created by arranging each fECG cycle in each row of $\boldsymbol{B}$ with the peak values in the same column.

Using the techniques that include subspace decomposition or reconstruction, some studies have removed the maternal component [Fatemi et al., 2013, Maier and Dickhaus, 2013]. In [Niknazar et al., 2013b], the maternal beats are identified and stacked in a three-dimensional array. The maternal ECG is then reconstructed and subtracted by using **tensor decomposition**.

Some studies have formulated the fECG extraction as a **blind source separation** (BSS) problem [Comon and Jutten, 2010]. BSS is based on the assumption that the abdominal ECG channel is composed of independent components. In this framework, the abdominal recordings are formulated as the instantaneous mixtures of maternal and fetal ECG sources [Zarzoso et al., 1997]. Considering each of the n abdominal channels as $x_j(t) = a_{j1}s_m(t) + a_{j2}s_f(t)$, $1 \leq j \leq n$, the problem is formulated as:

$$X = \boldsymbol{A}S + N, \text{ with} \tag{2.4}$$

$$X = [x_1(t), \cdots, x_n(t)]^{\dagger}, \; S = [s_m(t), s_f(t)]^{\dagger} \tag{2.5}$$

where $t \in \{t_1, \cdots, t_p\}$ for p number of samples, N is the additive noise and $\boldsymbol{A}$ is the mixing matrix which describes the propagation from source to sensor. The two main approaches which exist in this regard are Principal Component Analysis (PCA) and Independent Component Analysis (ICA). PCA tries to project the mixing signal onto the principal axis of its covariance matrix. Therefore, the PCA components are geometrically orthogonal by construction and also statistically orthogonal. This method is thus based on the removal of

second order dependencies of the observation signals [Di Maria et al., 2014, Castells et al., 2007]. ICA approach looks for components which are not necessarily geometrically orthogonal, but are statistically independent, and tries to remove the higher order statistics of the sources [Cardoso, 1998]. ICA has proved to be efficient on the several sets of recordings [Taylor et al., 2005]. The aim of ICA is to find the mixing matrix in equation (2.4) such that the sources are mutually statistically independent.

ICA is compared to PCA and is proved to perform better in the literature [De Lathauwer et al., 1995, Bacharakis et al., 1996]. It is also compared to adaptive filters in [Zarzoso and Nandi, 2001]. In [De Lathauwer et al., 2000], the maternal and fetal ECGs are considered as multidimensional signals; however, only different source subspaces are separated instead of all the source components in conventional ICA. In a more recent work, another improved version of the ICA is used as the periodic component analysis method to make use of the periodicity of the ECG signal [Sameni et al., 2008]. In this work, a measure of periodicity is defined and maximized to find the linear mixture $s(t) = \boldsymbol{w}^{\dagger}\boldsymbol{x}(t)$ with a maximal periodic structure that minimizes this measure. In order to treat the quasi-periodic ECG as a periodic signal, they used a time-warping function to assign the time instants of each beat with a phase between $[-\pi, \pi]$ setting the R-peaks to 0. As indicated by [Behar et al., 2013, Zaunseder et al., 2012], there is always a part of fECG remaining in the mECG components in the BSS methods; therefore, they may not be efficient in very low SNRs.

The **wavelet transform** (WT) is another approach that has been proposed for the problem of fetal ECG processing. Different techniques for noise removal and/or detection of fetal waveforms have been used. These techniques involve Gabor-8 wavelets and Lipschitz exponent's theory [Mochimaru et al., 2002], bi-orthogonal quadratic spline wavelet and modulus maxima theory [Khamene and Negahdaripour, 2000] and complex continuous wavelets [Karvounis et al., 2004]. Furthermore, wavelet-based multiresolution analysis has been proposed for noise removal [Mochimaru et al., 2002].

Kalman filter is a framework used in several biomedical applications. Using a single-channel data, [Sameni et al., 2005] was the first study to apply the Kalman filter for fECG extraction. This is based on a dynamic model comprising a phase information, which is obtained with the time warping already explained, and also on the mathematical description of the maternal heart beats which is based on the electrocardiogram model described in [McSharry et al., 2003]. This model approximates ECG waveforms by adding Gaussian kernels. Since Kalman filter models with a nonlinear model, its dynamical model has to be linearized before filtering. This extension is called the extended Kalman filter (EKF) [Sameni, 2008]. This model is highly reliant on the underlying dynamics assumed for the ECG signal. The model is then modified in [Niknazar et al., 2013a] to define a model for each of the components of the abdominal recording even in the case of twin

method	assumption	number of channels, n
ICA	independent components	$n > p$ ($n > 5$ [Zarzoso et al., 1997])
Adaptive filter	linearity	$n \geq 2$
Kalman filter	dynamical model	1

Table 2.2: The properties of the existing methods in fECG extraction. p is the number of sources existing in the mixtures.

pregnancy and claims to discriminate ECGs even if desired and undesired ECG waves overlap in time.

The mentioned techniques are the main approaches which have tackled the problem of fECG extraction; however, there are other researches which have used the fusion of two or several methods to obtain better performance results [Behar et al., 2014b]. For instance [Jafari and Chambers, 2005] has used the BSS in the wavelet domain. In [Gao et al., 2003] the authors used a single-channel recording and projected the data into higher dimensions. Consequently they assumed a statistical independence between the components, and used BSS for the their separation. SVD is used to contribute to the separability of each component, and ICA contributes to the independence of the two components. In another research done by [Andreotti et al., 2014] a template subtraction method is used for generating a maternal template beat. Then, based on the average maternal beat, Kalman filtering is applied to estimate maternal ECG. There are several other studies which use a fusion of existing methods [Vigneron et al., 2003, Varanini et al., 2013].

Beside the advantages that the mentioned methods have, every one of them has also some limitations. Some of the most well known approaches are listed in Table 2.2 with their two main characteristics: the pre-assumptions they must have about the data, and the number of data channels they need. As it is indicated in this table the first limitation of the methods could be the prior information that they demand. For example, in adaptive filters, the designed filter finds the best linear relationship between the input and desired response signals. In Kalman filter, although the number of the channels is minimum, there is an assumption on the dynamical state model. In ICA the large number of electrode sources may be impractical in the implementation of the device, and it is also based on the assumption on the independence of sources.

2.2.2 Fetal PCG

Hammacher and Gentner [Gentner and Hammacher, 1967] and Maeda [Maeda, 1965] invented external fHR monitoring with fetal heart sound for the full fetal monitoring in 1960s.

High pitched fetal heart sound listener and the fetal phonocardiography were studied by Maeda et al. [Maeda et al., 1980] before the introduction of ultrasound diagnosis of the fetus in Japan. Despite fECG, fPCG can be extracted from most of the abdominal noises using temporal filters [Varady et al., 2003]. The factors that can complicate the analysis of fetal PCG are the followings:

- The position of the fetus with respect to the sensor [Mittra et al., 2008, Ruffo et al., 2010].
- Acoustic noise sources like: fetal movements, maternal digestive and breathing sounds, maternal heart activity, and environmental noise.
- Acoustic damping through the fruit water and tissues [Varady et al., 2003].

The methods for fPCG have mainly focused on 3 aspects: the fetal abdominal PCG noise cancellation [Jimenez-Gonzalez and James, 2008, Vaisman et al., 2012, Varady, 2001, Moghavvemi et al., 2003, Jin and Sattar, 2013], , fPCG segmentation for detecting S1 and S2 sounds [Ortiz et al., 1999, Varady, 2001], and analysis of fHR and other medical characteristics from fPCG [Godinez et al., 2003].

2.3 Closing Remarks

The literature in the existing clinical devices and the signal processing methods in the fetal heart monitoring are presented in this chapter. However, despite the great number of studies in this regard, there is not yet a common solution to be implemented and used as a clinical tool. This can be due to several factors listed as followings:

- Some of the fECG components are missing in the extraction or are detected as the noise components,
- The method is sensitive to the temporal shape of the data and the electrode placements,
- The lack of precision in fHR detection and/or the estimation of the waveform of fECG,
- The computational cost of the algorithms,
- The lack of a common approach to record the signals, to be used in all methods.

Therefore, the existing methods are usually limited to provide a continuous monitoring of the fetal heart. On the other hand, all the mentioned researches are done to study noninvasive fECG and fPCG separately. Each of these signal modalities has its own limitations

and advantages (as listed in Table 2.1); and the information fusion of these modalities can be thus used in a multi-modal framework. Although a limited number of researches have studied the adult's ECG and PCG signals in one multi-modal approach [Phanphaisarn et al., 2011, Rawther and Cheriyan, , Fatemian et al., 2010, Wong et al., 2006], there is not yet a technique which studies these modalities for the fetus, despite the fact that the fPCG can provide some extra information on the extraction of fECG.

The multi-modal method which is presented in this study is based on the Gaussian process model [Rivet et al., 2012, Niknazar et al., 2012]. The method is a nonlinear approach and is a flexible tool to model the statistics of the mixture, and assumes little prior information about the source signals. This model will be described in the next chapters of this thesis.

3 A Study on Modalities

The information that we can obtain from the heart can be of different kinds. The two types of information in which we are interested are ECG and PCG. While these two signals are originating from a same body organ (the heart), they are carrying different information. ECG shows the propagation of the electrical impulse through the cardiac muscles and is thus a representation of the electrical activity of the heart, while PCG is the recording of the sounds made by the heart, and is thus a piece of data that demonstrates the mechanical activity of the heart. Therefore, the underlying natural processes which produce these two modalities are different and can depend on different natural or physiological variations.

In order to clarify a good framework for multi-modality, in this chapter, each of these signals are first analyzed. For this reason, the heart and its function producing these two signals are first described in Section 3.1, in order to shed light on the physiological process from which the modalities are originated. This section also contains the first definition of multi-modality (Section 3.1.3). After this brief description, the signals are mathematically analyzed and their relationship are discussed from a signal processing point of view in Section 3.2.

3.1 Physiological Origin

In this section, the used signal modalities are briefly presented in order to better understand the physiological process that causes the signals. These modalities are Electrocardiogram (ECG), and Phonocardiogram (PCG) which are first explained, following a definition of multi-modality.

The Heart

The anatomy and the function of the heart is first shortly presented to understand the physiological sources of the signal modalities and their relationships.

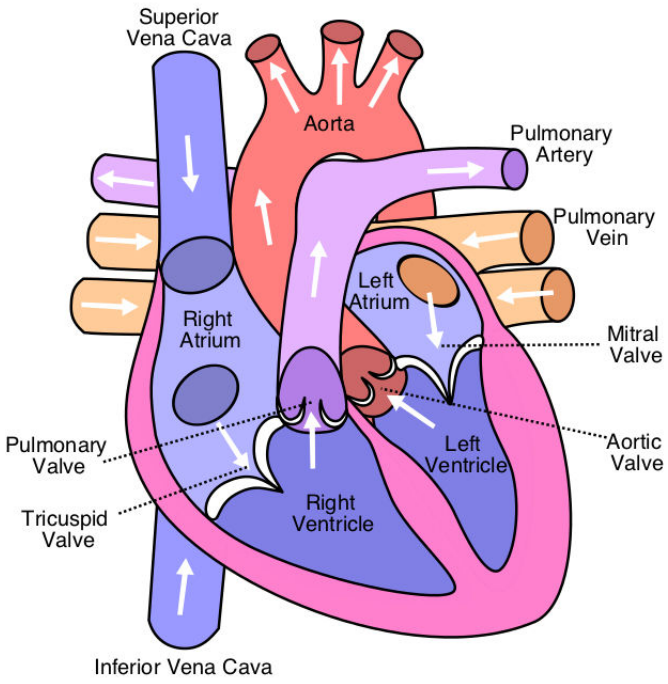

Figure 3.1: The anatomy of the heart. The white flashes show the directions of blood circulation.

Anatomy and Physiology of the Heart

The heart is actually a muscle whose main function is to pump the blood in the circulatory system. It consists of four chambers in which blood flows (see Fig. 3.1): 2 atria, and 2 ventricles. The heart is thus divided into two separate pumping systems [Moran, 2015]:

- The right side in which the blood enters by arriving to the right atrium and then passes through the right ventricle. The right ventricle pumps the blood to the lungs where it becomes oxygenated.
- The left side to which the oxygenated blood is brought back and enters the left atrium by the pulmonary veins. Blood then flows into the left ventricle from the left atrium. The left ventricle pumps the blood to the aorta which will distribute the oxygenated blood to all parts of the body.

Cardiac Conduction System

Having explained the function of the heart, it should be noted that the heart needs an electrical energy for the blood circulation, and it is able to create its own electrical impulse and to control the route that the impulses take in a specialized conduction pathway. This pathway has several elements:

- The sino-atrial (SA) node which releases electrical stimuli at a rate which depends on the needs of the body. Each stimulus first passes through the myocardial cells of

the atria creating a wave of contraction which spreads rapidly through both atria.

- The atrio-ventricular (AV) is then the second node to which the electrical stimulus reaches after the SA node, and it is delayed briefly so that the contracting atria have enough time to pump all the blood into the ventricles. Once the atria are empty of blood, the valves between the atria and ventricles are closed. At this point, the atria begin to refill and the electrical stimulus passes through the AV node and Bundle of His, into the Bundle branches and Purkinje fibers.

- At this point the ventricles are empty, the atria are full and the valves between them are closed. However, there is a third section to recharge the SA node and AV node for the next cycle.

The term used for the release (discharge) of an electrical stimulus is "depolarization," and the term for recharging is "repolarisation." Therefore, the 3 stages of a single heart beat are [Moran, 2015]

1. atrial depolarization,

2. ventricular depolarization,

3. atrial and ventricular repolarization.

3.1.1 Electrocardiogram

The voltage generated by the heart was first recorded in humans by Augustus D. Waller in St Mary's Hospital, London [Khan, 2004, Sykes, 1987]. However, it was Willem Einthoven who refined Waller's techniques and generated a clinically relevant ECG [Hurst, 1998]. Therefore, Einthoven is generally recognized as the father of ECG.

Electrocardiogram (ECG) is the electrical activity of the heart where electrical stimuli are initiated in the SA node, and are then conducted through the AV node and bundle of His, bundle branches and Purkinje fibers. Depolarization and repolarization of the atria and ventricles show up as 5 distinct waves on ECG. A unique labeling system is used to identify each wave: P, Q, R, S, and T [Einthoven, 1895]. The production of these waves is explored here and is depicted in Fig. 3.2.

P wave represents atrial depolarization. When the valves between the atria and ventricles are opened, the ventricles expand; therefore, due to the suction that they cause, most of the blood in the atria falls into the ventricles. However, atrial contraction is also required to pump all the blood and, therefore, a relatively small muscle mass is required. For that, only a relatively small amount of voltage is needed to contract the atria [Schamroth and Schamroth, 1990] (green wave in Fig. 3.2 marked with number 1).

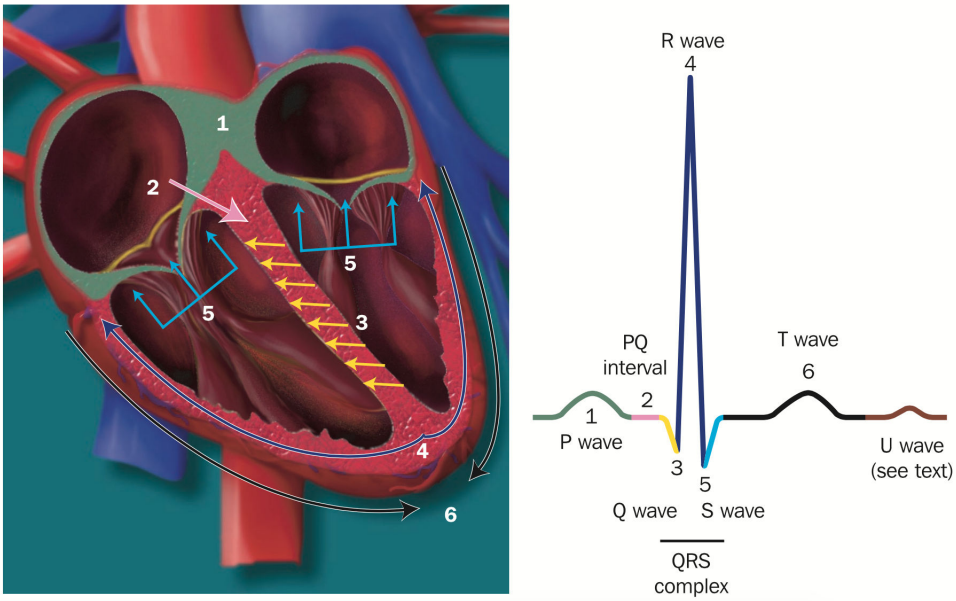

Figure 3.2: The simulation of PQRST heart beat (figure from [Khan, 2004])

After the first wave, there follows a short period where the line is flat. This is the point at which the stimulus is delayed in the bundle of His to give the atria enough time to pump all the blood into the ventricles. This segment is flat since there is only a small amount of tissue which is involved in this phase which generates a small electrical activity that cannot be perceived by surface ECG recordings [Khan, 2004, Waldo and Wit, 1993] (pink in Fig. 3.2 marked with number 2).

As the ventricles fill, the electrical stimulus passes from the bundle of His into the bundle branches and Purkinje fibers. The amount of the electrical generated energy is recorded as a complex of 3 waves known as the QRS complex. More voltage is required to cause ventricular contraction and therefore the wave is much bigger, so the largest wave in the QRS complex is the R wave. Q wave represents depolarisation in the septum (yellow in Fig. 3.2 marked with number 3); and the S wave represents depolarisation in the Purkinje fibers as shown in the figure.

Both ventricles repolarize before the cycle repeats itself and therefore a third wave (T wave) is caused which represents ventricular repolarization.

In some cases, an additional wave may be seen after the T wave, known as the U wave (brown in Fig. 3.2). It has been suggested that it is produced after depolarizations in the ventricles, by repolarization of the His/Purkinje system, or by prolonged repolarization of a specific cell layer (M-cells) in the mid-myocardium [Van Eck et al., 2003]. This wave is not always visible in the ECG recordings.

These main waves (P wave, QRS complex, and T wave) represent one cycle of the ECG, known as heartbeat. With the improvement of computerized automation and decrease in

prices of electronic technology, electrocardiogram is now accessible in almost every hospital and is available to doctors and clinicians. Better understanding of cardiac diseases is also now prompting healthcare professionals to use ECG interpretation skills.

A remark should be mentioned about the heart rate. This rate depends on the release rate of the electrical stimuli from the SA node, which depends on the needs of the body. This rate is thus not constant, and can vary from beat to beat. For example the heart rate increases while doing physical activity or in case of fear or stress.

3.1.1.1 Fetal Heart and Fetal Electrocardiogram

For the fetus, the blood circulation is different from when the baby is born, because despite a normal heart, the blood is not pumped to the lungs. Fetal heart has two main extra connections that will close after the baby is born (see Fig. 3.3).

The placenta accepts the deoxygenated blood from the fetus through blood vessels that leave the fetus through the umbilical cord (two umbilical arteries). When the blood goes through the placenta, it picks up the oxygen. This oxygenated blood then returns to the fetus via the umbilical vein. This blood passes through the fetal liver and enters the right side of the heart, and then goes through one of the two connections, already pointed out, in the fetal heart: *patent foramen ovale*, the hole between the right and left atrium. This hole allows the most oxygenated blood to go from the right atrium to left atrium and then to the left ventricle and then to the aorta, so the brain gets the blood with the most oxygen. Right atrium also receives the blood which has come back from the fetus's body, and the fetal heart sends this deoxygenated blood to the right ventricle. Despite a normal heart, in the fetus the blood that leaves the right ventricle bypasses the lungs through the second of the two extra fetal connections known as the *ductus arteriosus* which sends the blood to the organs in the lower part of the body. This also allows for the deoxygenated blood to leave the fetus through the umbilical arteries and get back to the placenta to pick up the oxygen [AmericanHeartAssociation, 2015]. Although there are differences between the heart of a fetus and the heart of an adult, the electrical activity and therefore ECG is rather the same, since the electrical impulse passes through the same cardiac nodes for depolarization and repolarization [Sameni, 2008].

A remark should be mentioned here about the clinical information that the doctors are interested to extract from the fetal ECG. First, they are interested in the heart rate which is normal in the range $[120, 160]$ bpm. They are also interested in the fluctuations in the baseline FHR. For instance, the moderate FHR variability is when the amplitude range varies between 6 bpm to 25 bpm [Freeman et al., 2012].

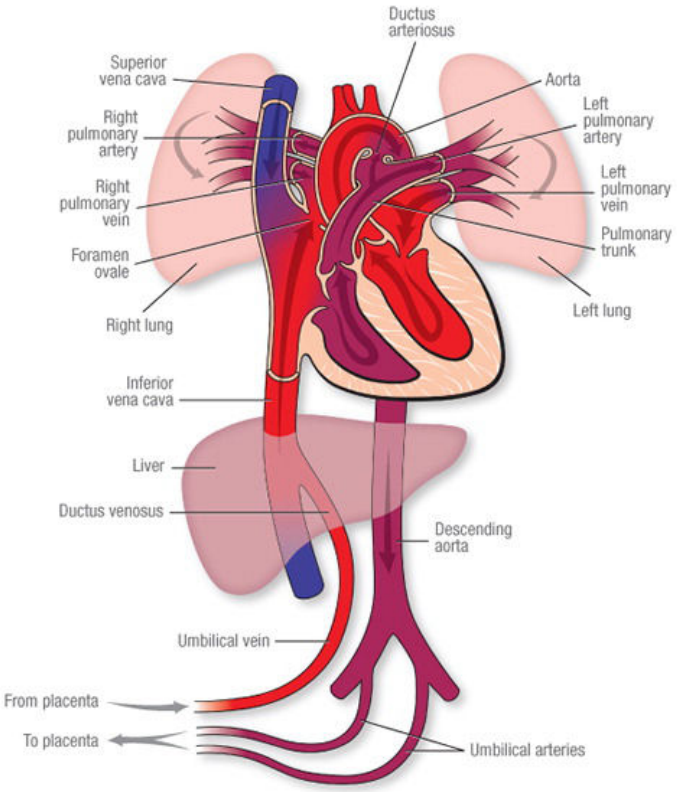

Figure 3.3: Fetal heart anatomy. There are 2 differences compared to a normal human heart: the opening, foramen oval, between the atria; and the shunts, ductus arteriosus and ductus venosus, which respectively bypass the lungs and liver (the organs that are not fully developed while the fetus is still in the womb). The Figure is Taken from [AmericanHeartAssociation, 2015]

3.1.2 Phonocardiogram

Having mentioned the function of the heart, we know that the right side of the heart pumps blood to the pulmonary (lungs) circulation, and the left side pumps blood to the systemic (the rest of the body) circulation. The blood from the pulmonary circulation returns to the left atrium, and the blood from the systemic circulation returns to the right atrium. The blood flow is controlled by two sets of valves: the atrio-ventricular (AV) valves (tricuspid and mitral) between the atria and the ventricles, and the Semilunar valves (aortic and pulmonary) between the ventricles and the arteries (see Fig. 3.1). The AV valves prevent backflow of blood from ventricles to atria during ventricular contraction (systole). The Semilunar valves prevent backflow of blood to ventricles during ventricular relaxation (diastole). The valves are opened and closed passively, and modulated by changes in

the contractility of the heart, the compliance of the chamber walls and arteries and the developed pressure gradients [Gill et al., 2005]. The sounds and murmurs produced by the heart is called phonocardiogram (PCG). Most researchers agree that heart sounds originate from the vibrations of the whole cardiovascular system [Durand and Pibarot, 1995]. The heart sounds are thus produced by a summed series of mechanical events:

- Valvular events; vibrations caused mostly by the closing of the heart valves (opening of the valves produces a vibration of lesser intensity.)
- Muscular events; vibrations of the myocardium during contraction.
- Vascular events; vibration produced by the sudden distension of the arterial walls during ejection.
- Vibrations caused by the acceleration or deceleration of the blood flow.

Not every sound is composed of all these components and, in the recordings, the most prominent component is due to the closure of the valves.

A normal cardiac cycle contains two major audible sounds: the first heart sound (S1) and the second heart sound (S2). As soon as the ventricular pressure exceeds the atrium pressure, the mitral and the tricuspid valves are closed and the vibrations of S1 begin. When the ventricles start to relax, the closure of the aortic and the pulmonary valves causes the S2 vibrations. Then ventricle pressure drops, and when it falls below the atrial pressure, the mitral valve is opened, and the rapid filling phase begins, and another audible sound (S3) is possible. A fourth heart sound, S4, may be heard sometimes due to atrial contractions displacing blood into the distended ventricles. In the presence of certain cardiovascular diseases, some murmurs can also be produced [Gill et al., 2005]. Using a microphone, all these sounds can be captured called PCG; however, a high skill is required for the interpretation of this signal. Therefore, the new technologies can serve the medical demands in digitization and automation of PCG signal. Fig. 3.4 shows a PCG signal with the S1 and S2 sounds.

The PCG signal can also vary from beat to beat (as in the ECG). The PCG signal (like the ECG) is thus a quasi-period signal, since the length of different beats are not the same.

3.1.2.1 Fetal Phonocardiogram

The differences between the fetal heart and an adult heart have already been studied in Section 3.1.1.1. Although the basic heart sounds are the same in adult and feta PCGs, there are some differences. Generally the systolic time interval is shorter that the diastolic time intervals (see figure 3.4), but at a high heart rate (fHR>180 beats/min), they may

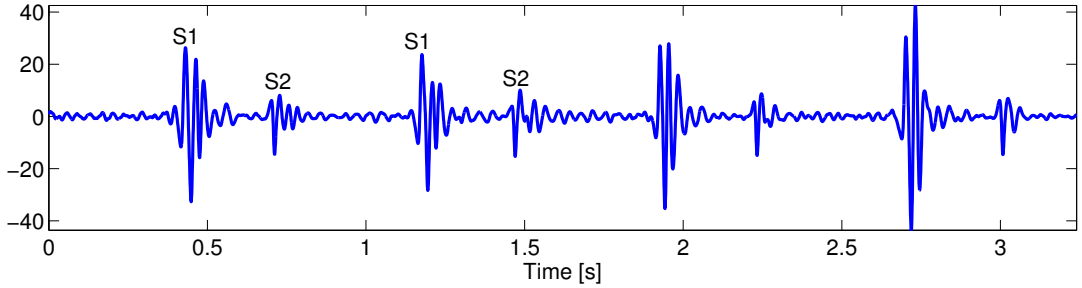

Figure 3.4: A Phonocardiogram signal with the closing sounds of mitral and tricuspidal (S1), and aortic and pulmonary (S2) vales. The systolic time interval is between S1 and S2, and the diastolic one is between S2 and S1.

be practically equal [Kovács et al., 2011]. However, from a signal processing point of view, we are not concerned with these differences.

3.1.3 Multi-Modal ECG & PCG Signals

Information about a phenomenon can be obtained by different types of instruments or measuring techniques. Natural processes and phenomena have numerous and different characteristics, and it is rare that a single type of acquisition can provide complete understanding of the phenomenon [Lahat et al., 2014]. Therefore a phenomenon can be captured through different sensors, and the data which is obtained by each sensor is called a modality. The modalities can be of different kinds and dimensions, and can represent different type of information about the same phenomenon. Multi-modality is referred to as the framework in which several modalities are used together in order to explain or describe a phenomenon, or to describe the relationship between the modalities. The applications in which multi-modality is used can be different. In multi-modality we are interested in making a composition in which certain kinds of information from one phenomenon come together in a particular way that best exemplifies or communicates what we want to mean, or to describe. Some known examples of multi-modality are use of EEG (electroencephalogram) and fMRI in one framework [Laufs, 2012] or the fusion of different biometric data for more accurate results [Patil, 2012].

Both the explained modalities are of interest in multi-modality. PCG and ECG are two signals coming from the same physiological organ, heart, and are providing complementary and redundant information about it. Complementary is referred to the knowledge about the cardiac activity which is not included in one modality but is existing in another; and redundancy is the knowledge which is in one of the modalities and it is also present in the other modality. The ECG and PCG cardiac modalities are providing complementary and

redundant knowledge about the cardiac activity. These cardiac modalities are recorded noninvasively; so, The electrical activity of the heart is recorded through electrodes as the ECG signal, and the heart sounds, referred to as PCG, are captured by microphones. The PCG signal is of interest because the type of noise that affects the PCG is different from the ECG. This fact makes the PCG signal easier to process as a reference modality. The physiological relation between ECG and PCG is explained in the following, which is actually a brief review of what has been explained in this section.

As the signal generated by the SA node spreads through atrial muscle, the atria respond by contracting (P wave). At this time, the ventricles are relaxing and the atrio-ventricular valves are open and the semilunars are closed. The ventricles are filling with blood, preparing for ejection. The AV node picks up the signal and-after a short delay that allows the atria to complete systole and enter diastole- sends the signal down the atrio-ventricular conduction system to the ventricles, stimulating them to contract (QRS complex). When the ventricles contract, ventricular pressure increases above atrial pressure and the atrioventricular valves are closed (S1 sound). Ventricular pressure continues to increase, and when it exceeds arterial pressure, the semilunars are opened and blood is rapidly ejected into the pulmonary trunk and aorta (T wave). The ventricles complete systole and enter diastole. As the ventricles relax, ventricular pressure falls below arterial pressure and the semilunar valves are closed (S2 sound). When ventricular pressure falls below atrial pressure, the atrioventrcular valves are opened and ventricular filling begins again. At this time, the atria and die ventricles are relaxed and awaiting the SA to signal the next cardiac cycle [Al-Qazzaz et al., 2014].

The relation between ECG and PCG is complex and multi-parametric in the physiological concept, about which we are not concerned. The main points of interests about the modalities, from a signal processing aspect, are explained in the following section.

3.2 Analyses of the Signals

The abdominal and thoracic ECG and PCG signals are respectively shown in Fig. 3.5 and Fig. 3.6 in both temporal and frequency domain. The signals are obtained through experiments explained later in Chapter 6. ECG signals are filtered between $[0.5, 60]$ Hz using a 4^{th} order butterworth filter applied in both direct and reverse directions to avoid phase distortions, and the power line 50 Hz frequency is eliminated using a notch filter. The PCG signals are filtered in the range of $[25, 100]$ Hz using a 4^{th} order butterworth filter. Because of the various structures of the sensors and physiological diversities of fetal heart sounds, different filters with different bandpass frequencies are applied on the PCG signal in the literature, mostly not wider than the band $[20, 200]$ Hz [Yang et al., 2012, Zuckerwar

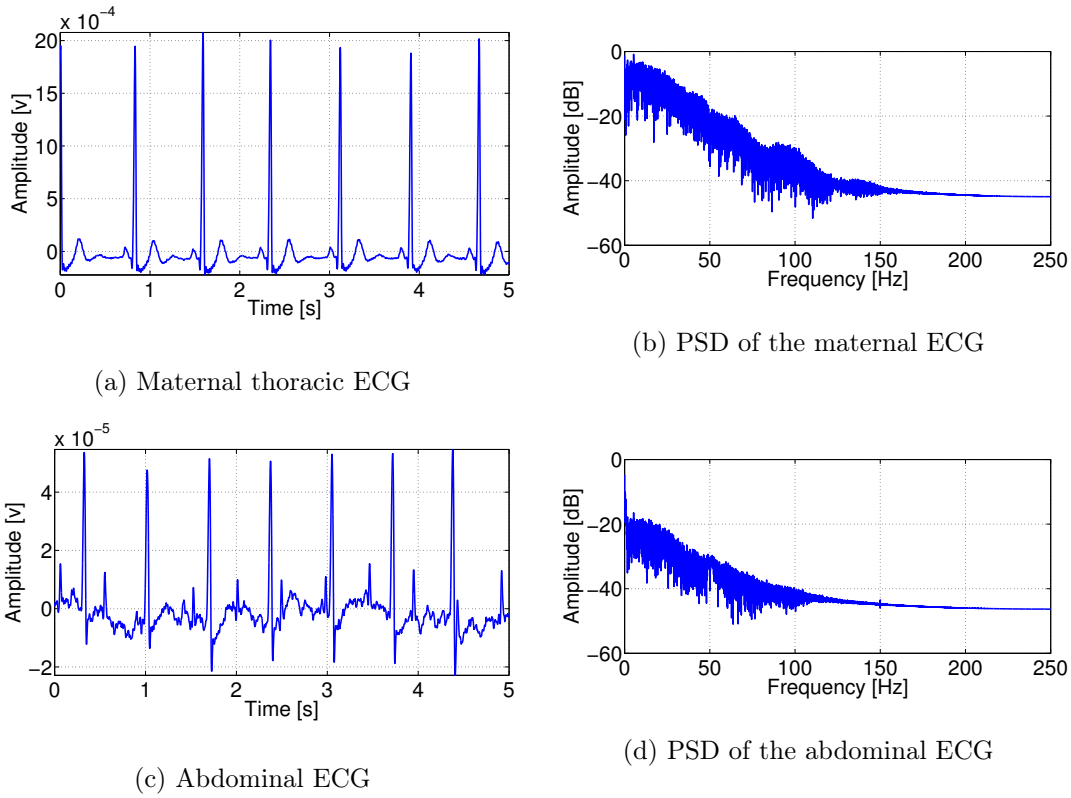

(a) Maternal thoracic ECG

(b) PSD of the maternal ECG

(c) Abdominal ECG

(d) PSD of the abdominal ECG

Figure 3.5: A representation of maternal and abdominal ECGs in time and frequency.

et al., 1993, Varady et al., 2003, Chen et al., 2006]. Here a passband of [25, 100]Hz is chosen, according to the recordings.

Clearly, the abdominal ECG contains both maternal and fetal ECGs, which cannot be separated in time (or frequency) domain (Fig. 3.5). This is not true for the abdominal PCG. Applying a bandpass filter on the abdominal PCG can provide us with the beats of the fetal PCG in the abdominal recording, as shown in Fig. 3.6. This figure shows the maternal and fetal PCGs from the thoracic and abdominal PCG recordings respectively. It is clear that the filtered abdominal signal shows a PCG with a different and higher heart rate than that of the mother's. This signal thus corresponds to the fetal PCG. The two frequency peaks in the frequency domain of the thoracic PCG, marked in the figure, show the frequencies of the two main heart sounds: S1, and S2.

One of the measures for calculating the heart rate is the detection of waves in any of these two signals. In electrocardiography, the detection of R-peaks, and in phonocardiography the detection of S1 waves can provide a good measure for the heart rate. This is shown in Fig. 3.7, where the R-peaks in ECG, and the heart sounds in PCG are marked. Moreover, because of the complex and highly non-stationary nature of PCG signals, the envelope of PCG (ePCG) is widely used instead of the full signal [Wu et al., 2012, Haghighi-Mood and Torry, 1995]. Here, the relative maxima in the amplitude of the envelope of the

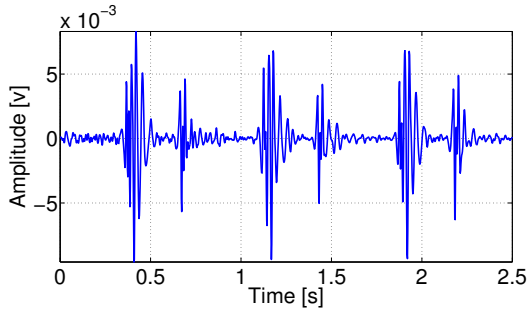

(a) Maternal thoracic PCG

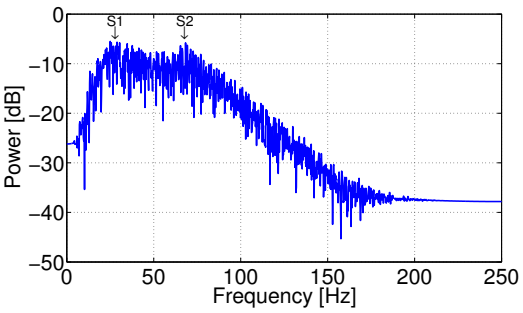

(b) PSD of the maternal PCG

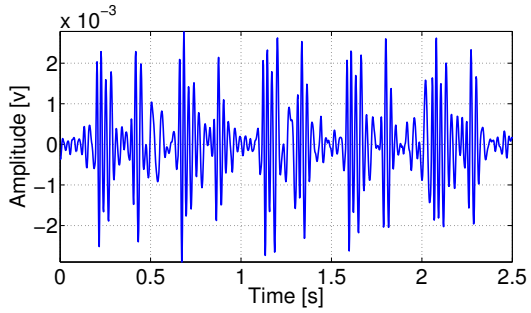

(c) Abdominal PCG (considered as fPCG)

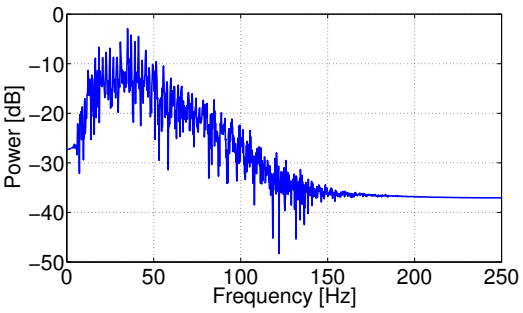

(d) PSD of the abdominal PCG

Figure 3.6: A representation of maternal and abdominal PCGs in time and frequency.

PCG is detected as the S1 and the S2 sound moments. There are several ways to calculate the ePCG signal. Here, the Hilbert transform, $\mathcal{H}(\,\cdot\,)$, is used to extract the analytical signal of the PCG, so the complex analytic signal of the PCG, $y(t)$, is expressed as [Choi and Jiang, 2008]:

$$A[y(t)] = y(t) + j\mathcal{H}\big(y(t)\big) = E(t)e^{j\phi(t)}, \tag{3.1}$$

where $E(t)$ is the envelope and $\phi(t)$ is the instantaneous phase. Therefore, using a hilbert transform the envelope can be extracted as:

$$E(t) = \sqrt{y^2(t) + \mathcal{H}^2\big(y(t)\big)} \tag{3.2}$$

This envelope might have some rapid variations due to the high sampling frequency, therefore a moving average filter is used in order to smoothen the envelope. The signals which are shown here (Fig. 3.7) are from an adult. Since the maternal and fetal cardiac signals have almost the same characteristics, as explained in the the previous section, what is explained here can be generalized to fetal cardiac signals.

3.2.1 Quasi-Synchronicity of ECG and PCG

Here, a basic model of the mixtures is presented to better understand the modalities. ECG observation signals can be modeled as linear instantaneous mixtures, considering a

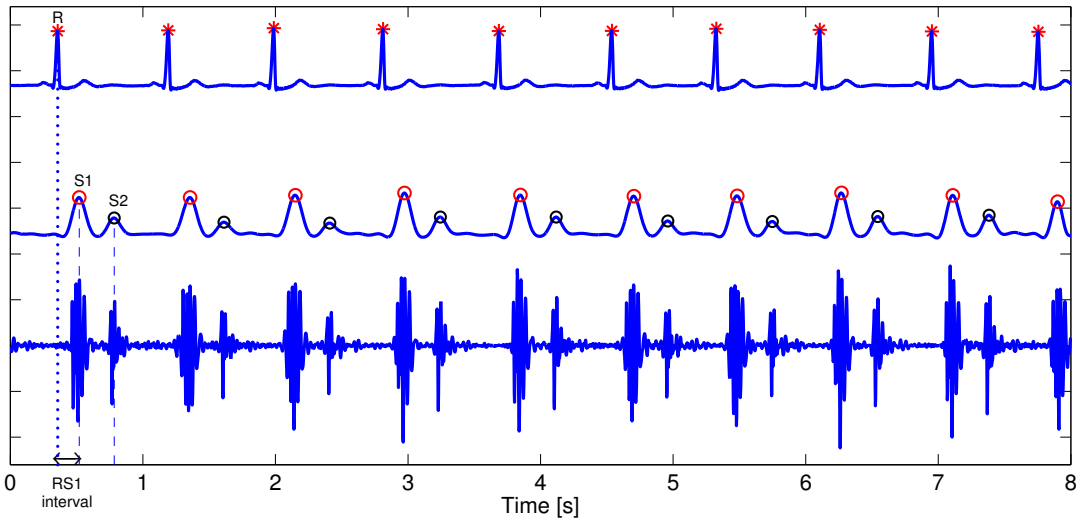

Figure 3.7: The detection of waves in ECG and PCG. The ePCG signal is detected and S1 and S2 sounds are detected according to this envelpe.

set of N source signals, $s_i(t)$, $1 \leq i \leq N$, which are observed by a set of P sensors, $x_j(t)$, $1 \leq j \leq P$. Let us denote $\boldsymbol{s}(t) = [s_1(t), \cdots, s_N(t)]^\dagger$ as the ECG sources ($\dagger$ is the notation of the transpose of a matrix), and $\boldsymbol{x}(t) = [x_1(t), \cdots, x_P(t)]^\dagger$ as the set of observed mixtures (see Fig. 3.8). So the instantaneous mixture of the cardio-electric sources can be noted as follows, considering $\boldsymbol{e}(t)$ as the remaining noise:

$$\boldsymbol{x}(t) = A\boldsymbol{s}(t) + \boldsymbol{e}(t). \tag{3.3}$$

The mixing phenomenon results from the simultaneous propagation of all signals from their emission locations. The linear instantaneous mixture model assumes that no propagation delay of the cardio-electric signals exists in the human body, and A is the scalar mixing matrix. This fact however is not true for the sound, which propagates to the microphones placed on the surface of the body. In this case the delayed contributions are considered in the generation of the observed signals. This is because of the speed of the sound which is passed through the body tissues to be recorded via the microphones. Therefore, the measurements $\boldsymbol{y}(t) = [y_1(t), \cdots, y_P(t)]^\dagger$ captured by P microphones can be well represented by a convolution of the cardiac sources of the PCG signal with the filter $\boldsymbol{H}(t)$:

$$\boldsymbol{y}(t) = \boldsymbol{H}(t) * \boldsymbol{u}(t) + \boldsymbol{n}(t), \tag{3.4}$$

where $*$ denotes the convolution operation, and $\boldsymbol{n}(t)$ denotes the noise. The transmission path between sensors and sources are hence modeled as the filter $\boldsymbol{H}(t)$, which is a $P \times N$ matrix whose $(j,i)^{th}$ entry is the filter convoluted by the source i to contribute as a component in microphone j.

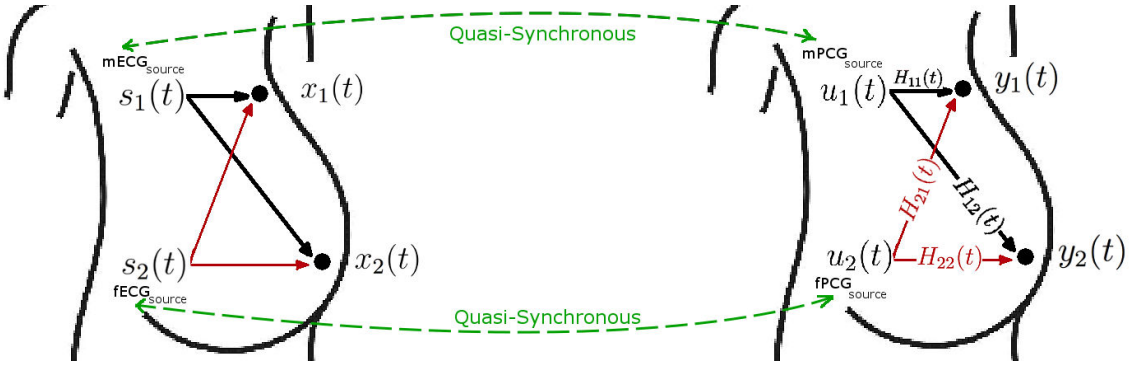

Figure 3.8: The mixture models of the ECG and PCG measurements. ECG is modeled as the linear mixture and PCG is modeled as the convolutive mixture.

The mentioned mixture models are depicted in Fig. 3.8. In this application, we have two maternal and fetal sources ($N = 2$). And thus, each of the cardiac source signals $\boldsymbol{s}(t)$ (ECG sources), and $\boldsymbol{u}(t)$ (PCG sources) consists of two maternal and fetal sources.

Accordingly, the heart produces two signals: $s_i(t)$ and $u_i(t)$. Each of these signals are quasi-periodic signals due to the function of the heart, as explained in Section 3.1. However, The former one is originated from the electrical activity of the heart and the latter one is caused by the mechanical activity of the heart, and that is why the two signals are not totally synchronized. Due to this quasi-synchronicity, a delay exists between the corresponding beats of $s_i(t)$ and $u_i(t)$ signals, which can vary from beat to beat. This phenomenon is illustrated in Figs. 3.9a and 3.9b, where 50 ECG beats are synchronized on the basis of the R-peaks $\{\tau_b\}_{1\leq b\leq 50}$, and thus the b^{th} reference time segment is considered to be $E_b = [\tau_b - t_c, \cdots, \tau_b, \cdots, \tau_b + t_d]$ with a duration of $t_c + t_d$ seconds. Both ECG and PCG beats are then plotted on these reference time segments and they are stacked in Fig. 3.9a. This synchronization is crucial since ECG (and also PCG) are quasi-periodic signals, meaning that its period (and possibly the amplitude) is varying over time [Miaou and Chen, 2001]. In Fig 3.9b, the reference segments are based on the detected S1 waves, $\{\tau_b^r\}$, of ePCG. In this figure, the reference time segments (according to which the beats are stacked) are $P_b = [\tau_b^r - t_c, \cdots, \tau_b^r, \cdots, \tau_b^r + t_d]$ for each beat b. It is clear that there is a variable delay between the ECG and PCG waves, which is caused by either the signal propagation or more commonly by the natural functional activity of the heart. This latter phenomenon is widely seen in multi-modal signals since the modalities show different functions of the same phenomenon. Here, ECG and PCG beats may be affected by different physiological and environmental effects like respiration or sensor movements respectively. This time-varying delay between the beats of the modalities is also comprehensible by looking at the phase diagram showing S1 (Fig. 3.10a) and S2 (Fig. 3.10b) waves in different beats of ePCG, when synchronized by ECG reference segments.

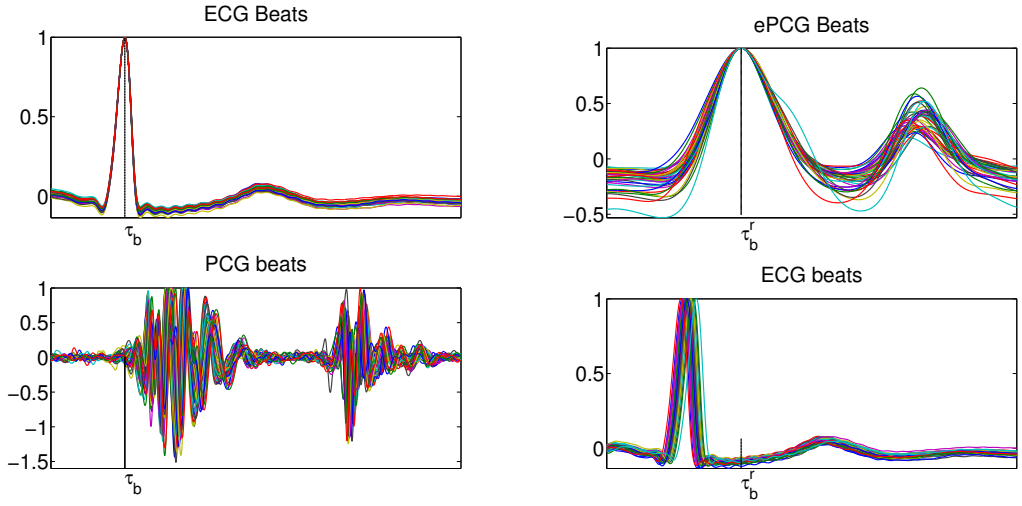

(a) Synchronization of R-Peaks (b) Synchronization of S1

Figure 3.9: Illustration of delays between ECG and PCG beats.

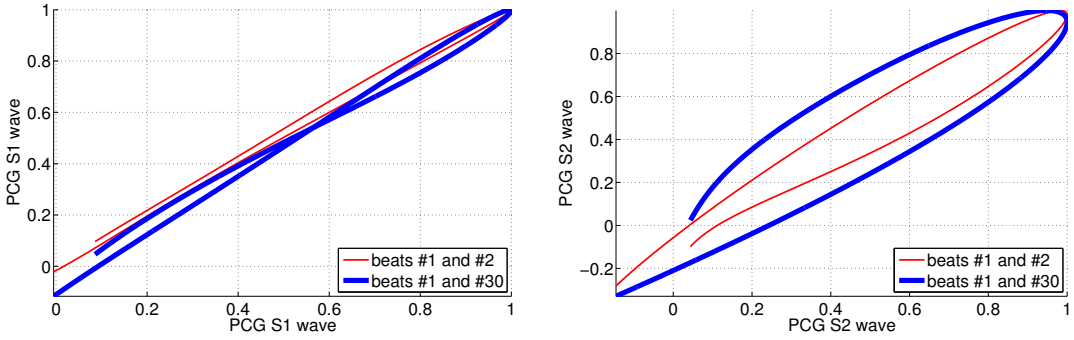

(a) Phase diagram of two pairs of S1 waves (b) Phase diagram of two pairs of S2 waves

Figure 3.10: Phase diagram of S1 and S2 waves.

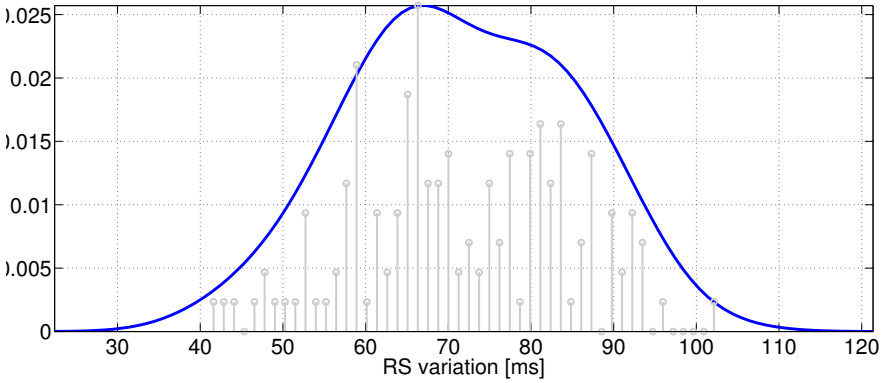

Figure 3.11: The probability Density Function of RS variations.

The distribution of the variations of this value is shown in Fig. 3.11 for a total number of 200 beats on our experimental data. The histogram of the delays is depicted in gray and the probability density in blue is estimated using the kernel smoothing estimator based on a normal kernel function with a bandwidth equal to 6 ms [Wand and Jones, 1994]. According to this estimation, the delays between R-peak and S1 wave, called the RS variations (see Fig. 3.7), can thus be said to follow a normal distribution with mean and standard deviation of 70 ms and 20 ms respectively:

$$\mathrm{RS} \sim \mathcal{N}(70, 20)[ms] \tag{3.5}$$

3.3 Closing Remarks

This chapter studied the ECG and PCG signals from the physiological aspect, and also the signal processing aspect. First, the anatomy of the heart is presented and its function is explained to clarify the origin of both electrical and mechanical activities of the heart referred to as ECG and PCG respectively. The definition of multi-modality is then presented to understand the framework that this study deals with. Second, the two mentioned signal modalities are demonstrated and their characteristics are studied from a signal processing point of view.

These two modalities are presented as quasi-periodic signals. Moreover, the study showed that these two signals are not completely synchronized, meaning that the delay between the corresponding ECG and PCG beats is not always constant and that lead to quasi-synchronous modalities. The quasi-synchronous characteristic may lead to some difficulties, when the two signals are being used in a multi-modal framework. The methods which are presented in the following chapter will explain how the varying delay between the modalities is handled in the multi-modal concept.

4 Modeling Quasi-Periodic Signals

In this chapter, a Gaussian process (GP) approach is studied as a general method which is applicable not only on ECG or PCG signals, but can also be employed to model and denoise any kind of pair of signals which has the quasi-periodicity characteristic, and which are (quasi-) synchronized. In Section 4.1, the GP is defined and the denoising procedure using GP is explained. Then in Section 4.2, the properties of the quasi-periodic signals are investigated and appropriate GPs are introduced in order to model these properties using the previous methods [Rivet et al., 2012, Niknazar et al., 2012], so that the general class of quasi-periodic signals can be modeled with this approach. Subsequently, the problem of detecting cycle indexes and the possible techniques are presented as the solution. The techniques presented in this section are actually uni-modal, meaning that the procedure of modeling is done only using one type of data and a single channel. This section is depicted as red in the schema of Fig. 4.1. Then in Section 4.3, as depicted in green in Fig. 4.1, the first multi-modal approach, called partial multi-modality, is suggested to index the cycles of the desired signal. In Section 4.4, a multi-modal approach, called natural multi-modality, is proposed in order to naturally model and extract the desired signal without an explicit cycle indexation. Finally, using the presented methods, the results of denoising the ECG signal (as an example of quasi-periodic signals) are shown and analyzed in Section 4.5.

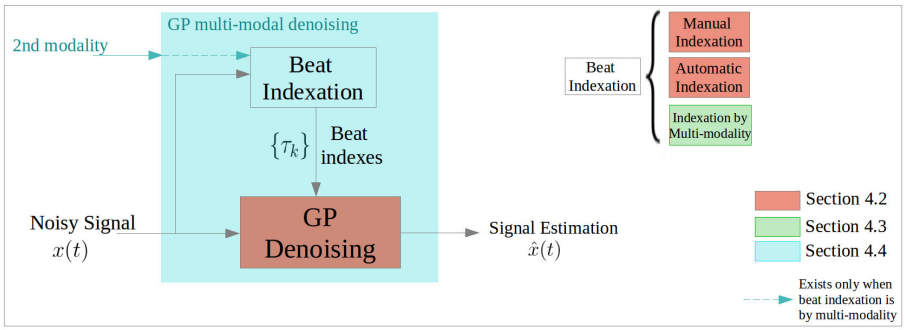

Figure 4.1: General Scheme of the techniques presented in Chapter 4.

4.1 Gaussian Process

Gaussian processes (GPs) are practical tools which are used to define a probability distribution over functions. Since a decade, GP has become a very popular tool in machine learning applications like supervised and non-supervised learning [Kuss and Rasmussen, 2005, Lawrence, 2005]. Regression, which is categorized as a supervised algorithm, is one of the main applications for which the GP is used in order to predict the target or output values for the unobserved inputs and is first introduced by [Rasmussen, 2006] as a concept in machine learning. Since then, the class of GPs is one of the most commonly used families of stochastic processes for modeling the observed data. The GP is the extension of multivariate Gaussian distribution to infinite dimensions, meaning that it contains an infinite-size collection of random variables. Therefore, a stochastic process say $y(t)$ is a Gaussian process if any finite number of these random variables has a joint Gaussian distribution. For instance, consider $\boldsymbol{y} = [y_1, y_2, \cdots, y_n]^\dagger$ as a set of random function variables for the corresponding input set $\boldsymbol{t} = [t_1, t_2, \cdots, t_n]^\dagger$, where the sign $\dagger$ is used to show the transpose of a matrix. In the GP, such set of random function variables are distributed multivariate Gaussian:

$$\boldsymbol{y}|\boldsymbol{t} \sim \mathcal{N}(\boldsymbol{m}, \boldsymbol{K}), \tag{4.1}$$

where $\mathcal{N}(\boldsymbol{m}, \boldsymbol{K})$ is a Gaussian distribution with mean vector $\boldsymbol{m} = \{m_1, \cdots, m_n\}$ and the $n \times n$ covariance matrix $\boldsymbol{K}$. In a GP, the probabilistic model of the inputs is not studied, meaning that the distribution of the inputs is undefined, and only the conditional distribution of the output random variables as in equation (4.1) is modeled [Snelson, 2007].

One of the advantages of the GP is that it is used in a Bayesian setting where the GP is a prior on the functions and can provide a probability measure over the function space. In other words, the GP prior governs the set of possible unobserved functions. The likelihood of these functions and the observations then produce the posterior probabilistic estimates. Consequently, the joint distribution of the training (observation) and the test (predicting) data is a multidimensional Gaussian, and the estimation of the predicted distribution is done by conditioning on the training data. So, first of all, GP modeling provides the possibility of flexible models. Afterwards, the prediction can be done in a straightforward way within a Bayesian framework. Another advantage is that the GP is a flexible, non-parametric model so that the parameters are determined by the training data and not by the model and, thus, the complexity of the model increases as more data points are received. Another practical characteristics of the GP is that it can be defined only by the first and the second order moments of the process. One of the other interesting features of the GP model is its ability to solve nonlinear estimation [Pérez-Cruz et al., 2013] meaning that the flexible prior function would handle the nonlinearity, and the nonlinear estimation

can be treated within a Bayesian framework. Beside the mentioned advantages, GP has difficulties as in the computational cost which is dependent on the size of the data.

4.1.1 Modeling with GP

The key point in the GP, to be remembered, is that it is a collection of random variables any finite subset of which has a multivariate Gaussian distribution as equation (4.1); however, the probability distribution can be specified not only over random variables, but also over functions with an infinite-size domain.

A GP is completely determined by only its mean and covariance functions. This property facilitates model fitting as only the first- and second-order moments of the process require specification. Thus, a random function, $y(t)$, as a statistical process, can be fully described at the second order by its mean function, $m(t)$, and its covariance function, $k(t, t')$ defined as:

$$\begin{aligned} m(t) &= \mathbb{E}[y(t)], \\ k(t,t') &= \mathbb{E}[\big(y(t) - m(t)\big)\big(y(t') - m(t')\big)]. \end{aligned} \tag{4.2}$$

The set of real valued functions, $y(t) \in \mathbb{R}$, can then be described as a Gaussian process:

$$y(t) \sim \mathcal{GP}\big(m(t;\boldsymbol{\theta}), k(t,t';\boldsymbol{\theta})\big). \tag{4.3}$$

By choosing particular mean and covariance functions for the GP, we can introduce some hyperparameters, notated as the set $\boldsymbol{\theta}$, to the prior of the GP. These hyperparameters control the behavior of the functions over which the GP is defined. Now, considering equation (4.3), it can be said that a collection of random variables $y(t)_{t\in\boldsymbol{t}}$ is drawn from a GP with mean function, $m(t;\boldsymbol{\theta})$, and covariance function, $k(t,t';\boldsymbol{\theta})$, if the associated finite set of $\{y(t_1), \cdots, y(t_n)\}$ indexed by the inputs $\{t_1, \cdots, t_n\} \in \boldsymbol{t}$ has a distribution as:

$$\begin{bmatrix} y(t_1) \\ \vdots \\ y(t_n) \end{bmatrix} \sim \mathcal{N}\left(\begin{bmatrix} m(t_1) \\ \vdots \\ m(t_n) \end{bmatrix}, \begin{bmatrix} k(t_1,t_1) & \cdots & k(t_1,t_n) \\ \vdots & \ddots & \vdots \\ k(t_n,t_1) & \cdots & k(t_n,t_n) \end{bmatrix} \right). \tag{4.4}$$

In the following, some notations, which will be used later in this chapter, are defined:

Definition 1 *Given a signal $x(t)$ with M number of samples, and $k.(t,t')$ a covariance function:*

- $\boldsymbol{x} = [x(t_1), \cdots, x(t_M)]^\dagger$ *denotes the column vector indicating signal $x(t)$ with $t \in \boldsymbol{t} = [t_1, \cdots, t_M]^\dagger$,*
- $\boldsymbol{m} = [m(t_1;\boldsymbol{\theta}), \cdots, m(t_M;\boldsymbol{\theta})]^\dagger$ *denotes the mean vector,*

- $\boldsymbol{K}_{\cdot}$ *denotes the covariance matrix where* (p, q)*-th entry is* $k_{\cdot}(t_p, t_q; \boldsymbol{\theta}_{\cdot})$*, where* $\boldsymbol{\theta}_{\cdot}$ *is the set of hyperparameters defined for* $k_{\cdot}$*,*
- $\boldsymbol{k}_{\cdot}(t^*) = [k_{\cdot}(t^*, t_1), \cdots, k_{\cdot}(t^*, t_M)]^\dagger$ *denotes a covariance column vector for any* t^* *time instant.*

One way to estimate the hyperparameters of the model, defined in Eq. (4.3), is maximization of the evidence (log marginal likelihood) given by [Rasmussen, 2006]:

$$\log p\big(\boldsymbol{x}|\boldsymbol{\theta}\big) = -\frac{1}{2}(\boldsymbol{x}-\boldsymbol{m})^\dagger\big(\boldsymbol{K}\big)^{-1}(\boldsymbol{x}-\boldsymbol{m}) - \frac{1}{2}\log\Big|\boldsymbol{K}\Big| - \frac{M}{2}\log(2\pi), \tag{4.5}$$

The maximization of equation (4.5) can be obtained by an optimization method such as gradient ascent [Nocedal and Wright, 2006] or DIRECT optimization algorithm [Finkel, 2003].

The problem of modeling a signal using Gaussian Process is to consider the signal as a collection of random variables indexed by time inputs, and to define an appropriate model with mean and covariance functions which matches the characteristics of this signal. Very often, the mean of the prior Gaussian Process is defined to be zero at any input point: $m(t) = 0$, which is also the case in the present study; therefore, it is only the covariance function which defines the GP and relates the observation points to each other. Accordingly, considering the zero-mean assumption, the problem of modeling is defined as the problem of finding a suitable covariance function for the signal we intend to model.

4.1.2 Denoising with GP

The GP models can be used to model different signals, if we can choose an appropriate covariance function with the parameters/hyperparameters which are estimated to best fit the signal to be modeled. If a good GP model can be found, it can be used in denoising or separation applications.

In the denoising problem a desired quasi-periodic signal, say $s(t)$, is contaminated by an additive noise, $n(t)$, and thus the observation signal, $x(t)$, is defined as:

$$x(t) = s(t) + n(t). \tag{4.6}$$

Assuming that the signal, $s(t)$, and the noise, $n(t)$, are uncorrelated, we intend to estimate the desired signal as $\hat{s}(t)$, which is modeled as a zero-mean GP here. According to the characteristics of the noise, a zero-mean GP can also be defined for $n(t)$. Therefore, the signals $s(t)$ and $n(t)$ are denoted as:

$$s(t) \sim \mathcal{GP}\big(0, k_s(t, t'; \boldsymbol{\theta}_s)\big), \tag{4.7}$$

$$n(t) \sim \mathcal{GP}\big(0, k_n(t, t'; \boldsymbol{\theta}_n)\big), \tag{4.8}$$

where $\boldsymbol{\theta}_s$ and $\boldsymbol{\theta}_n$ are the hyperparameters of the desired and noise signals respectively, which should be well defined to match the characteristics of the signals. For the moment, let us assume that the covariance function and its hyperparameters are already estimated according to the type of signals which we can have in different applications. The definition of suitable covariance functions for the quasi-periodic signals is explained later in the next sections.

Consider again the notations defined in Definition 2 and consider $s(t^*)$ defined on time instant $t^* \in \boldsymbol{t}^* = [t_1^*, \cdots, t_S^*]^\dagger$, where $\boldsymbol{t}^*$ is a vector of time instants with length S. Now, according to the priors defined in equations (4.7) and (4.8), the observed values of $\boldsymbol{x}$ and the $s(t^*)$ are jointly Gaussian distributed [Rasmussen, 2006]. This joint prior distribution is written as:

$$\begin{bmatrix} \boldsymbol{x} \\ s(t^*) \end{bmatrix} \sim \mathcal{N}\left(\boldsymbol{0}, \begin{bmatrix} \boldsymbol{K}_s + \boldsymbol{K}_n & \boldsymbol{k}_s(t^*) \\ \boldsymbol{k}_s(t^*)^\dagger & k_s(t^*, t^*) \end{bmatrix}\right). \tag{4.9}$$

It is seen that the time domain of the estimated signal, can be different from that of the observation. Here, for $s(t^*)$, the time instants are $t^* \in \boldsymbol{t}^*$ with a length different from that of the observation ($S \neq M$ if desired). To obtain the posterior distribution, one may think of conditioning the joint Gaussian prior distribution on the observation, $\boldsymbol{x}$. This gives:

$$s(t^*) \mid \boldsymbol{x}, \boldsymbol{t}; \boldsymbol{\theta} \sim \mathcal{N}(m^*, K^*), \tag{4.10}$$

$$m^* = \boldsymbol{k}_s(t^*)^\dagger (\boldsymbol{K}_s + \boldsymbol{K}_n)^{-1} \boldsymbol{x}, \tag{4.11}$$

$$K^* = k_s(t^*, t^*) - \boldsymbol{k}_s(t^*)^\dagger (\boldsymbol{K}_s + \boldsymbol{K}_n)^{-1} \boldsymbol{k}_s(t^*). \tag{4.12}$$

The values of $s(t^*)_{\forall t^*}$ can be sampled from the joint posterior distribution by computing the Cholesky decomposition C of the positive definite symmetric covariance matrix of $\boldsymbol{K}^*$ in (4.12). Then the Gaussian random scalars are generated as $u \sim (0, \boldsymbol{I})$ and a sample function is consequently computed as $\boldsymbol{m}^* + C\boldsymbol{u}$.

Finally the estimation that we consider for the denoised signal is the mean of the posterior distribution (4.11) which is given by:

$$\forall t^*,\ \hat{s}(t^*) = \boldsymbol{k}_s(t^*)^\dagger (\boldsymbol{K}_s + \boldsymbol{K}_n)^{-1} \boldsymbol{x}. \tag{4.13}$$

It should be recalled that the denoised estimated signal is not limited on the sample points of the observation ($[t_1, ...t_M]$), but it can be calculated for any set of samples even if it is different from the existing samples, and the length of the estimated signal can thus also be different from the observation, if needed.

4.2 GP Based on Uni-Modality

As explained before, the problem of modeling in GP is the problem of finding a suitable covariance function for modeling the signal in which we are interested; and in order to define a suitable covariance function for the GP prior, the characteristics of the signal has to be studied in order that the chosen covariance function best fit the signal. A quasi-periodic signal, $s(t)$, can be considered to have two main characteristics which have to be taken into account for the definition of the covariance function. The first property is of course the quasi-periodicity, meaning that the signal, $s(t)$, is the concatenation of quasi-similar patterns called pseudo periods (or cycles in this study), so although the cycle, $c(t)$, is being repeated, the period of the signal is time-varying. A quasi-periodic signal, with N cycles, can thus be written as follows by considering τ_n the n^{th} cycle index of this signal:

$$s(t) = \sum_{n=1}^{N} c(t - \tau_n), \text{ with} \tag{4.14}$$
$$\Delta_{\tau_n} = \tau_n - \tau_{n-1},$$

where Δ_{τ_n} is not a constant but it varies from cycle to cycle.

The second property, called the shape-form, is the shape of the signal, as in the smoothness, the amplitude, or different components of the cycle. For instance, in the case of ECG signal, we know that it is composed of three main entities: P wave, QRS complex, and T wave, as already shown (see Fig. 3.2). These entities have different characteristics from each other. P and T waves have lower amplitudes than the QRS complex; in addition, the QRS shows a sharper behavior than the P and T waves.

Having mentioned the two properties of the quasi-periodic signals, the quasi-periodicity and the shape-form, two strategies are considered to define the covariance functions that can model these characteristics. The first covariance function, called the time-varying covariance, is defined to first model the shape-form property by modeling each cycle with time-varying hyperparameters, and then the whole signal will be modeled as the concatenation of the individual cycles at the cycle indexes to model the quasi-periodicity. This method is introduced in [Rivet et al., 2012]. The second covariance function, called the periodic covariance, first models the quasi-periodicity and then the shape-form. This is done by using a linear time warping for the quasi-periodicity following by a periodic covariance function, and is introduced in [Niknazar et al., 2012]. A summary of the covariance functions and how they can model the quasi-periodic signals, is found in Table 4.1.

	Covariance Func.	
Properties	Time-varying	periodic
Quasi-periodicity	summation on cycles	linear time-warping from time to phase domain
Shape-form	modeling cycles with time-varying hyperparameters	periodic function

Table 4.1: The methods that each of the two uni-modal covariance functions use to model each property of quasi-periodic signals.

4.2.1 Time-Varying Covariance

As stated before, this covariance function first models the shape-form of the signal by modeling each cycle separately with a GP whose covariance function is $k_c(t, t'; \boldsymbol{\theta})$. This covariance function is defined for describing the shape-form of the cycles and its set of hyperparameters, $\boldsymbol{\theta}$, depends on the shape-form characteristics of any signal that we want to model.

Next, in order to model the quasi-periodicity, the full signal is modeled as the succession of cycles and is, thus, also a GP whose covariance function is given by:

$$k\big(t, t'; \widetilde{\boldsymbol{\theta}}\big) = \sum_{n=1}^{N} \sum_{n'=1}^{N} k_c\big(t - \tau_n, t' - \tau_{n'}\big), \tag{4.15}$$

where $\widetilde{\boldsymbol{\theta}} = \big\{\boldsymbol{\theta}, \{\tau_n\}\big\}$, and $\{\tau_n\}_{1 \le n \le N}$ is the set of cycle index instants that has to be detected from the mixture. This index set contains the common points of the cycles which can be used as the reference point of each cycle to measure the period variability. For example in the ECG signal this can be the R-peak instants (Fig. 4.2a), or in the PCG signal this can correspond to S1 waves (Fig. 4.2b), or in the acceleration signal of the humain gait [Mäntyjärvi et al., 2005], these indexes can be the maxima/minima of each

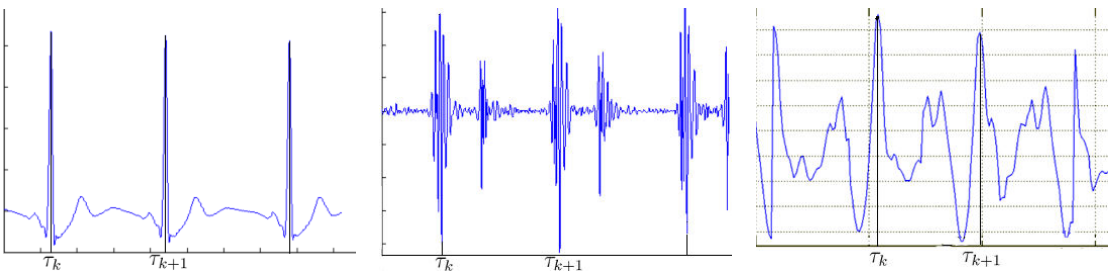

(a) ECG signal. (b) PCG signal. (c) Gait acceleration signal.

Figure 4.2: Cycle indexation of quasi-periodic signals.

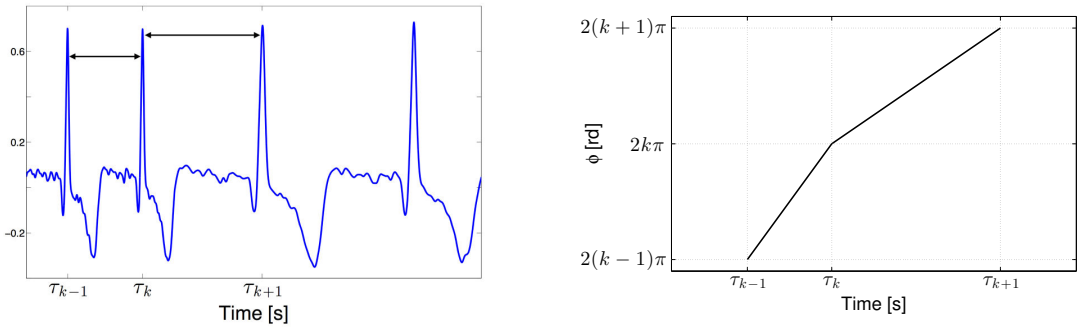

(a) Quasi-periodic ECG beats.

(b) ECG linear time warping to phase.

Figure 4.3: Mapping ECG from time to phase domain.

cycle (Fig. 4.2c).

As an example, the model by time-varying covariance function used for modeling ECG, as a quasi-periodic signal, is explained in Appendix A. The covariance function in (4.15) can be efficient for modeling the quasi-periodic signals since it models each of the cycles separately; however, it suffers from several drawbacks. First, the hyperparameters have to be time-varying to cover accurately the whole signal and this leads to a complicated model and therefore it is not an easy task to optimize all the hyperparameters. Moreover, from a computational point of view, the double summation is quite CPU intensive. Consequently, another alternative formulation is presented which is called here the periodic covariance function.

4.2.2 Periodic Covariance

This covariance function first models the quasi-periodicity by using a linear time-warping to map each cycle's time point to a phase value. So $\phi(t;\{\tau_n\})$, with $\{\tau_n\}$ as its parameters, is defined such that each interval $[\tau_n, \tau_{n+1})$ is mapped into interval $[2(n-1)\pi, 2n\pi)$ (Figure 4.3) [Sameni et al., 2005]. In this case the quasi-periodic signal, $s(t)$, is a periodic signal in the phase domain, $s(\phi)$. Afterwards, a periodic covariance function is presented using time-independent hyperparameters to model the shape-form property. If the cycles are decomposed of parts with different behaviors, for example the waves with different smoothness which cannot be modeled by a single parameters, the signal can be decomposed into few frequency sub-bands where each sub-band has different specific parameters. The signal $s(t)$ can be decomposed via a filter bank into i sub-signals each of them can then be warped to 2π periodic signals $s_i(\phi)$ using $\phi(t;\{\tau_n\})$. In each sub-band, i, this warping allows to use a periodic covariance function defined by the following expression [Niknazar

et al., 2012]:

$$k^{(i)}(t,t';\widetilde{\boldsymbol{\theta}}) = \sigma^2(i)\exp\left(-\frac{\sin^2\Big(\phi(t;\{\tau_n\})-\phi(t';\{\tau_n\})\Big)}{2l_d^2(i)}\right), \tag{4.16}$$

where $\widetilde{\boldsymbol{\theta}} = \big\{\boldsymbol{\theta},\{\tau_n\}\big\}$ is the set of hyperparameters and $\boldsymbol{\theta} = \big\{\{\sigma^2(i), l_d^2(i)\}_i\big\}$, where $\sigma^2(i)$ and $l_d^2(i)$ are power, and correlation length scale of the i^{th} sub-signal, respectively.

The quasi-periodic signals might have different cycles. For example, different cycles may have different amplitudes from each other. Using $\sigma(i)$ to model the amplitude does not consider this variability between different cycles. Therefore, in order to model this variability, we replace the non-varying amplitude by a GP:

$$\sigma^2(i)\exp\Big(-\frac{(t-t')^2}{2l^2(i)}\Big), \tag{4.17}$$

where $l(i)$ defines the correlation between the cycles. If this value is large the correlation between the cycles is varying smoothly and otherwise, we see a less smooth variation over cycles. This modification is necessary since the signal is modeled using one covariance function over all time instants of the signal, while the cycles amplitudes can be different from each other because of different natural phenomenon or noise. The variation of amplitude in the time-varying covariance function in (4.15) is modeled using the time-dependent hyperparameters. Considering equations (4.16) and (4.17), the periodic covariance function can finally be defined as:

$$k^{(i)}(t,t';\widetilde{\boldsymbol{\theta}}) = \sigma^2(i)\exp\Big(-\frac{(t-t')^2}{2l^2(i)}\Big)\exp\left(-\frac{\sin^2\Big(\frac{\phi(t;\{\tau_n\})-\phi(t';\{\tau_n\})}{2}\Big)}{l_d^2(i)}\right), \tag{4.18}$$

for which another $l(i)$ parameter should be added to the set of hyperparameters: $\boldsymbol{\theta} = \big\{\{\sigma^2(i), l_d^2(i), l^2(i)\}_i\big\}$.

Fig. 4.4 shows two randomly drawn priors from equation (4.18) and their corresponding covariance functions.

It is worth noting that this covariance function allows to fit well quasi-periodic signals using the linear warping $\phi(t;\{\tau_n\})$, which maps each cycle into an interval with a length of 2π. Moreover, using such a nonparametric model, no assumption is made about the shape of the signal but its (quasi-) periodicity and its smoothness which are defined by $\phi(t;\{\tau_n\})$ and $l_d(i)$, respectively.

4.2.3 Hyperparameters and Cycle Indexes

Having introduced the covariance functions which can describe the quasi-periodic signals, an important remark should be made considering the cycle indexes, $\{\tau_n\}$: these indexes were either assumed to be the known parameters, or they are detected manually from

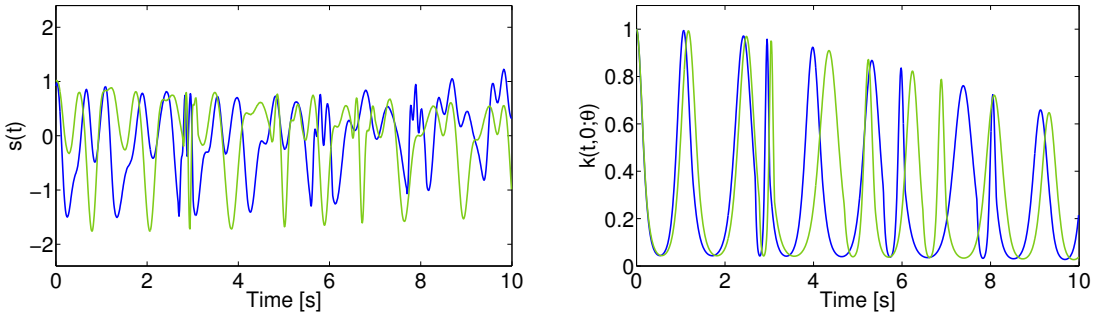

(a) Two randomly drawn priors.

(b) Corresponding cov. functions, $t' = 0$

Figure 4.4: Illustration of the flexibility of the GP modeling: two functions randomly drawn from $\mathcal{GP}\big(0, k(t, t'; \boldsymbol{\theta})\big)$ with the same covariance function in (4.18) but two different sets of τ_n.

the noisy signal in the previous studies. However, the detection of these indexes can be a difficult task considering the signal and the application. One alternative solution is to consider the cycle indexes as the hyperparameters of the method. These hyperparameters can then be automatically estimated just like the other hyperparameters, according to the maximum likelihood framework, which was already presented in Section 4.1.1. However, the maximization of the likelihood function can be complex due to the high-dimensional optimization problem. Maximization of likelihood may poorly estimate the parameters in this case. The existence of local maxima in the likelihood surface also makes the problem more complicated. It is thus proposed to maximize the posterior function. Using the maximum a posteriori estimation allows to first benefit from prior information on the hyperparameters to reduce the complexity of the estimation. Second, it tackles the problem of cycle index detection by using the GP model.

The maximum a posterior estimation is thus a procedure which incorporates a prior distribution over the parameters that we intend to estimate. Therefore, the hyperparameters are estimated as:

$$\hat{\widetilde{\boldsymbol{\theta}}} = \arg\max_{\widetilde{\boldsymbol{\theta}}} p(\widetilde{\boldsymbol{\theta}}|\mathbf{x}). \tag{4.19}$$

According to the Bayesian scheme,

$$p(\widetilde{\boldsymbol{\theta}}|\mathbf{x}) \propto p(\mathbf{x}|\widetilde{\boldsymbol{\theta}})p(\widetilde{\boldsymbol{\theta}}), \tag{4.20}$$

we can then benefit from the prior distribution functions (PDFs) considered for the hyperparameters according to the knowledge obtained from the signal shape and characteristics. As an example the prior $p(\boldsymbol{\theta})$ defined in equation (4.21), is the prior distribution of the hyperparameters defined in the periodic covariance function in equation (4.18):

$$p(\widetilde{\boldsymbol{\theta}}) = p(\sigma^2)p(l^2)p(l_d^2)p(\{\tau_n\}). \tag{4.21}$$

If we wish to consider the cycle indexes as the known hyperparameters, $p(\{\tau_n\})$ would be equal to one.

According to Bayesian scheme, the prior should be multiplied by the likelihood, and integrated over the resulting posterior:

$$\int p(\boldsymbol{x}|\widetilde{\boldsymbol{\theta}})p(\widetilde{\boldsymbol{\theta}})d\widetilde{\boldsymbol{\theta}}. \tag{4.22}$$

But, the likelihood has a complex form which makes the analytical integration impossible. So the integral is approximated using a Markov chain Monte Carlo (MCMC) algorithm [Gamerman and Lopes, 2006]. The MCMC algorithm used here is the Metropolis-Hastings algorithm. An advantage of MCMC over deterministic approximate inference is that it gives a precise approximation to the posterior distribution in the limit of long runs. Another advantage is that the sampling scheme will often not depend on details of the likelihood function [Lawrence et al., 2009].

Making advantage of the prior distribution functions on hyperparameters would reduce the complexity that we could have with the likelihood function, and can lead to an accurate estimation of the hyperparameters. The detected cycle indexes, $\{\hat{\tau}_n\}$, are of high precision, when considered as the hyperparameters of the method. The time values detected as the location of cycle indexes are not restricted to be on the existing samples, but they can be even between data samples. Thereby, firstly the method can be efficient in the detection of R-peaks even when there are not enough samples in the source data, or when there is a data loss on the data. Secondly, the signal can be purposely down-sampled to decrease the size of the covariance matrix and decrease the computational cost. Then, after hyperparameter estimation, the samples can be reconstructed according to the precise location of cycle indexes.

4.3 Partial Multi-Modality

The previous sections explained the basics of modeling quasi-periodic signals with GP. The described methods are based on the definition of covariance functions. It has also been said that one of the essential information for the definition of such covariances is the indexes of cycles, τ_n of equation (4.14). The main approaches to detect these indexes are the manual detection, or the maximization of posterior. The manual detection of indexes is not always possible, if the observation signal is very noisy or too long. The maximum a posteriori estimation detects the indexes which are defined as the hyperparameters of the GP, and demands a large amount of computational time due to the number of hyperparameters.

The mentioned methods are uni-modal methods, meaning that only one type of signal is used (e.g. ECG) in the modeling; however, another data modality (e.g. PCG) can also

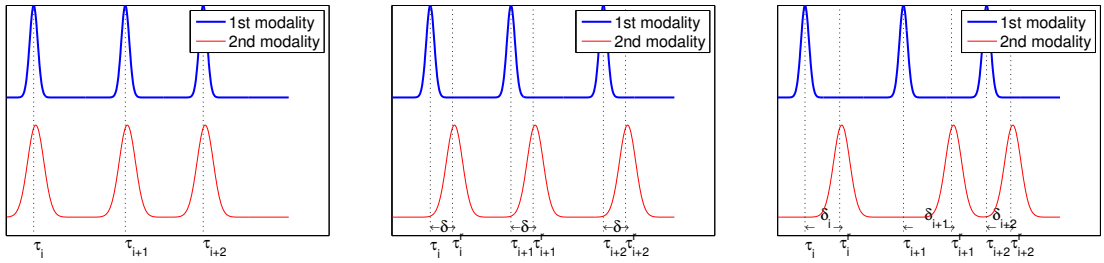

(a) First Scenario (b) Second Scenario (c) Third Scenario

Figure 4.5: The schematic of the 3 possible scenarios for cycle synchronization of modalities.

provide some complementary information which can be useful in indexing the cycles. Beside the quasi-periodic signal that we want to model, we can have other measurements. These measurements are correlated to the desired signal; thus, they also have a quasi-periodic characteristic. The other modality can be either recorded from the same phenomenon which is producing our desired signal, or from another phenomenon which is synchronized to the desired one. Assume that we have two modalities: $s(t)$, the quasi-periodic signal that we want to model, and $r(t)$, the second modality that we will use as the reference. The quasi-periodic signal, $s(t)$, is already defined in equation (4.14). Considering $\{\tau_n^r\}$ the set of cycle indexes of the reference signal modality, this signal is also written in the same way:

$$r(t) = \sum_{n=1}^{N} c_r(t - \tau_n^r). \tag{4.23}$$

Some notations should be reminded: according to equations (4.14) and (B.19), c and c_r are the cycles of $s(t)$ and $r(t)$ respectively with N cycles. The sets of cycle indexes are respectively noted as $\{\tau_n\}$, and $\{\tau_n^r\}$.

If the different nature of the reference modality lets us to detect the indexes $\{\tau_n^r\}$ more easily that using $s(t)$, these reference indexes can provide us with the estimation of $\{\tau_n\}$. In the first approach the reference indexes can provide a good prior distribution on the instants of the indexes of $s(t)$, and this prior can be used in maximizing the posterior as explained before in Section 4.2.3. But, even in this case, the problem of time complexity of maximum a posteriori estimation still remains. For this reason, we introduce the partial multi-modal method.

According to this method, three different scenarios can occur in different multi-modal data. The first scenario is when the two signal modalities are completely synchronous, meaning that the indexes are occurring exactly at the same time instant:

$$\{\tau_n\} = \{\tau_n^r\}. \tag{4.24}$$

This is illustrated schematically in Fig. 4.5a. The second scenario is when the signals are

again synchronous, like the previous case; however, there is a constant delay between the indexes (Fig. 4.5b):

$$\tau_n - \tau_n^r = \delta, \quad \text{for all } 1 \leq n \leq N. \tag{4.25}$$

In these two cases the reference cycle indexes, τ_n^r, can directly index the cycles, τ_n, of $s(t)$. In the case of the second scenario, the model and thus the estimation can usually be done considering $\{\tau_n^r\}$ as the indexes of the $s(t)$ signal; however, the constant delay δ can also be considered as an extra hyperparameter of the GP. The third scenario occurs when the delay between the indexes of two modalities is not constant:

$$\tau_n - \tau_n^r = \delta_n, \tag{4.26}$$

and δ_n depends on the number of the cycle, n. This delay varies from cycle to cycle. In this scenario, which is shown in Fig 4.5c, if the reference cycle indexes are directly used to index the signal cycles, the method may show some flexibilities considering the observations and the amount of delay, however it may also lead to some conflicts in the modeling.

This method is called partial multi-modality since the second modality is used only in indexing the cycles. So, first the indexes of cycles of $s(t)$ are detected using the reference modality. Second, these indexes are given to any of the two uni-modal approaches presented in Sections 4.2.1 and 4.2.2. Afterwards, these methods will not handle the reference modality anymore, and the desired signal is modeled only based on the provided cycle indexes.

4.4 Natural Multi-Modality

4.4.1 The General Method

The method introduced in the previous section makes use of the second modality in the cycle indexation. After that, the GP modeling is still based on a single modality. The approach which is introduced here is a multi-modal one which uses the reference modality naturally in the GP prior model. In the uni-modal approach two covariance functions were presented: the time-varying and the periodic covariance functions. Both of the functions require a previous knowledge about the cycle indexes of the signal. For the time-varying covariance, the double summation on the beats to generate the covariance matrix is pretty time consuming. The periodic covariance however requires a time-warping which can change the shape of the cycles by dilating or compressing them. To overcome these limitations, a more natural way of multi-modality is presented here which includes the presentation of a new covariance function which requires another channel of signal data.

Let us first reconsider the square exponential covariance function which is a popular kernel in describing natural phenomenon. This covariance function is defined by equation (4.27), for the real process $s(t)$. A modification of this covariance was also used to model $s(\phi)$ with the periodic covariance function in equation (4.18).

$$k(t,t';\boldsymbol{\theta}) = \exp\big(-\frac{||\vec{u}(t)-\vec{u}(t')||_2^2}{2l^2}\big). \tag{4.27}$$

Here $||.||_2^2$ denotes the L_2 norm, and l is the length-scale which defines the smoothness of the function which is the hyperparameter of the covariance function $\boldsymbol{\theta} = l$. This covariance function is defined as the function of the input space, $\vec{u}(t)$. The input space can be either the time points where $\vec{u}(t) = t$,as the previously-defined covariance functions; or any other inputs which can be mapped by a function f to the output $s(t)$ as:

$$s(t) = f(\vec{u}(t)) + \epsilon(t), \tag{4.28}$$

where $\epsilon(t)$ is the additive noise. Any signal related to the $s(t)$ can be used as the input of the GP which models $s(t)$. Thus, the reference modality, $r(t)$, can also be used: $\vec{u}(t) = \vec{r}(t)$. It is important to note that this relationship, between input $\vec{u}(t)$ and output $s(t)$ is not assumed to be linear [Pérez-Cruz et al., 2013].

Now, the GP of the signal $s(t)$ can then be described as:

$$f\big(\vec{\mathbf{u}}_L(t)\big) \sim \mathcal{GP}\Big(0, k_u\Big(\vec{\mathbf{u}}_L(t), \vec{\mathbf{u}}_L(t')\Big)\Big), \tag{4.29}$$

where

$$\vec{\mathbf{u}}_L(t) = [u(t), \cdots, u(t-L+1)]^\dagger.$$

We will then propose the following covariance function which depends on the window of the reference modality:

$$k(t,t';\boldsymbol{\theta}) = k_u\big(\vec{\mathbf{u}}_L(t), \vec{\mathbf{u}}_L(t')\big) = \sigma^2 \exp\big(-\frac{\big(\vec{\mathbf{u}}_L(t)-\vec{\mathbf{u}}_L(t')\big)^\dagger\big(\vec{\mathbf{u}}_L(t)-\vec{\mathbf{u}}_L(t')\big)}{2l^2}\big), \tag{4.30}$$

where σ is used to model the amplitude of the signal, and l is the length-scale and models the smoothness of the signal. L is also the length of the window of the input of the covariance function. Consequently, the hyperparameter set is defined as $\boldsymbol{\theta} = \{\sigma^2, l^2, N\}$, and the signal is modeled as:

$$s(t)|r(t) \sim \mathcal{GP}\big(0, k(t,t';\boldsymbol{\theta})\big), \text{ with } k(t,t';\boldsymbol{\theta}) \text{ from } (4.30). \tag{4.31}$$

As mentioned before, the $u(t)$ signal that we use as the reference can be of any kind as long as it is related with the signal that we want to model. So, instead of using the full reference, we can use the 1-bit version of that. In other words, $u_q(t) = \text{sign}(u_t)$ can also be used as the reference (when the mean of the $u(t)$ signal is zero). With the same reason,

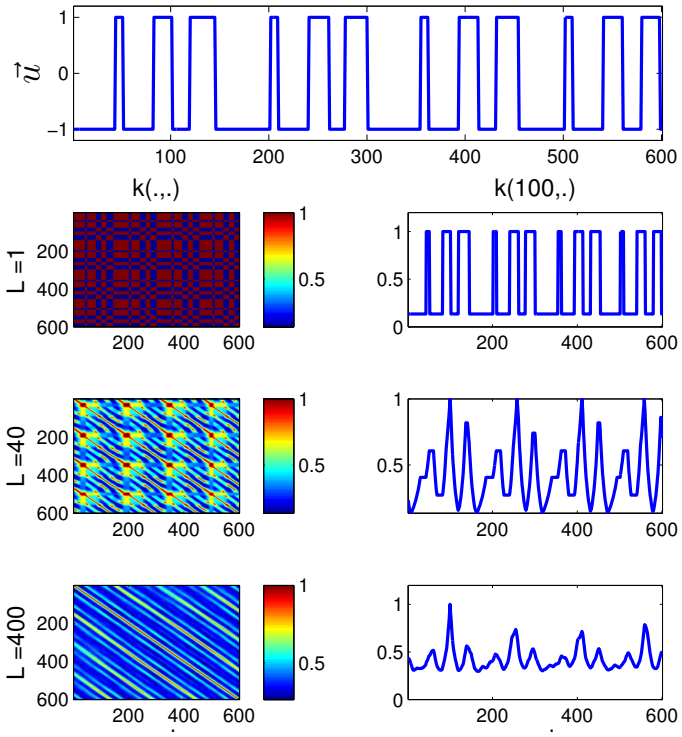

Figure 4.6: The effect of the length of the window in the multi-modal covariance.

this approach works not only with the full reference modality signal, $r(t)$, but also with the 1-bit version of this modality, $r_q(t)$. The use of 1-bit reference signal is proposed for a less-costly device since it can be recorded using cheap sensors or a 1-bit ADCs. This signal is also more memory-efficient and has less time complexity to be processed.

Remarks

The first remark should be mentioned about the window size L. This value determines the length of the windows of the signals whose similarities are compared to each other in order to create the covariance matrix of the signal. Therefore, a small value for the size causes the result to be very dependent on small variations and shape and details of the reference; and a large window size can result in a noisy result, since the covariance shows the similarities of more number of samples or more cycles. The effect of the length of the window on a natural multi-modal covariance function which uses a 1-bit quasi-periodic reference is shown in Fig. 4.6.

The natural multi-modal approach can be compared to the two uni-modal approaches. The time varying method assumes a cycle which is being repeated on different cycle indexes, but the shape of the cycle is assumed to be unchanged. However, the time-warping done in the periodic method assumes that the length of the cycles are different, and so

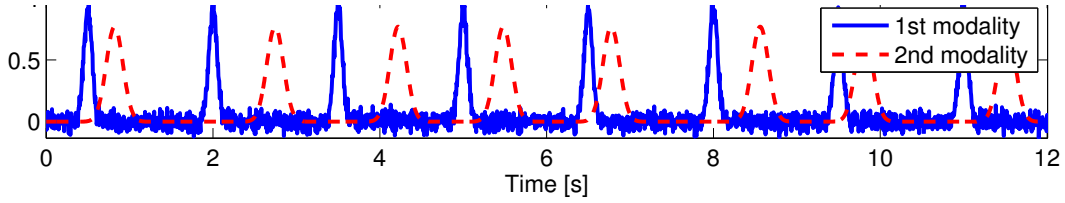

Figure 4.7: A synthetic noisy periodic signal, and a reference signal with delay variations between cycle indexes.

compresses or dilated the cycles by the time warping function to make all the beats have an equal size. Although none of the above methods considers the perfect assumption, the former one seems to consider a more reasonable approach about the natural quasi-periodic phenomenon. The multi-modal approach is based on the comparison of beats and finding their similarities. This method is thus closer to the time-varying method, since a window (a cycle) of the signal is compared to the natural shape of other windows (cycles).

4.4.2 Natural Multi-Modality with Delay Control

Using multi-modality may provoke different complexities as explained before, for example in some modalities, there might be a non-predictable delay between the events in the modalities if they are quasi-synchronized. The delay for each cycle can be different from the other cycles. The use of natural multi-modality can also result an incorrect model. Considering the reference signal as the input of the GP, if its cycles are not synchronized with the cycles of the observation signal, the model which is defined for the observation would not be completely accurate. To better understand this phenomenon, consider a periodic signal generated as the first modality. The second modality is also generated so that its indexes have varying delays with the indexes of the first modality. This is shown in Fig. 4.7. A white Gaussian noise is added to the observation signal (first modality), so that we can use GP to denoise it as explained in Section 4.1.2.

The natural multi-modal covariance function is illustrated in Fig. 4.8a and it is clear that the repeating values in the covariance, which is expected as a good model for the periodic signal, are corrupted by this covariance function, since the reference signal is not synchronized with the first modality. So we propose to replace this covariance function by a covariance function which predicts these delays. Therefore a vector of delays is defined as $\boldsymbol{d} = [d(1), \cdots, d(C)]$, where C is the number of cycles and $d(c)$ represents the variation of the delay between the peaks of modalities in the c^{th} cycle. This can be written as: $d(c) = \tau_c^r - \tau_c$.

Considering R the average period of the signal, the natural multi-modal covariance

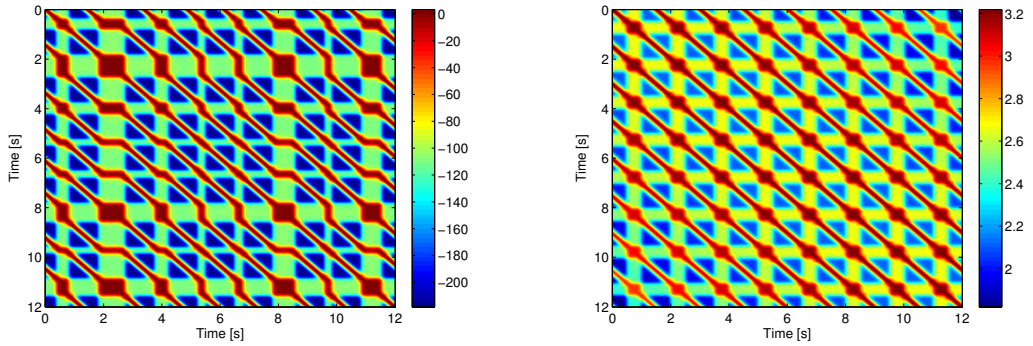

(a) With the existing delays

(b) After the estimation of delays

Figure 4.8: Natural multi-modal covariance matrices of the synthetic periodic modality, when the second modality is given as the reference.

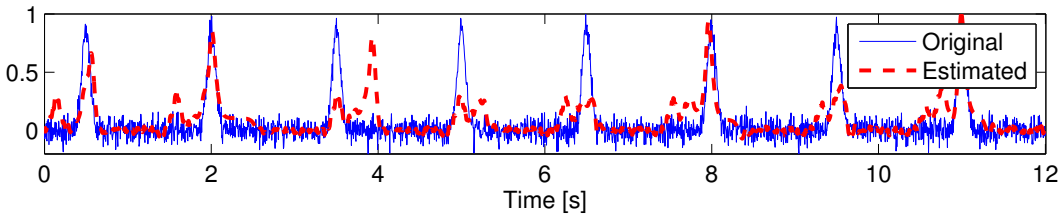

(a) Estimation without delay hyperparameters

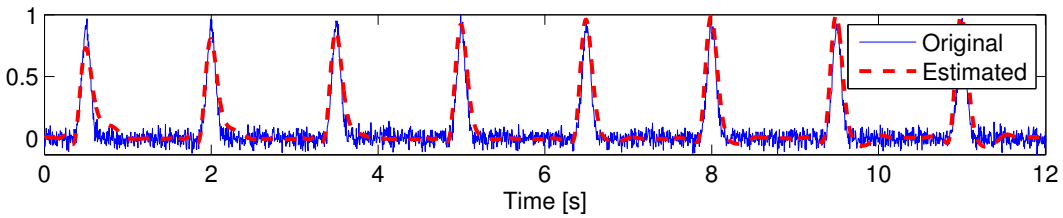

(b) Estimation with using delay hyperparameters

Figure 4.9: Comparison of denoising by natural multi-modality with and without delay parameters.

function between the points in cycle i and the points in cycle j would be

$$k^{i,j}(t,t') = k\Big(\vec{\boldsymbol{r}}_N\big(t+d(i)\big), \vec{\boldsymbol{r}}_N\big(t'+d(j)\big)\Big), \tag{4.32}$$

if $t \in [iR, 2iR)$ the delay $d(i)$ is used for the points in the interval, and $d(j)$ is considered as the delay for the points in the interval $t' \in [jR, 2jR)$. The delays, $\{d(c)\}_{1\leq c\leq C}$, are not necessarily known in advance; therefore, they are considered as the hyperparameters of the method and should be estimated according to any of the parameter estimation techniques described in Section 4.2. This can be done by maximum likelihood; but, it is not recommended due to the complexity of likelihood function in the parameter space. The maximum a posteriori estimation is thus used to estimate the delay parameters (Section 4.2.3). This new multi-modal covariance function is then applied on the synthetic data of Fig. 4.7, and the new covariance matrix is illustrated in Fig. 4.8b. In this figure, the periodicity of the signal is clearly seen in the covariance matrix of the model. The estimation of the signal, as the mean of the posterior distribution, is consequently shown in Fig. 4.9. This figure shows both estimations with and without delay control. It is clear that due to the very large delay variations that we have considered in synthesizing the signal, the observation cannot be denoised using the reference (Fig. 4.9a), since the prior model does not fit the observation. However, when the delays are estimated as the hyperparameters of the method, the denoising gives a more acceptable result as in Fig. 4.9b

4.5 Results and Analysis

In this section the methods which have been explained are tested on the synthetic data. As explained before, the signals can be of any type if they have the quasi-periodicity characteristic. Here, the ECG is chosen as an example to be modeled and denoised. The reference signal that is used here, is the PCG which is modeled to be quasi-synchronized with the ECG. First, the method used for synthesizing the data is described and the evaluation metrics which are used are explained, and finally the results of denoising an ECG signal are illustrated and analyzed.

4.5.1 Synthetic Data Generation

To synthesize the ECG signal, each ECG beat is modeled as the summation of 5 Gaussian-shaped functions [Sameni et al., 2007]. Each of these Gaussian-shaped functions models one of the P, Q, R, S and T waves (see Figure 4.10a):

$$s(t) = \sum_{i\in\{P,Q,R,S,T\}} a_i \exp\left(-\frac{(t-\mu_i)^2}{2b_i^2}\right), \tag{4.33}$$

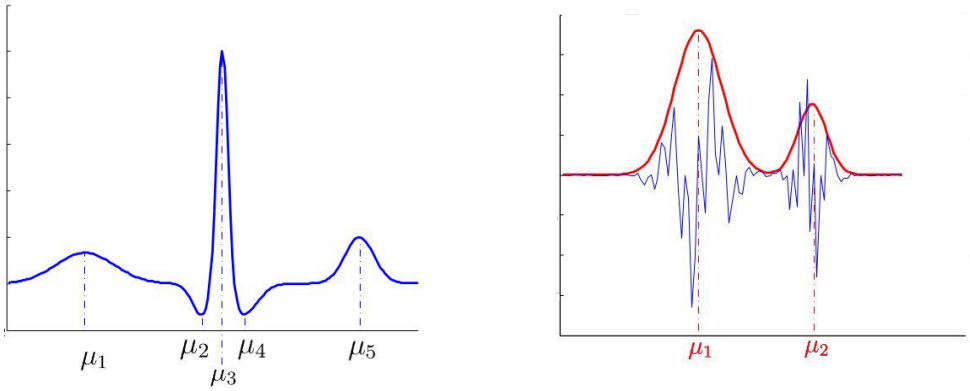

(a) A synthetized ECG beat

(b) A synthetized PCG beat

Figure 4.10: Synthetic ECG and PCG signals.

where a_i, b_i, and μ_i show the amplitude, width, and center of the gaussian functions. In this experiment, each beat of the ECG signal is generated by this model. In order to mimic the variability presented in an actual ECG, the waves amplitudes and P-R and R-T intervals are randomly changed around their mean values. The ECG signal is then obtained as the concatenation of several beats with random global amplitudes and random R-R intervals, to model the quasi-periodicity.

The synthetic PCG data is modeled to contain two Gaussian functions as S1 and S2 waves each of which are multiplied by two sine functions with different frequencies. This is a simple method with less possible number of parameters which is inspired from the work done by [Almasi et al., 2011] who considered two Gabor kernels for modeling each of the S1 and S2 sound waves. The PCG signals we have used are generated as follow:

$$p(t) = \sum_{i \in \{S1,S2\}} \alpha_i \exp\left(-\frac{(t-u_i)^2}{2\beta_i^2}\right) \sin(2\pi f_i t + \phi_i) \sin(2\pi g_i t + \psi_i), \tag{4.34}$$

where α_i, β_i, and u_i are again the amplitude, width, and the center of the Gaussian functions, and f_i and g_i are the frequencies of the waves (since S2 is of higher frequency, the f_i and g_i used for S2 wave can also be higher than that of the S1). In this experiment, the initial phases ϕ_i, ψ_i are randomly drawn from a uniform distribution to allow the variability between the beats. The S1-S2 and the S2-S1 are also varying according to values drawn from Gaussian distributions. The PCG signal is then generated as the concatenation of several beats. If the PCG signal is generated to be used with the ECG, it should be quasi-synchronous with the ECG signal. This means that the S1 peaks are generated to be after the corresponding R-peaks, and the RS variability is also considered. RS variability indicates that the delay between R-peak and S1 wave of one beat can be different from other beats.

A remark should be mentioned about synthesizing the modalities with (RS) delay vari-

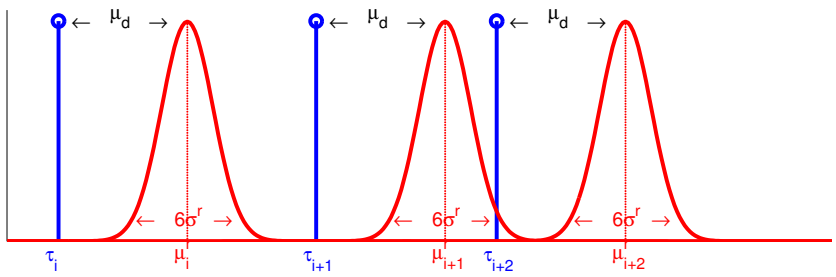

Figure 4.11: A schema of generating the delays between synthetic ECG and PCG.

abilities. Imagine that the i^{th} cycle index, τ_i^r, of the reference signal (here it correspondents to S1 of PCG) is sampled from a Gaussian distribution:

$$\tau_i^r \sim \mathcal{N}(\mu_i^r, \sigma^r), \text{ with } \mu_i^r = \tau_i + \mu_d, \tag{4.35}$$

where μ_d is the mean of the delay variations, and τ_i in the cycle index of the first modality (here R-peak of the ECG). This is shown in Fig. 4.11 for three beats. In generating the reference data two rules should be respected. First, the distribution of cycle i of the reference signal should not collide with that of the $(i+1)^{th}$ cycle (the red distributions should not collide) and second, this distribution should not pass the generated $(i+1)^{th}$ cycle index of the first modality. This is formulated as follows for the reference cycle i: $\mu_i^r + 3\sigma^r < \mu_{i+1}^r - 3\sigma^r$, and $\mu_i^r + 3\sigma^r < \tau_{i+1}$.

The effect of the delay variability is depicted in the result section. In the case of ECG and PCG, a good physiological model of the delay variability is already explained in Section 3.2, and the values for RS interval can thus be sampled from the previously modeled distribution: $\mathcal{N}(70, 20)[ms]$.

4.5.2 Performance Metrics

Both the R-peak detected from the estimations and the quality of the estimated signals are evaluated using two measures. The former is done using the difference between the real R-peak instants, $\{\tau_i\}_{1\leq i\leq N}$, and the estimated R-peak instants, $\{\hat{\tau}_i\}_{1\leq i\leq N}$. The error for each beat is computed as

$$|\tau_i - \hat{\tau}_j|, \tag{4.36}$$

and the average R-peak error is

$$\frac{1}{N}\sum_{i=1}^{N}(|\tau_i - \hat{\tau}_i|). \tag{4.37}$$

The second measure is Signal to Noise Ratio (SNR) which is measured as the level of the desired signal to the noise level. For instance, for an estimation of desired ECG, $\hat{s}(t)$,

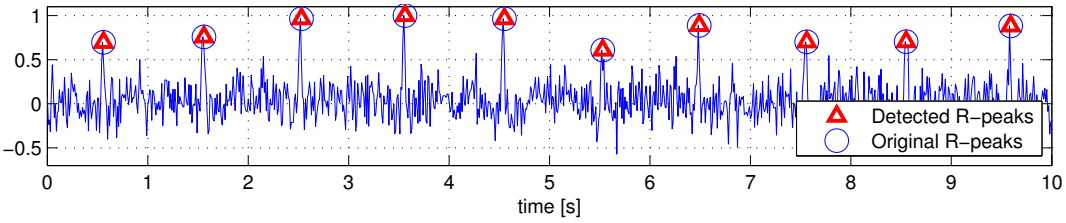

(a) Detection of R-peaks as hyperparameters.

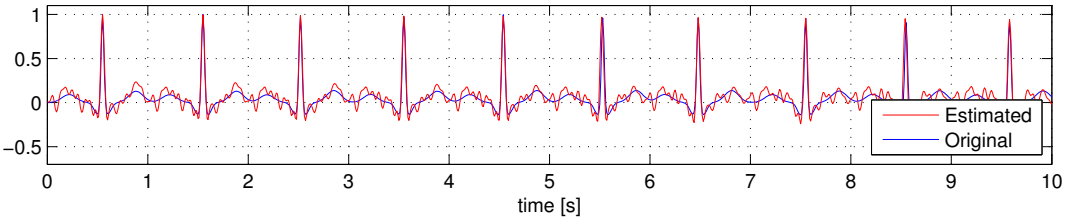

(b) The Estimation of ECG

Figure 4.12: The estimation of ECG and R-peaks as hyperparameters, from a synthetic noisy ECG.

and an estimation of noise, $\hat{n}(t)$ from a noisy observation, $x(t) = s(t) + n(t)$, the output SNR is calculated as

$$\text{SNR} = \frac{\sigma^2_{\hat{s}}}{\sigma^2_{\hat{n}}}, \tag{4.38}$$

where σ^2_v, for any signal $v(t)$, defines its variance.

4.5.3 Results

An ECG signal is generated at the sampling frequency of 100 Hz and the parameters to generate the signal are chosen so that it corresponds to an adult ECG signal, e.g. the mean of the R-R interval is 1 second. This signal is summed with a white Gaussian noise, $n(t)$, to form the noisy signal $x(t) = s(t) + n(t)$. This signal is then normalized, meaning that the mean is subtracted and the data is scaled by the standard deviation; and it is finally shown in Fig. 4.12a. The desired $s(t)$ signal is then modeled by a GP according to the periodic covariance function introduced in Section 4.2.2: $s(t) \sim \mathcal{GP}\big(0, k(t, t'; \widetilde{\boldsymbol{\theta}}_s)\big)$, where $\widetilde{\boldsymbol{\theta}}_s = \{\sigma^2, l^2, l_d^2, \{\tau_n\}\}$. The noise is also modeled by a GP: $n(t) \sim \mathcal{GP}(0, k_n(t, t'; \boldsymbol{\theta}_n)$, whose covariance function is defined by

$$k_n(t, t'; \boldsymbol{\theta}_n) = \sigma_n^2 \delta(t - t'), \tag{4.39}$$

where $\delta(t)$ is a Dirac delta function and so the noise hyperparameters are $\boldsymbol{\theta}_n = \sigma_n$. The set of the hyperparameters of the model, $\widetilde{\boldsymbol{\theta}} = \widetilde{\boldsymbol{\theta}}_s \cup \boldsymbol{\theta}_n$, is then estimated by using the maximum a posteriori estimation, using the prior distribution, $p(\widetilde{\boldsymbol{\theta}})$. Since the parameters

	Adult ECG
σ^2 [V^2]	$\Gamma(5, .2)$
l_d^2 []	$\Gamma(5, .005)$
l^2 [s^{-2}]	$\Gamma(5, 40)$
$R-R$ interval [s]	$\mathcal{N}(1, .002)$
σ_n^2 [V^2]	$\Gamma(5, .2)$

Table 4.2: Values of hyperparameters of prior distributions on $\widetilde{\boldsymbol{\theta}}$ for ECG.

are independent, the prior distribution function can be written as:

$$p(\widetilde{\boldsymbol{\theta}}) = p(\sigma^2)p(l^2)p(l_d^2)p(\{\tau_n\})p(\sigma_n^2). \tag{4.40}$$

The hyperparameters σ, l, l_d, and σ_n are considered to be of Gamma PDFs respectively defined as $\Gamma(\alpha_\sigma, \beta_\sigma)$, $\Gamma(\alpha_l, \beta_l)$, $\Gamma(\alpha_{l_d}, \beta_{l_d})$, and $\Gamma(\alpha_{\sigma_n}, \beta_{\sigma_n})$. Since the set of R-peak instants is also assumed to be unknown, it is considered as the hyperparameter of the model whose prior distriution, $p(\{\tau_n\})$, is derived from the distribution of R-R intervals which are independent and identically distributed with a Gaussian PDF of mean μ_R and variance σ_R^2. Therefore, $p(\{\tau_n\})$ is defined as a multivariate Gaussian distribution with mean vector $\boldsymbol{\mu}$, and covariance matrix $\boldsymbol{\Sigma}$. The i^{th} element of $\boldsymbol{\mu}$ is defined as $\tau_0 + i\mu_R$, and the $(i,j)^{th}$ entry of $\boldsymbol{\Sigma}$ is $\min(i,j)\sigma_R^2$. The values which are used for the prior Gamma and normal distributions are shown in Table 4.2. These values are chosen to match the properties of any ECG signal, so they can be used on real data as well. The posterior distribution is then sampled by Metropolis Hasting's algorithm and the hyperparameters including R-peaks are detected. The detected R-peaks are shown in Fig. 4.12a. Then these detected R-peaks are given to the periodic covariance function to model and denoise the ECG. The estimation of the ECG, $\hat{s}(t)$, is shown in Fig. 4.12b. As it can be seen, this method is able to detected the R-peaks almost perfectly; however, due to the number of hyperparameters, the time complexity of this method is quite high. Therefore, the multi-modal approaches can be good solutions to reduce this complexity.

To apply the multi-modal approaches, a reference signal is needed. The PCG signal is synthesized with S1 wave instants, $\{\tau_n^r\}$, which are d ms after R-peak instants, where $d \sim \mathcal{N}(70, 20)[ms]$. The ePCG is then calculated and is shown in Fig. 4.13b. First, the partial multi-modal method is used. The values detected as S1 intants are given as the reference points of the ECG beats by imagining that $\{\tau_n\} = \{\tau_n^r\}$. Then one of the uni-modal approaches (periodic or time-varying) can be used. Here the periodic covariance function is used, and the results of the estimation is shown in Fig. 4.13c. It is clear that due to the varying delays between the τ and τ^r there are some R-peaks which are not

accurately detected. This is more obvious in the beats which are marked with the circle. The shown errors, between the estimated and the original R-peaks, is dependent on the variation of the delay between the observation and reference indexes.

Afterwards, the natural multi-modal approach is used. It is recalled that in this approach, the whole ePCG is given as the input to the GP which defines the desired ECG. The result of the estimation is depicted in Fig. 4.13d. This result shows a good detection of the ECG. The R-peaks are also precisely matched with the original R-peaks. In Fig. 4.13e, the 1-bit version of the PCG signal, shown in Fig. 4.13b, is used as the reference to the GP by the natural multi-modal method. The estimation is almost the same as when the full-bit ePCG is used, while the 1-bit reference is less costly to be recorded and consumes less memory as explained before.

The results shown in Fig. 4.13 are on the signals which are synthesized to match the physiological delay variations between R-peak and S1. However, if we consider the general class of quasi-periodic signals, the delay between cycles in the modalities can have different amount of variations.

Afterwards, the effect of the variability of the delay between modality indexes is investigated. The PCG signal as the reference is synthesized with $\mu_d = 70$ ms and different standard deviations, σ^r of equation 4.35. The ECG signal is then modeled and estimated with both the partial and natural multi-modal methods. Then, the R-peaks of the detected ECGs are computed and its average error is calculated for every trial of signal generation as equation (4.37). This test is done for 100 generations of different signals and the distributions of these average errors over all the trials are depicted in Fig. 4.14. According to this figure the cycle indexes of the reference signal is almost always perfectly detected using the natural method since the error is always around zero. However, in the partial multi-modal method, this error increases with the increase of the variance of the reference cycle index distribution. For example, in partial multi-modality, when the variance of the delay variation is around 5 ms, the average error has a median of 8 ms, and this error will increase to 39 ms in the case that the standard deviation of the delay variation is 55 ms. If the variance of the error gets larger that this value, the partial method would be unable to have a good estimation, and the natural method will also encounter some problems. In this case the delays could be estimated as hyperparameters to re-synchronize the cycles of the reference modality to find a good GP model as explained in Section 4.4.2.

The output SNR of the different methods are calculated from equation (4.38) and are compared in Fig. 4.15 for only 5 trials. The small number of trials is due to the fact that estimating the delays as hyperparameters takes a large amount of time. The methods are compared with the uni-modal periodic method when the R-peaks are assumed to be known, and the best result is obtained when the delay between the modalities is considered

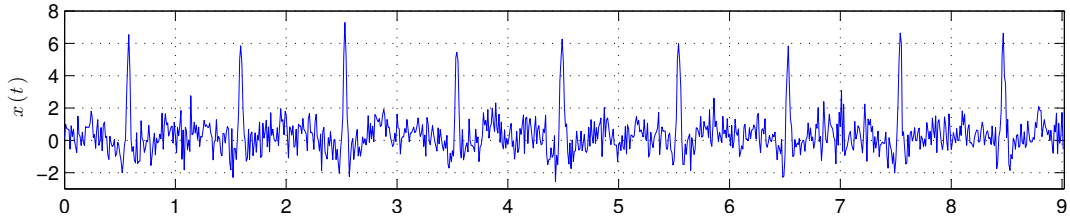

(a) Noisy ECG.

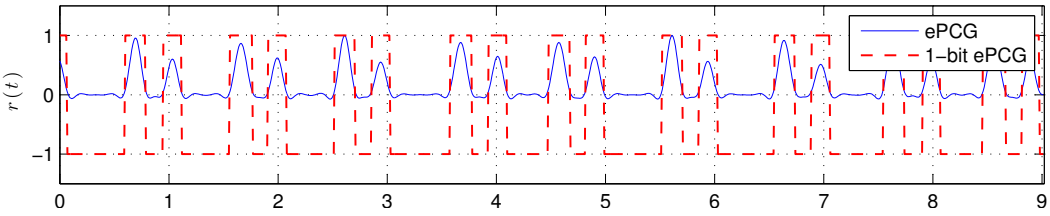

(b) The reference signals.

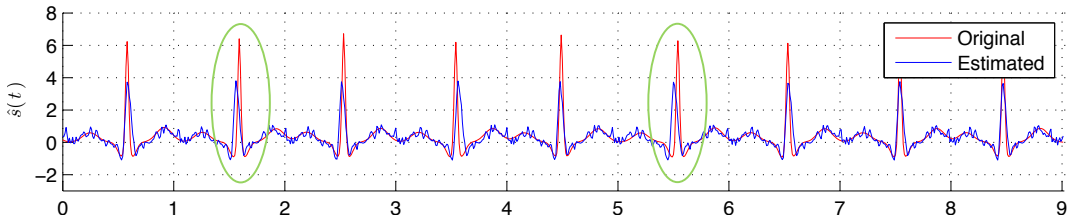

(c) The estimation of ECG by partial multi-modality.

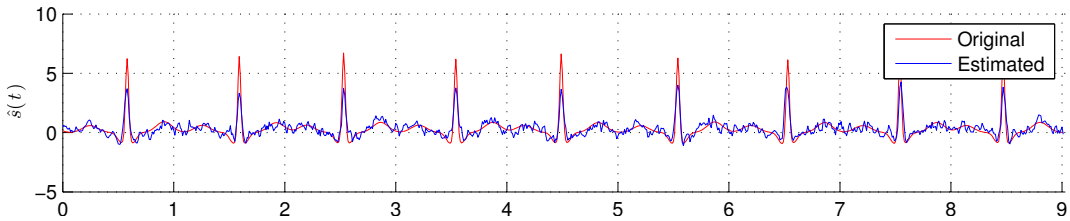

(d) The estimation of ECG by natural multi-modality with full-bit reference.

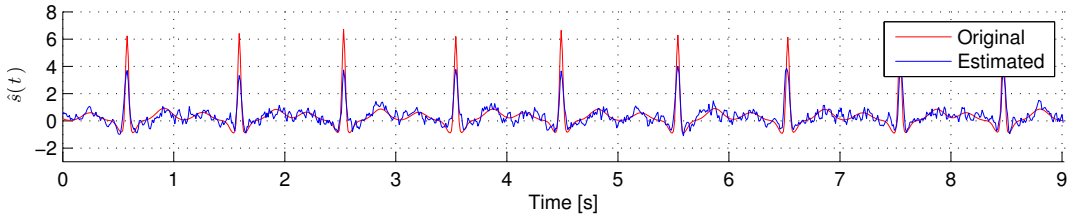

(e) The estimation of ECG by natural multi-modality with 1-bit reference.

Figure 4.13: The estimation of ECG by multi-modal methods from a synthetic noisy ECG.

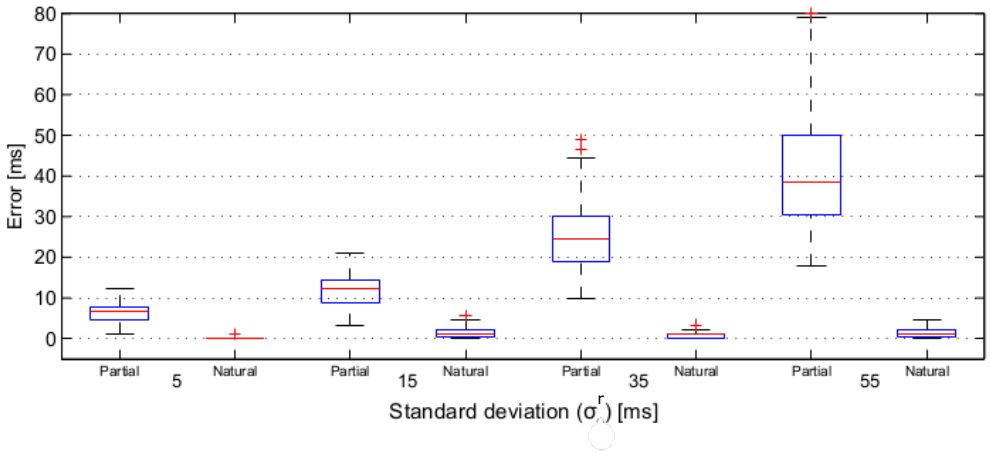

Figure 4.14: The effect of the variation of the delay between modalities on the estimation of R-peaks.

as hyperparameters. If these hyperparameters are assumed to be known, the two modalities are perfectly synchronized and the best SNR is obtained. In this case, the SNR is almost the same as the SNR obtained when the R-peaks are known in the uni-modal approach. However the estimation of all these delay hyperparameters is not an easy optimization task. That is why the SNR is lower, when the delays are estimated as hyperparameters.

As mentioned before, this optimization problem is also very time-consuming, as it takes about 30 minutes to estimate the delays between the 10 beats of a signal samples at 100Hz, while the partial and natural multi-modal approaches take about 2 minutes for the same signal to estimate the hyperparameters and the denoised ECG. In the case of partial and natural multi-modalities, once the parameters are estimated they can be reused for all the segments of the signal and may also be usable for other signals. However the delay parameters vary from beat to beat and are not reusable. Despite the advantages mentioned for the partial and the natural multi-modal approaches, they result in lower output SNRs as depicted in Fig. 4.15.

4.6 Closing Remarks

In this chapter, first, the Gaussian process (GP) modeling was presented as a general method to model any quasi-periodic signals. GP describes the signal according to its mean and covariance function. The existing uni-modal approaches were described which are called time-varying and periodic methods. Both of the methods however assume the availability of the cycle events. So, the cycle-indexes should already be given or they should be detected manually.

An automatic cycle index detection was then presented, and the results were shown that

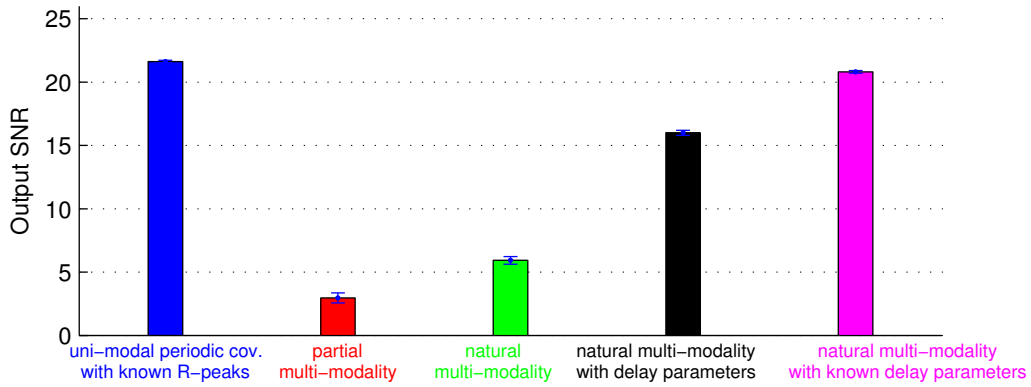

Figure 4.15: Comparison of SNRs of the estimated ECG from the synthesized noisy signal.

it can detect the instants of the cycle indexes perfectly, however it is pretty time-consuming to detect any of the cycle indexes as a hyperparameter of the method.

Consequently, two multi-modal approaches are presented based on the GP modeling. In the first one, called partial multi-modality: the second modality was used as a cycle indexation alternative; and in the second one, called natural multi-modality: the second (reference) modality was used as a natural way to model the first signal.

Finally, the signals were generated to test the presented methods. ECG is a good example of a biomedical quasi-periodic signal which was modeled according to the presented methods, and PCG was considered as the reference modality. The results showed the performance of both of the multi-modal approaches. An analysis was done on different amount of delay variations between the indexes of the first and the second modalities. The natural multi-modal approach was shown to be more efficient in handling the problem of beat synchronization in the two signal modalities. Natural multi-modality is also efficient when the reference signal is only a 1-bit signal. The 1-bit recording could result in a less implementation complexities. The following chapter explains the application of the presented methods on the extraction of fetal ECG.

5 Fetal ECG Extraction

In this chapter the methods which were explained on modeling the quasi-period signals are applied on the extraction of the fetal ECG from the maternal abdominal ECG channels. The method is used in modeling both maternal and fetal ECG signals, and estimate them based on the GP model. Finally, the results on the synthetic data are presented and analyzed.

5.1 Maternal ECG Modeling and Subtraction: a Deflation Approach

Consider the noisy abdominal ECG channel which is a mixture of maternal ECG, $s_m(t)$, fetal ECG, $s_f(t)$, and other noises like the EMG of the mother's and/or the fetus' or the environmental noise, $n(t)$:

$$x(t) = s_m(t) + s_f(t) + n(t). \tag{5.1}$$

This problem is the same as the denoising problem demonstrated in Chapter 4, if we consider the summation of the fetal ECG and noise $\bar{n}(t) = s_f(t) + n(t)$ as the sources which contaminate the maternal ECG contribution in the abdomen: $x(t) = s_m(t) + \bar{n}(t)$. Therefore, $s_m(t)$ can be modeled and extracted according to any of the uni-modal methods explained before (Section 4.2).

Here, it is explained how multi-modality approaches can be used in the case of fetal ECG extraction. Consider a maternal reference channel, $r(t)$, which can be the maternal ECG recorded from the maternal chest which mainly contains the maternal ECG, $r_m(t)$, and the noise, $r_n(t)$:

$$r(t) = r_m(t) + r_n(t). \tag{5.2}$$

Maternal R-peak instants can be detected using the reference $r(t)$ signal. Using these indexes, the first scenario explained in the partial multi-modality section (Section 4.3) is applicable since the thoracic ECG and the maternal ECG which appears in the abdomen are completely synchronized, therefore these indexes can be used to model and extract the maternal ECG, $s_m(t)$, from the abdominal channel. If the reference maternal signal is

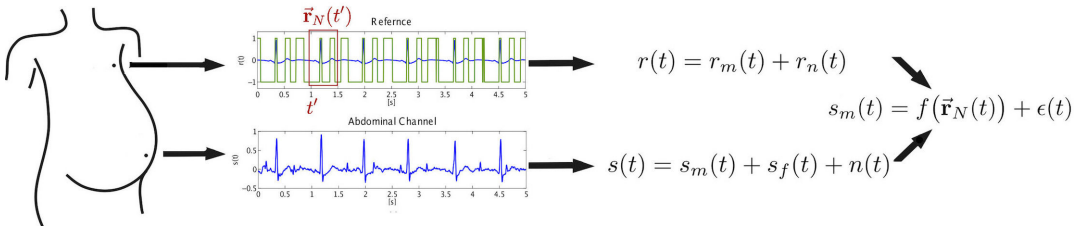

Figure 5.1: A schema of the reference-based covariance model to model maternal ECG in the abdomen, $s_m(t)$. The reference, $r(t)$, can be the full signal or the 1-bit signal.

chosen to be the thoracic PCG instead of the ECG, the R-peak indexation can be done according to the second scenario of Section 4.3 of partial multi-modality method.

The covariance function explained in natural multi-modality approach is also useful in this regard. The two signals $s_m(t)$ and $r_m(t)$, which are attributed to the maternal ECG, are actually highly correlated; while, they are decorrelated with the fetal ECG, $s_f(t)$, and with the noises $n(t)$ and $r_n(t)$. Now, considering the mentioned assumptions, the maternal ECG, $s_m(t)$, is modeled to depend on a window of the reference ECG, $\vec{\mathbf{r}}_N(t)$, by a Gaussian process. So having

$$s_m(t) = f\big(\vec{\mathbf{r}}_N(t)\big) + \epsilon_m(t), \tag{5.3}$$

where $\epsilon_m(t)$ is the additive noise, the GP is written as:

$$f\big(\vec{\mathbf{r}}_N(t)\big) \sim \mathcal{GP}\Big(0, k\Big(\vec{\mathbf{r}}_N(t), \vec{\mathbf{r}}_N(t')\Big)\Big), \tag{5.4}$$

where the covariance function is defined as equation (4.30):

$$k_m(t, t'; \boldsymbol{\theta_m}) = k\Big(\vec{\mathbf{r}}_N(t), \vec{\mathbf{r}}_N(t')\Big), \text{with} \tag{5.5}$$

$$\boldsymbol{\theta}_m = \{\sigma_m, l_m, N_m\}. \tag{5.6}$$

The advantage of using such a covariance function is that there is no need for a prior knowledge on the beats and the R-peaks or even the quasi-periodicity of the ECG signal, but the points' relations of mECG are assumed to be well defined by the covariance function which depends on a reliable reference signal.

The rest of the abdominal signal can then be modeled by a GP using the covariance function

$$k_n(t, t') = \sigma_n^2 \delta(t - t'), \tag{5.7}$$

where σ is a delta Dirac function. Then the maternal ECG that is modeled with the GP can be extracted using equation (4.13).

Finally, the estimated maternal ECG can be omitted from the abdominal recording to leave an estimation of fetal ECG:

$$\hat{s}_f(t) = x(t) - \hat{s}_m(t). \tag{5.8}$$

Apparently, this estimation can result in a noisy fetal ECG: $\hat{s}_f(t) = s_f(t) + n(t)$. However, the main noise source, which is the maternal ECG, is eliminated; and the task of maternal and fetal ECG separation is accomplished.

It should be recalled that the reference signal, $r(t)$, can be replaced by a 1-bit signal recorded from the maternal chest noted as $r_q(t)$. Since r and r_q are highly correlated the assumption of the correlation between s_m and r_q is also true; according to this fact, the GP model for the maternal ECG can use the 1-bit signal as the input of the covariance function. This model is schematically shown in Fig. 5.1.

5.2 Fetal ECG Modeling by Multi-Modality: a Joint Approach

Consider again the components of the abdominal ECG explained in equation (5.1). In the previous section only the maternal ECG component, $s_m(t)$, in the abdominal signal is modeled using the maternal reference signal obtained from the chest, $r(t)$. However the fetal ECG contribution in the abdomen, $s_f(t)$, can also be modeled using the reference-based covariance if we can find an appropriate reference signal correlated to fetal ECG.

The reference used here for the fetal ECG is the envelope of a PCG signal which is recorded from the abdomen as the fetal PCG. This reference signal is denoted as $p(t)$. With a GP model, we can express the fetal ECG to be correlated with the fetal PCG envelope:

$$s_f(t) = f\big(\vec{\mathbf{p}}_M(t)\big) + \epsilon_f(t), \tag{5.9}$$

$$f\big(\vec{\mathbf{p}}_M(t)\big) \sim \mathcal{GP}\Big(0, k\Big(\vec{\mathbf{p}}_M(t), \vec{\mathbf{p}}_M(t')\Big)\Big). \tag{5.10}$$

Using the definition of the covariance in (4.30) the fetal covariance is written as:

$$k_f(t, t; \boldsymbol{\theta}_f) = k\Big(\vec{\mathbf{p}}_M(t), \vec{\mathbf{p}}_M(t')\Big), \text{ with} \tag{5.11}$$

$$\boldsymbol{\theta}_f = \{\sigma_f, l_f, N_f\}. \tag{5.12}$$

In order to summarize the GP modeling of the abdominal signal and the extraction of fetal ECG, the following is presented to review the GP method step by step.

1. Define $k_m(t, t'; \boldsymbol{\theta}_m)$, $k_f(t, t'; \boldsymbol{\theta}_f)$, and $k_n(t, t'; \boldsymbol{\theta}_n)$ with unknown parameters, and define all hyperparameters $\boldsymbol{\theta} = \boldsymbol{\theta}_m \cup \boldsymbol{\theta}_f \cup \boldsymbol{\theta}_n$.

2. Estimate the hyperparameters to create the covariance matrices.

3. Create $\boldsymbol{K}$ as the covariance of the observation between all observation instants: $\boldsymbol{K} = k_m(t, t'; \hat{\boldsymbol{\theta}}_m) + k_f(t, t'; \hat{\boldsymbol{\theta}}_f) + k_n(t, t'; \hat{\boldsymbol{\theta}}_n)$

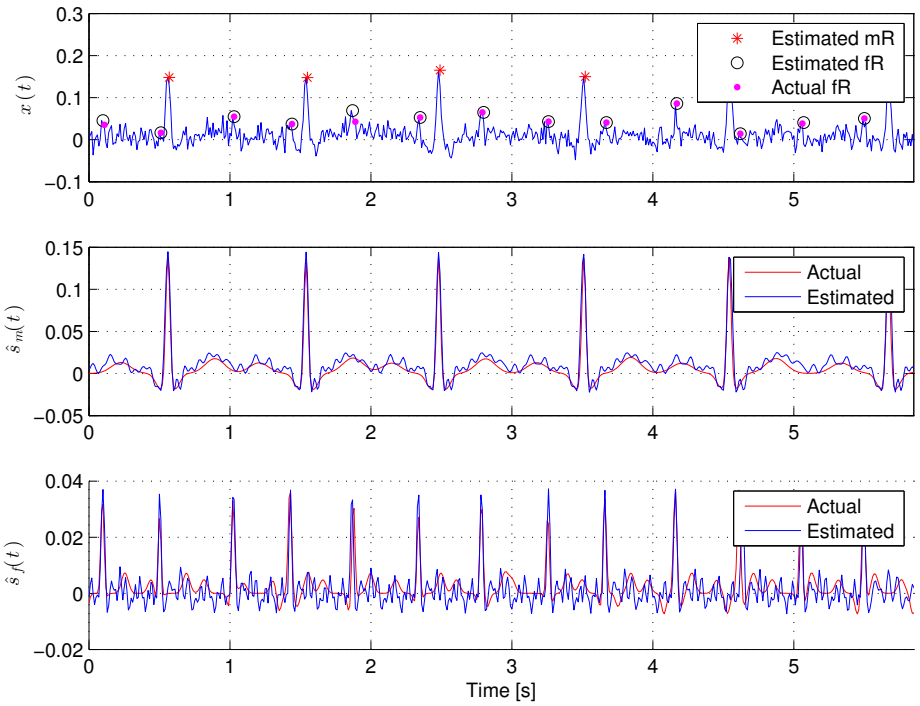

Figure 5.2: Detection of fetal R-peaks (noted as fR) and maternal R-peaks (notes as mR) by considering R-peaks as hyperparameters, and the estimation of mECG and fECG from a noisy synthetic signal.

4. Create the covariance between the desired prediction instants, t^*, and the observation instants, i.e, the fetal covariance $k_f(t^*, t; \hat{\boldsymbol{\theta}}_f)$

5. Estimate the mean of the posterior for the prediction:
   $\hat{s}_f(t^*) = k_f(t^*, t; \hat{\boldsymbol{\theta}}_f)^\dagger \boldsymbol{K}^{-1} \boldsymbol{x}$

5.3 Results and Analysis

The results shown here are obtained by the synthetic data which are generated with the same procedure explained in Section 4.5.1. The maternal ECG, $s_m(t)$, fetal ECG, $s_f(t)$, and noise, $n(t)$, are separately synthesized at 100 Hz and summed up to generate the synthetic abdominal ECG, $x(t)$.

First, the power of the noise, $n(t)$, is considered to be sufficiently high to visually hide the fetal ECG R-peaks in the synthesized $x(t)$ observation. The observation is shown in Fig. 5.2. It is clear that the peaks cannot be manually indexed. So the automatic R-peak detection is applied, to estimate the R-peaks and other hyperparameters by the maximization of the posterior (Section 4.2.3). The prior distributions which is used for the maternal ECG (which is the same as Table 4.2) and the ones used for the fetal ECG and noise are shown in Table B.2. It should be reminded that these distributions correspond to

	Maternal ECG	Fetal ECG	noise
σ^2 [V^2]	$\Gamma(5, .2)$	$\Gamma(5, .001)$	$\Gamma(5, .2)$
l_d^2 []	$\Gamma(5, .005)$	$\Gamma(5, .002)$	
l^2 [s^{-2}]	$\Gamma(5, 40)$	$\Gamma(5, 10)$	
RR interval [s]	$\mathcal{N}(1, .002)$	$\mathcal{N}(.5, .004)$	

Table 5.1: Values of hyperparameters of prior distributions on $\widetilde{\boldsymbol{\theta}}_m$, $\widetilde{\boldsymbol{\theta}}_f$, and $\widetilde{\boldsymbol{\theta}}_n$ for mECG, fECG, and noise respectively.

the hyperparameters defined by the periodic covariance function in equation (4.18). The periodic covariance function is used to model both maternal and fetal ECGs. The values shown in Table B.2 are also applicable on the real data. The results of R-peak detection and ECG estimation are then shown in Fig. 5.2. Both maternal and fetal R-peaks are almost precisely detected as the hyperparameters; and using the estimated R-peaks the ECG signals are finally extracted. It is seen that most of the R-peaks are precisely detected even when the power of the fetal ECG is very low comparing to maternal ECG and the other noises.

Returning to the multi-modal approaches, Fig. 5.3 shows a synthetic abdominal ECG and the two references, $r(t)$ and $p(t)$, generated as the reference modalities for modeling the maternal and fetal ECGs respectively. $r(t)$ corresponds to a thoracic ECG and $p(t)$ corresponds to the detected envelope of an abdominal PCG as shown in the figure. In synthesizing the thoracic ECG, the parameters are chosen to be different from the parameters used to generate $s_m(t)$ in order to verify that the method is not dependent on the temporal shape of the reference signal or the electrode positions or leads of recording. There is no delay between the R-peaks of the abdominal and reference ECGs, and the delay between the fetal R-peaks and S1 waves are sampled from a Gaussian distribution with a mean of 70 ms and a standard deviation of 20 ms, to match the physiological delay as explained before in the previous chapters.

Considering the observation signal $x(t)$, we intend to estimate fetal ECG, $s_f(t)$. Two ways can be considered here: using only one reference signal to model $s_m(t)$ [Noorzadeh et al., 2015b] and subtract it from the abdominal signal, or using two references to model both $s_m(t)$ and $s_f(t)$ [Noorzadeh et al., 2015c]. The two mentioned ways are tested to extract fetal ECG. In the former one we use only the $r(t)$ signal as the reference for the maternal ECG. In the second approach beside using the maternal reference, we also use the envelope of the synthetic PCG, to model fetal ECG.

The quadratic errors of estimated fetal ECGs, $\big(s_f(t) - \hat{s}_f(t)\big)^2$, are shown in red in Fig.5.4. By comparing the two red bars, it is clear that two models for maternal and fetal

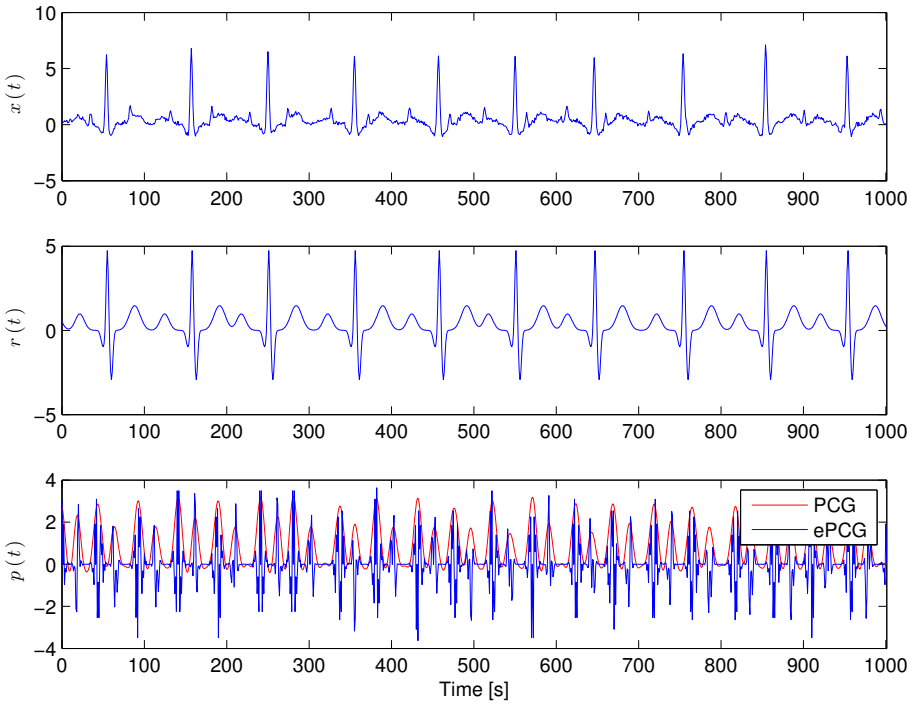

Figure 5.3: The synthetic abdominal signal and the maternal and fetal references. $x(t)$ is the abdominal ECG, $r(t)$ is the maternal reference, and $p(t)$ is the fetal reference.

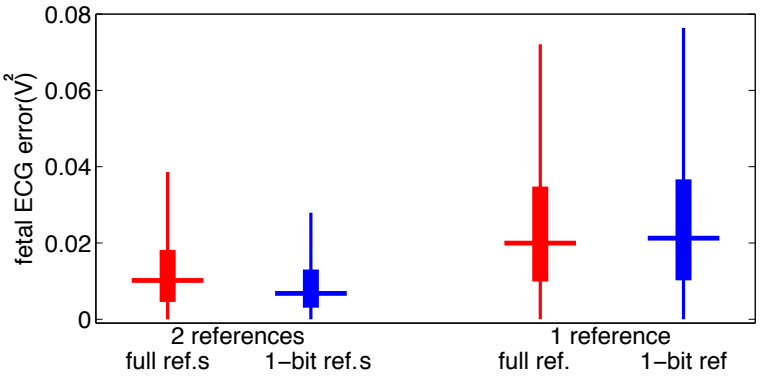

Figure 5.4: The comparison of the error of the estimated ECG with only maternal model, and with both maternal and fetal models.

ECGs can improve the performance to a large extend, since the error of detection is less when having two references. We have then replaced the references of both approaches with 1-bit signals, and the error results are depicted in blue in this figure. It is seen that when using 1-bit signals, two references still give a better performance. By comparing the performance using full reference and 1-bit reference (comparing the red bars to the blue ones), it is seen that using the 1-bit reference signals, the method has almost the same error as when using the full reference signals. By looking at the estimations with two references, we see that the means of the fetal quadratic estimation error is around 0.01 for both the full and the 1-bit references. Moreover, sing only a full or a 1-bit maternal reference signal gives almost the same error bars as shown in this figure. The next results which are shown are obtained by modeling both maternal and fetal ECGs using their corresponding references.

Figs. 5.5a, and 5.5b illustrate the extraction of mECG and fECG using partial and natural multi-modality. The perfect estimation of mECG in the latter one shows that a highly correlated reference can result in a very good estimation. As before, the fetal R-peaks may be wrongly estimated using the partial method because of the delay between the non-synchronized delays between fECG and fPCG. The beat circled in Fig. 5.5a shows an example of such error. However, in the natural method the estimated R-peaks are correctly located.

The error of the detected instants of the fetal R-peaks for both of these methods are calculated on 100 generations of the signals. Then, the error of the detected fetal R-peaks is calculated for each generation trial as equation (4.37). The values of all the trials are then depicted in boxplots in Fig. 5.6. The standard deviation of the Gaussian distribution from which the delay between fetal R-peak and S1 instants are sampled, is varied between 5 ms and 45 ms. The depicted results of the partial method show that the error increases as the variation of the delay increases. When the standard deviation of the delay is 5 ms and 15 ms, the median of the detected error is around 10 ms. This value increases to 30 ms, when the standard deviation of the delay is 45 ms. However, by looking at the obtained results from the natural method, we see that the amount of variation of the delays between the two modalities does not affect the detected fetal R-peaks. The error of these detected R-peaks are almost always around zero.

Since the information that the clinicians need to monitor the fetal heart is usually the heart rate, this information is extracted from the data and is shown on a signal detected by the two multi-modal methods in Fig. 5.7. The figure shows the original fHR and the fHR detected by the two methods. The fHR obtained by the partial multi-modality is seen to be sometimes smoother than the real one. For instance, at the time point around 22 ms, there is an almost rapid variation in the fHR; but, the partial method results in a smooth fHR. This could cause difficulties in detecting the cardiac problems, and may lead

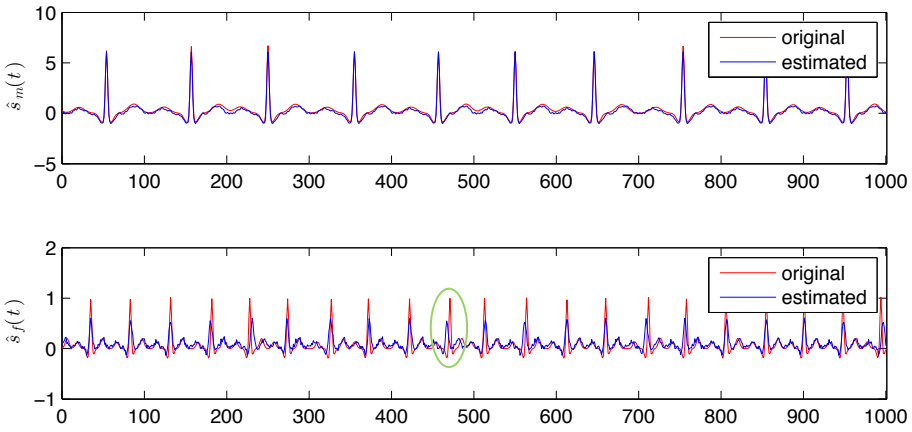

(a) Extraction using partial multi-modality

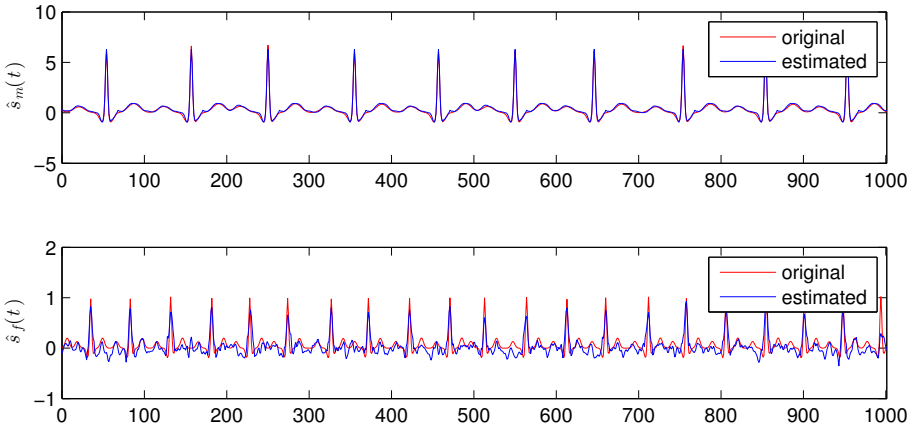

(b) Extraction using natural multi-modality

Figure 5.5: Estimation of mECG and fECG by multi-modality from the synthetic signal.

to a false positive error which causes an ignorance of some of the possible diseases.

The error of the fHR detected by two methods is also calculated for the two multi-modal approaches. This error is calculated according to the heart rate error described in [Andreotti et al., 2014], and equals to:

$$Error_{FHR} = \sqrt{\frac{1}{I}\sum_{i=1}^{I}(RR_i - RR_i^d)^2}, \tag{5.13}$$

where i is the detection index, RR_i and RR_i^d are the real and detected R-R interval of the i^{th} beat as $\tau_i - \tau_{i-1}$. The scores obtained by 100 trials of signals are depicted in Fig. 5.8. This figure shows that the natural multi-modality could be a more reliable method in the detection of fHR.

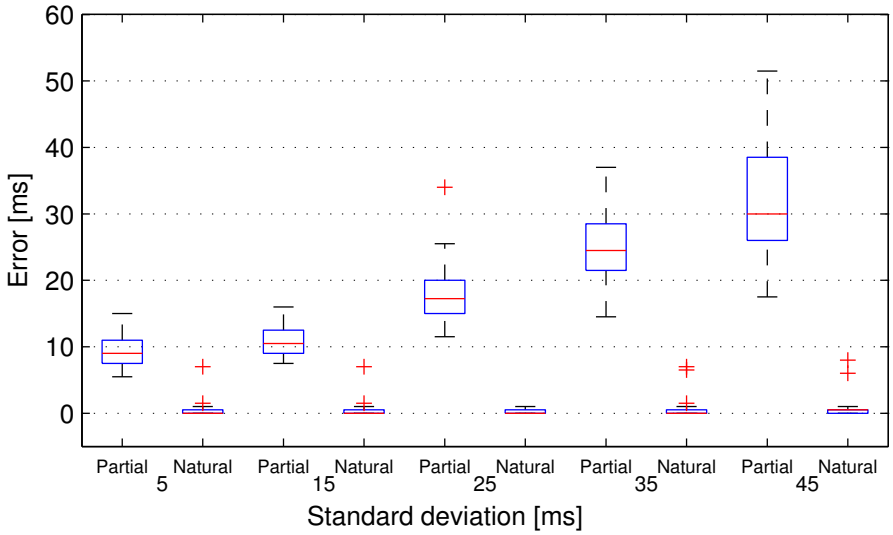

Figure 5.6: The error of detected fetal R-peaks using multi-modality.

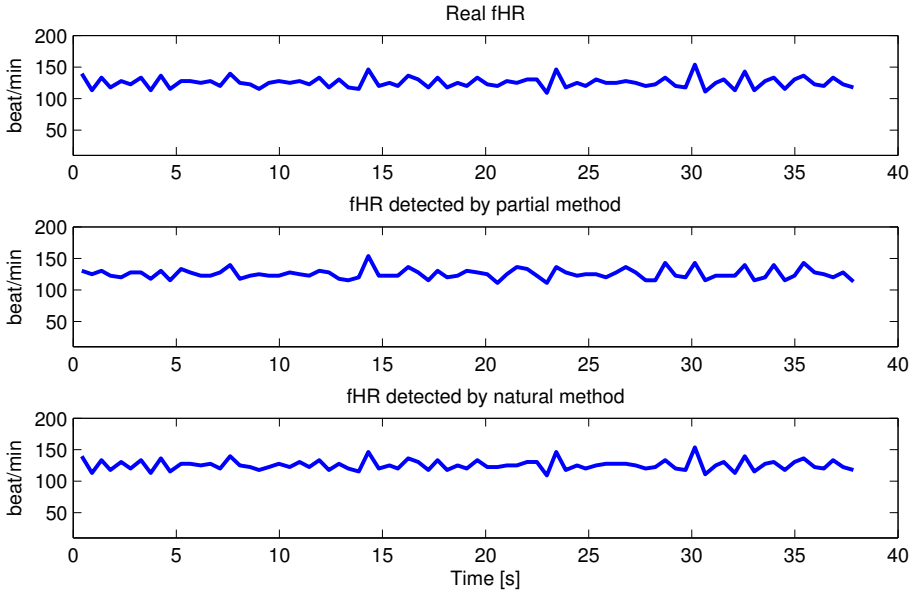

Figure 5.7: The fHR detected by multi-modal approaches.

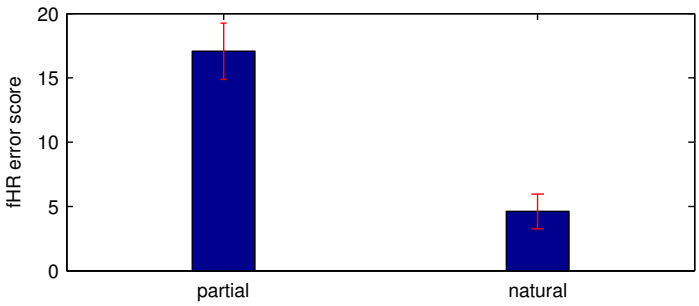

Figure 5.8: The fHR error detected by multi-modality.

5.4 Closing Remarks

This chapter used the methods explained in the previous one to separate the fetal ECG from the maternal abdominal ECG. Both the maternal and fetal ECG contributions in the abdomen were modeled using their corresponding reference signals, maternal ECG, and fetal PCG. All the signals were simulated and in summary the results show that the natural multi-modality can be efficient in both the extraction of fetal ECG, the detection of fetal R-peaks and also the extraction of fHR which is an important information to the specialists.

6 Data Acquisition and Results

There are lots of published methods concerning fetal ECG extraction. The existing studies on fetal ECG have used hundreds of different electrode configurations [Martens et al., 2007, Vullings et al., 2009,Rabotti et al., 2010,Vigneron et al., 2005]. There is a great number of phenomena which can influence the recorded signals. To date, no general agreement exists for the data acquisition.

The methods that were explained in previous chapters, have been tested on synthetic data. In order to apply the methods on real data, we have recorded the synchronous ECG and PCG signals. Such multi-modal data set does not exist in advance, so we have recorded our own data, and observed some parameters that influence the quality, or the shape of the data. Theses observations are mentioned here to facilitate the task of ECG and PCG signal acquisition. However we do not address the complex problem of finding the sensor placements or the optimal signal recording, and do not provide the experimental results about this task. Here some preliminary signals are demonstrated to be used in validation of the method.

6.1 Description of the Experiments

Platform

Data have been acquired with the help of the local facility (PRETA Platform) which belongs to the LSI Carnot Institute Platform Network, and benefits from an official authorization for noninvasive recordings. The used data acquisition hardware is Powerlab (AdInstruments), provided with biological amplifiers, which are connected in parallel to give the possibility of recording several channels of synchronized signals. The ECG is recorded using the disposable electrodes, and for the PCG recording, a condenser microphone device from AdInstrument is used which is suitable for the phonocardiography.

Uni or Bi-polar

Both uni-polar and bi-polar electrodes have been used in different studies to record cardiac electrical activity [Kimber et al., 1996]. Here, the bi-polar electrode configurations are used

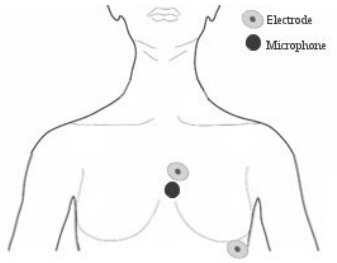

Figure 6.1: The maternal electrode and microphone configuration.

as they are less sensitive to the common interference. The lead vectors associated with Einthoven's lead system are conventionally found based on the assumption that the heart is located in an infinite, homogeneous volume conductor. The recording field of the uni-polar ECG in this volume conductor is uniform in all directions, while the bi-polar recordings vary with the angle between the electrical heart vector and the axis of the bipole. Therefore, the signal captured with the uni-polar configuration is composed of the global activity, and it is possible that the local activity of the signal of interest is hidden in the recording, while the bi-polar recording contains less distant interference. That is why the bi-polar configurations are used in our experiments. However, the directional sensitivity of the bi-polar configuration makes the electrode placements complicated [Graczyk et al., 1995].

Subjects

The signals were registered from 9 pregnant healthy women between the 22^{nd} and the 38^{th} week of gestation, from which 4 subjects were in the 9^{th} month, since this period can provide best quality signals consistent for the presented method. According to the medical checks that the subjects had, the mother and the fetus were in complete health at the time of ECG recordings. The data is recorded through both thoracic leads (to record maternal signals) and the abdominal leads (to contain fetal signals). These two recordings are explained subsequently.

6.2 Maternal Signals

One channel of maternal ECG and one maternal PCG is recorded from the chest of the mother. The maternal sensor placements are shown in Fig. 6.1.

6.2.1 ECG

The poles of the ECG electrodes are placed on the axis of lead II of Einthoven's triangle; however, the distance of the electrodes is decreased in order to reduce the sensitivity of the recording to distant activities or noises.

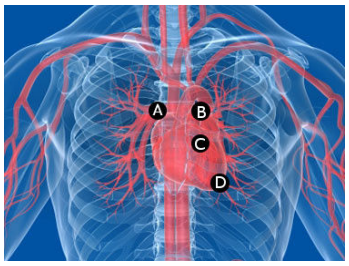

Figure 6.2: Placements of microphone for PCG recording: the traditional auscultation. A refers to the aortic valves, B the pulmonic valves, C the tricuspid valve, and D the mitral valves sound.

6.2.2 PCG

The placement of cardiac microphones on the rib cage on the chest can record the PCG signal. However, some placements are known to better correspond to cardiac valve sounds [Ahlström, 2006]. We have placed the microphone very close to the sternum on the left to record both S1 and S2 sounds (at the center of A, B, and C positions in Fig. 6.2). The microphone A string belt is used to fix the microphone considering the comfort of the subject.

6.3 Fetal Signals

Despite the fact that maternal ECG and PCG signals can be recorded according to appropriate configurations, fetal cardiac signals are simply influenced by the physiological or experimental factors which make it more difficult to define a fixed configuration of sensor placements [Rooijakkers et al., 2014]. There are many factors of this kind, among which the ones observed through our experiments are described here. The fetal signals are recorded via large number of sensors as depicted in Fig. 6.3, without any prior assumption about the location of the fetus. Afterwards, the best quality signal is selected among these recordings.

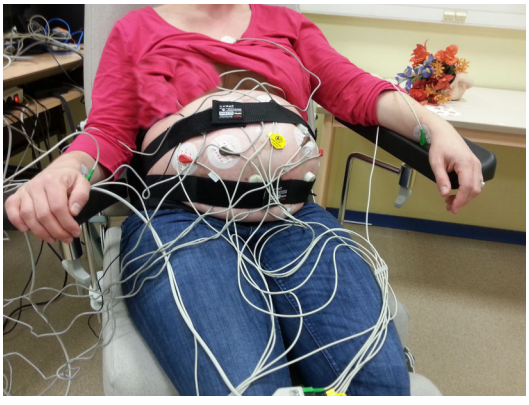

Figure 6.3: A pregnant woman during a data recording session.

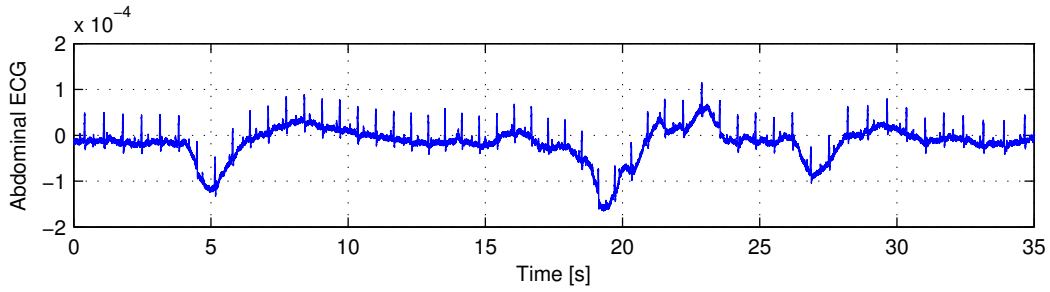

Figure 6.4: An ECG recording with large motion artifacts.

6.3.1 ECG

First the physiological, environmental and factor of these kinds which affect the quality of the fetal ECG recorded through registration sessions are described. These factors are listed as follows.

Fetal Age

The fetal ECG cannot be recorded earlier than about the 20^{th} week of gestation, and even afterwards, we know that the fetus is surrounded by different anatomical layers which have different conductivity. In the early stages, the fetal heart is very small, and in the late pregnancy vernix caseosa, a thin fatty layer is developed on fetal skin [Stinstra, 2001]. The conductivity of the vernix caseosa is much lower than that of the surrounding tissues and severely reduces the measured fECG amplitude. Therefore, the 36-38^{th} week can result in the best quality of the fetal ECG signal since the fetal heart is large enough and the vernix caseosa has dissolved.

Electrode Motion Artifacts

The movement of the electrodes or lead wires can change the electrode-skin impedance and also the skin potential due to deformation of the skin [de Talhouet and Webster, 1996]. Electrode motion artifacts are from 100 to 500 ms in length and their amplitudes are up to five times higher than that of the mECG [Rooijakkers et al., 2014]. This artifact is shown in Fig. 6.4 at time instances around 5s and some large electrode motion artifacts can also be seen between 19s and 29s. However, this artifact can be removed by signal processing methods like temporal filters (high-pass filters) or adaptive ones.

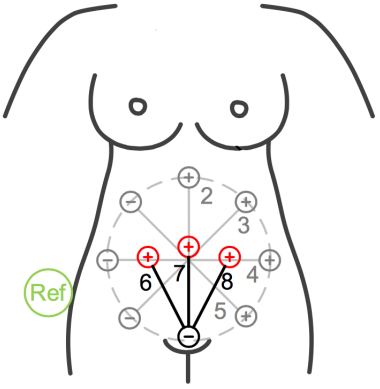

Figure 6.5: The proposed leads 6-8 by [Andreotti et al., 2014]

Artifacts Caused by the Mother

Maternal ECG is the main source noise which can have an amplitude of 4 to 20 times higher than the fetal ECG. Beside mECG, electromyographic signals produced by the propagation of action potentials trough uterine cells is one of the most important sources of noise. These signals are also known as electrohysterogram (EHG). There is not a certain uterine pacemaker found yet and any myometrial muscle cell is capable of acting as a pacemaker which results in the variation in the extent of electrical propagation, as well as the pacemaker current. Maternal sitting or lying down position can also affect the artifacts of the recorded signal.

Fetal Orientation and Movements

In obstetrics, the orientation of the fetus in the womb is categorized into different positions. Since the fetus is most of the time in a vertical position (most of the time the head-down position) the vertical or diagonal configuration of electrode poles is preferred to a horizontal placement. This configuration has also been used in [Andreotti et al., 2014] as in Fig. 6.5. Unlike the maternal pole electrodes which can be placed closer to reduce the effect of noise, the fetal electrodes should not be placed very close to each other, since the position and location of the fetal heart cannot be precisely determined in advance. Two abdominal recorded ECGs are compared in Fig. 6.6 with different configurations. In Fig. 6.6b, the fetal R-peaks are completely hidden. This can be caused by different factors: the close distance of the electrodes, or the horizontal placement of the bi-poles, or the vernix caseosa which is not yet disappeared since this signal corresponds to the 29^{th} week of pregnancy when the vernix caseosa is developing, while Fig. 6.6a corresponds to the 38^{th} week. In the latter figure, fetal ECG R-peaks can be seen in most of the times.

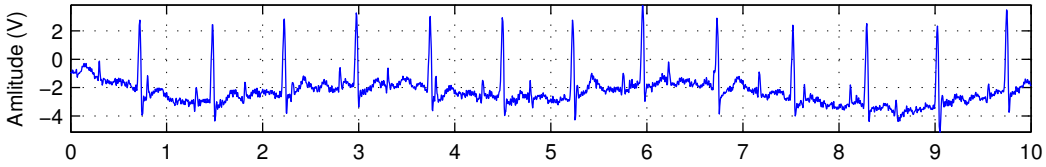

(a) Diagonal electrode placements.

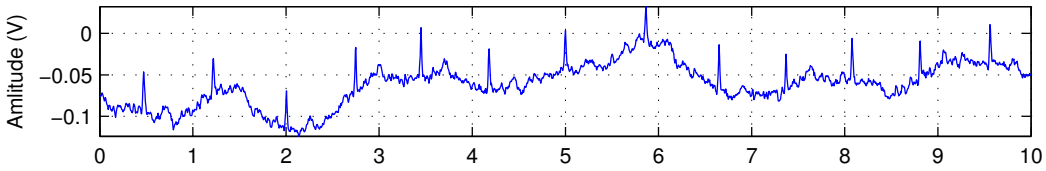

(b) horizontal electrode placements.

Figure 6.6: Comparison of two abdominal ECG recordings.

6.3.2 PCG

Fetal heart sound can be recorded from the maternal abdomen. Vibrations caused by movement of the fetal heart propagate through the abdominal tissue and reach the membrane. The membrane moves in response to the vibrations and the waves will encounter a transducer and are converted into electrical pulses. For our experiments the microphones are fixed on the abdomen by spring belts as in Fig. 6.3 considering the comfort of the mother. The microphones are placed in two rows on the top abdomen and the lower part of the abdomen.

Fetal Age

The fetal PCG can be theoretically recorded as soon as the noninvasive fECG can be recorded since the heart is formed as in functioning; however, due to the small size of the fetal heart, it is difficult to record the PCG before around the 30^{th} week, or the microphone should be placed on the abdomen in a circle (with diameter not larger than 5cm) around the fetal heart. This can be done only by a specialist.

Fetal Position

One of the most common positions in pregnancy is Left OccipitoAnterior (LOA) [Osei and Faulkner, 1999], which suggests that one of the best placement of the microphone is possibly on the left of the abdomen. Thus, to locate the best recording place, it is suggested to start with the lower left part of the abdomen.

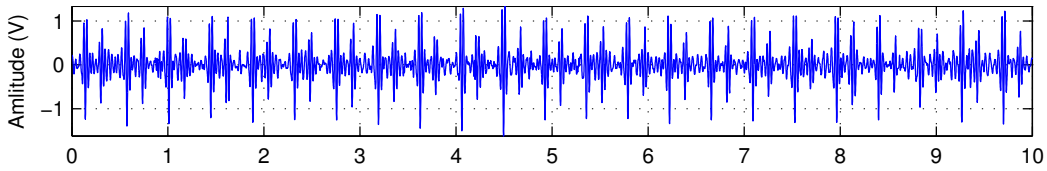

(a) 38^{th} week

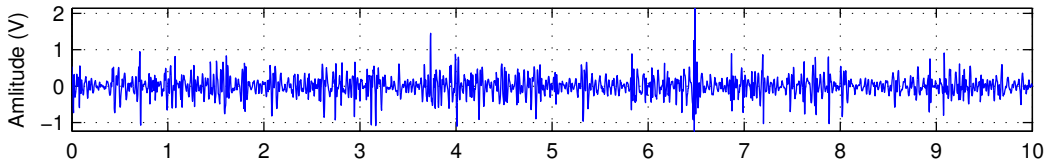

(b) 24^{th} week

Figure 6.7: Comparison of two abdominal PCG registrations.

Artifacts

The sound of umbilical cord and the sound of the arteries in the placenta are two of the acoustical noises which may be captured from the fetus. Beside these two artifacts, the environmental noise can be recorded through the microphone. A mechanism should be found to secure microphone device on the maternal abdomen so that there is no need for another person to manually hold the device in place. It would also reduce noise interference caused by slight positional changes of the device when the person holding the sensor shifts his/her weight or adjusts the sensor. Two abdominal recordings are shown in Fig. 6.7. They are filtered in the frequency range of $[25 - 100]$ Hz. One can see that in Fig. 6.7a, fetal PCG is clear, however in Fig. 6.7b no clear fPCG is observed.

In summary, the PCG signal is easy to be recorded as long as the fetus is in a good position which is actually the 9^{th} month of gestation.

6.4 Results and Analysis

So far, it is shown that the natural multi-modal method is more efficient than the partial one. Therefore, this method is applied on the signal registered from a subject in the 9^{th} month of gestation. The reference signal for the mother is the thoracic ECG recorded from the chest, and the abdominal PCG is pre-processed to correspond to the fetal cardiac sounds which is then used as the reference to model the fetal ECG. The abdominal ECG and the reference signals are depicted in Fig. 6.8. As it is depicted in the figure, the reference signals can be either full signals or the 1-bit signals. One should note that $x(t)$ is referred to as the abdominal ECG, and $r(t)$ and $p(t)$ are the maternal thoracic ECG and the abdominal fetal PCG respectively.

The first results shown in Fig. 6.9a are obtained by using only one maternal reference

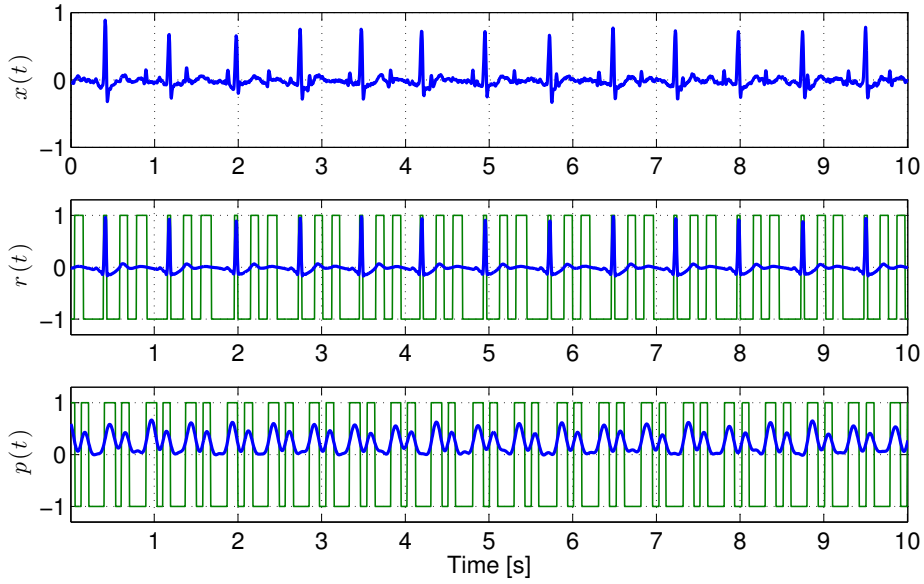

Figure 6.8: The abdominal observation ECG and the two references. $x(t)$ is the abdominal ECG, $r(t)$ is the reference for mECG, and $p(t)$ is the reference for the fECG.

to estimate $\hat{s}_m(t)$ and subtracts it from the observation signal to obtain an estimation of the fECG, $\hat{s}_f(t)$. The maternal signal is thus modeled using the thoracic ECG as the reference modality. This reference is used as the input of the GP and is estimated with the natural multi-modality technique explained in Section 5.1. This is done to compare the results obtained by adaptive filtering. This figure shows that adaptive filter gives almost the same result as the Gaussian Process. Now, in the next figure the reference signals of the two methods are replaced with the 1-bit signal. Fig. 6.9b shows this point; although the GP is capable of detecting maternal and fetal ECGs, adaptive filter is not. The reason is that the 1-bit version of the reference cannot be linearly transformed to the maternal ECG contribution in the abdomen. However, GP can nonlinearly provide the estimations.

Now, the natural multi-modality is applied using both maternal and fetal reference signals which were demonstrated in Fig. 6.8. Both of the maternal and fetal ECG contributions in the abdomen are modeled according to the joint multi-modal approach explained in Section 5.2. This result is shown in Fig. 6.10. By comparing this figure to the left columns of Fig. 6.9, it is clear that the estimation using 2 references (one for the mother and one for the fetus) is less noisy than when only maternal signal is modeled. This result contains also less errors; for example, in Fig. 6.9b, natural multi-modality has detected two close peaks in the estimation of $\hat{s}_f(t)$ at time instant 3.5s, while this error has been corrected in Fig. 6.10 due to the model of the fetal ECG.

Now, imagine that a data loss appears in the ECGs which are recorded. This could

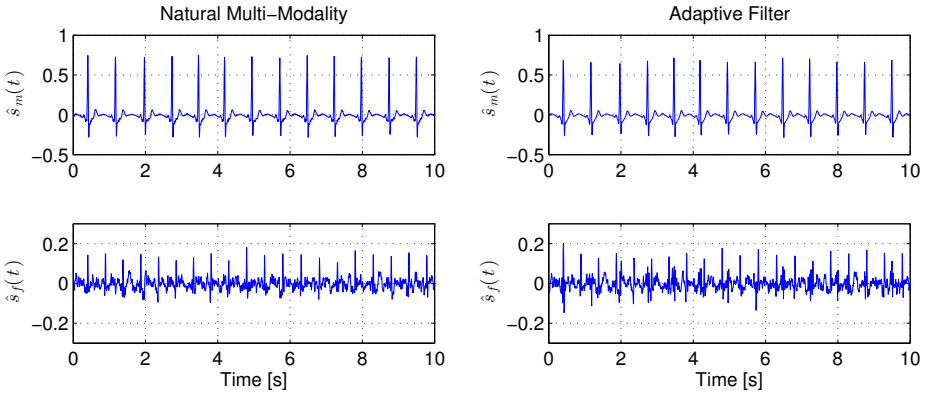

(a) Extraction of mECG and fECG using only the full thoracic maternal reference.

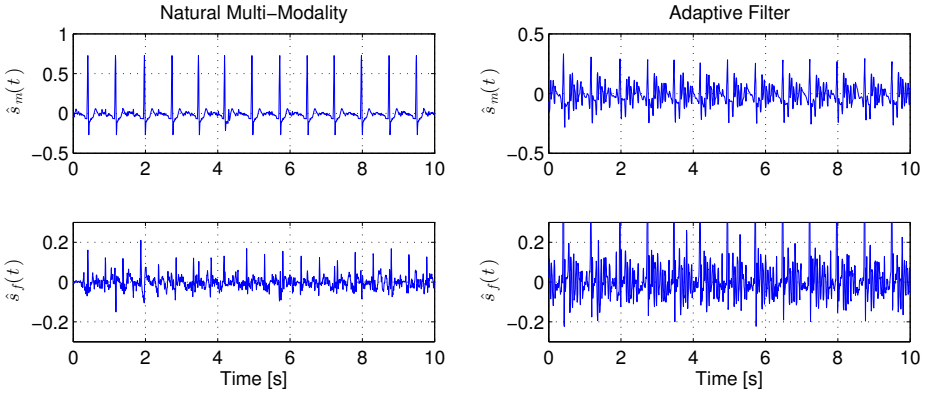

(b) Extraction of mECG and fECG using only the 1-bit thoracic maternal reference.

Figure 6.9: Comparison of the extraction using GP and adaptive filter.

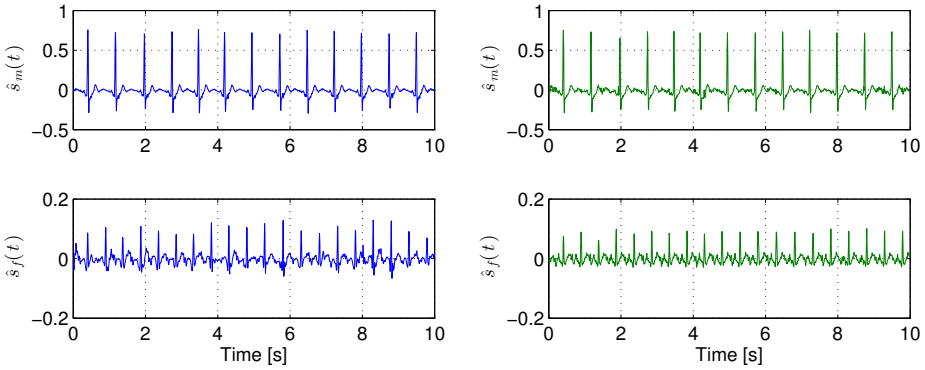

Figure 6.10: Estimation of mECG and fECG from the real data using full and 1-bit references by natural multi-modality. The signals in blue are the estimations using the full references and the ones in green are the estimation using 1-bit references.

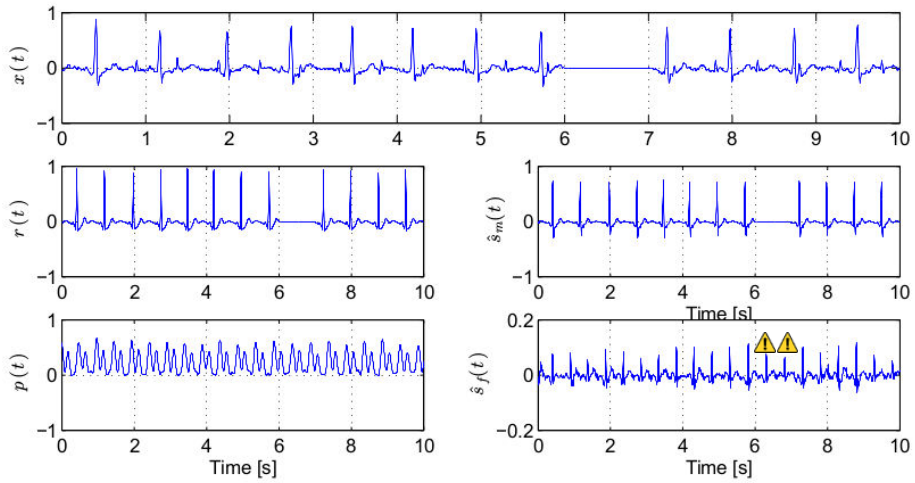

Figure 6.11: Estimation of mECG and fECG from the data by natural multi-modality in the presence of data loss. The warning flags on the detected beats of the fECG, represents the data loss of the observation.

appear in the abdominal and/or thoracic ECG as shown in Fig. 6.11, and it is seen that the method still detects the fECG according to the model obtained from the reference signal (fPCG). Therefore, the estimated signal is only based on the model although there is no observation signal. The reference modality is actually telling the system that the fetal activity is still present according to the presence of fPCG. Thus, along with the two beats detected based on the model, a warning is also displayed, meaning that the estimation is done only based on one modality.

Having proposed the hyperparameter estimation method in Section 4.2.3, we will show the precision of R-peak detection by considering them as hyperparameters of the model. We have first recorded one channel of abdominal ECG from a pregnant woman with a sampling frequency of 4kHz leading to a ground truth of $250\mu s$. This means that the original R-peaks detected from this signal are considered as the reference R-peaks. The large number of samples of this signal makes the method very time-consuming; as a result, we reduce the number of samples by a factor of 50 (after filtering with a low-pass filter with 40 cut-off frequency) so that the new signal have the sampling frequency of 80Hz. The R-peaks of this new down-sampled signal is detected manually and are compared to the original R-peaks in the original signal. The mean of the error is seconds and a confidence interval with the level of 99%, is shown in Figure 6.12 by black bars. This new down-sampled signal is then modeled by GP using the periodic covariance function as the summation of maternal ECG, the fetal ECG, and the noise. Both maternal and fetal R-peaks are assumed to be unknown and are then estimated as the hyperparameters of the method. The error of

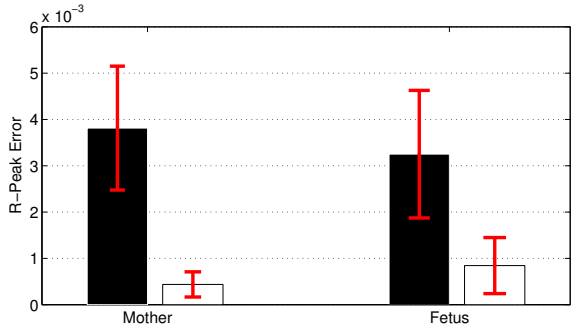

Figure 6.12: R-peak detection precision. The white bar shows the error of detected R-peaks of the down-sampled signal by maximizing posterior, and the black bar is the R-peak error with manual detection.

the estimated R-peaks, knowing the original signal's R-peaks as the reference, is shown in white bars in the same Figure (Fig. 6.12). It is clear that the method can precisely detect the R-peaks of both maternal and fetal ECGs even using the down-sampled signal. As mentioned before, considering R-peaks as the hyperparameters of the GP model can avoid the need of the prior knowledge about the data and can automatically detect the R-peak instances. Having the mentioned results, this method can also be useful in decreasing the computational cost of the GP by down-sampling the signal and detecting the precise location of R-peaks (even between data samples) on the new signal automatically. The original signal can then be restored without loss of information. With the same reasoning, this method can be advantageous when there is a data loss in the signal.

Next, the fHR from a signal in about one minute is calculated. Here, the estimation of fECG, $\hat{s}_f(t)$, is based on the natural multi-modal joint approach using 2 references: the 1-bit maternal thoracic ECG and a 1-bit fetal ePCG. The fetal R-peaks are then extracted from the $\hat{s}_f(t)$ signal and the fHR is then calculated in beats per minute as the following (considering that R fetal peaks are detected):

$$\frac{60}{\tau_i^f - \tau_{i-1}^f}, \; 2 \leq i \leq R, \tag{6.1}$$

where τ_i^f is the i^{th} detected fetal R-peak. The detected fHR is then depicted in Fig. 6.13. The depicted result is the fHR calculated at every fetal R-peak and is therefore the instantaneous result of fHR. The fHR detected from the noninvasive ECG could be validated with the data recorded from CTG.

A word should also be told about the detected morphology from the signal. This has never been analyzed yet by the healthcare specialists since there was no access to such kind of information during pregnancy. Here, although the detected fetal beats could be almost noisy, their average over several beats shows the shape form of an ECG beat whose

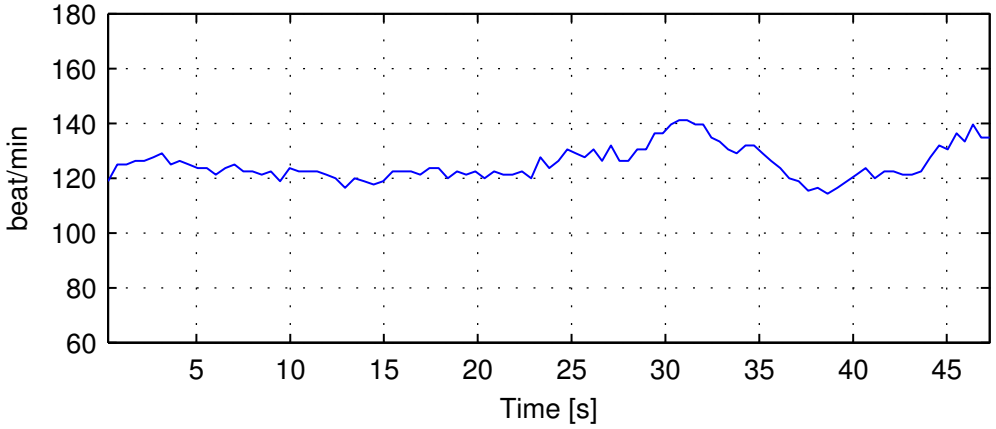

Figure 6.13: Calculation of fHR from the detected fECG from the real data by natural multi-modality.

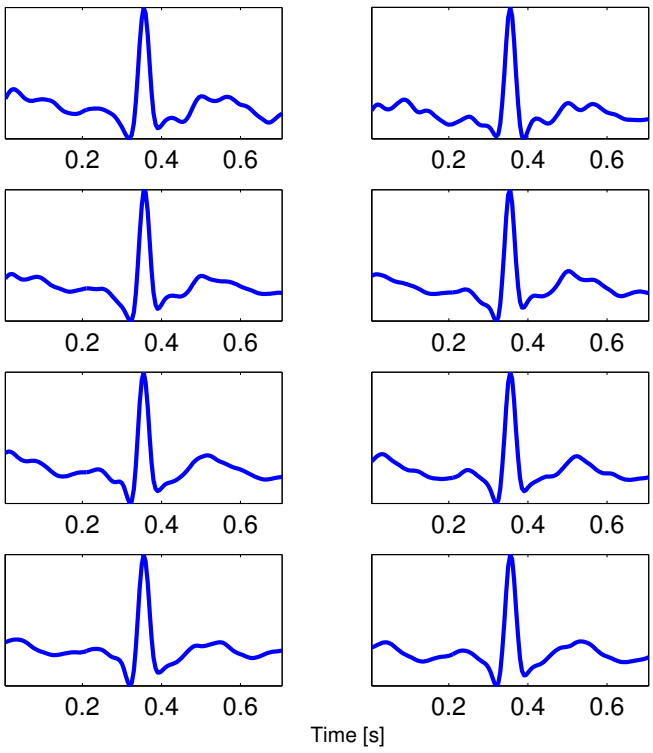

Figure 6.14: Estimated fetal ECG beats by natural multi-modality averaged every 4 beats.

correctness and precision should be validated according to a ground truth (like fetal scalp ECG) or by the clinicians of the field. The average over every 4 beats is enough to have a smooth shape of the beats. This is illustrated in Fig. 6.14.

6.5 Closing Remarks

In this chapter, the data which is recorded through preliminary experiments were discussed, and the parameters which affect the quality of signals are studied. The data were recorded from pregnant women in different months of pregnancy with one mECG channel and one mPCG. The abdominal data, however, is recorded through a number of channels whose optimization is not in the scope of this study. The observations about the factors which influence the recordings are explained in order that they can be used in further studies as initial standard for data registration. The intention is not to introduce a protocol in data recording but to collect some synchronous ECG and PCG data and examine our observations through the experiments, and also to finally apply the method (which has already been tested on the synthetic data) on the real data. The experiments provide us with signals from a pregnant subject in 9 month of pregnancy and the proposed method yields good results from this data. In order to propose a faithful protocol, subjects in great number are required along with more experimental designs with different parameters. This, however, is out of the scope of our study.

The results obtained by the multi-modal approach showed that this method can provide the clinicians with the information about both the fHR and the morphology of the ECG. Moreover, the multi-modal approach is proven to be more practical than the adaptive filter, which also employs a reference signal. This is due to the nonlinear estimation of GP in the natural multi-modal approach. The models which are calculated, for the mECG and fECG in the mixture, are also helpful in producing results even if there is a data loss in the abdominal observation signal, or the lack of any one of the modalities. The reason behind this fact is that these models are based on another data modalities (or another data channels in the case of maternal ECG model) which are bringing extra (and different) information beside the information obtained by the abdominal ECG channel.

Conclusion and Perspectives

This research studied the extraction of fECG signal, through recordings which are recorded noninvasively from the mother's abdomen. With regard to the limitations of the conventional technologies, like CTG or *invasive* fECG, it was argued that *noninvasive* fECG could be an appropriate replacement to detect fetal heart rate, and could also bring information to specialists about the morphology of the fECG beats. However, the extraction of noninvasive fECG is still a challenge of research. The study introduced a multi-modal approach using two cardiac signals: ECG (the electrical activity of the heart) and PCG (the mechanical activity of the heart). Multi-modality would then benefit from the complementary information that these signal provide about the heart function. Here, multi-modality is employed based on the Gaussian process model, while it could be applied on any of the existing methods. Gaussian process is a nonlinear estimation approach with few assumptions and little prior information about the desired signal. The implementation issues of such technology is equally important, and thus some of the practical aspects in realizing such device were considered in the proposed approach.

One of the main issues in this research is the prior knowledge that many of the previous methods consider about the R-peaks of the maternal and/or fetal ECGs, while this information is an essential one that the clinicians need to extract. For this purpose, first, an automatic solution was presented in Section 4.2.3 which estimated the R-peaks by modeling the desired signals as Gaussian processes in a uni-modal framework, and using maximum a posteriori estimation to detect the R-peaks. Second, the concept of multi-modality was presented, whose intention is making use of another signal modality to complete the information that can be obtained from the ECG signal. PCG, the audio signal produced by heart valves, is considered as the reference modality, because it has a different nature from ECG, and is contaminated by other kinds of noise. That is why, it can provide complementary information in modeling the fECG signal.

To this end, two approaches called partial multi-modality (Section 4.3) and natural multi-modality (Section 4.4) were introduced. The former is a solution to detect the R-peaks and is followed by a uni-modal method on ECG signals. The latter is a more natural way to consider the second modality as the input of the Gaussian process. It is worth

noting that the methods are not only applicable on ECG, but they can be used to model any quasi-periodic signal, since this class of signals shares common properties which were discussed and modeled using Gaussian process. The methods can also be applied on other kinds of signals as long as there is a reference modality. For instance, in [Noorzadeh et al., 2015a], the eye movement artifact is modeled and removed from EEG, considering the Gaze signal as the reference modality.

The performance achieved by the proposed methods was first assessed by simulation experiments. Then, the method was applied on the actual data which has been recorded during this thesis. Although the experiments are preliminary ones, they allowed us to achieve some high quality signals in the last month of pregnancy. This can be a good model for the intrapartum period of pregnancy regarding the fact that the fetus' position is almost stabilized. Through the experiments, several factors which can affect the quality of ECG and PCG data recordings, are also studied (Chapter 6).

The obtained results showed that the maximization of posterior function would give precise detection of R-peaks. Thus, by using this method, there is no need for knowing the R-peaks in advance. As the results showed, this method can be useful in applications where the observation signal is very noisy; moreover, its ability to detect R-peaks between data samples would be efficient even if there is a data loss in the observation, for example, when the peaks of QRS waveforms are cut off due to the saturation in amplifier which is caused by high electrode offset voltage, or improperly calibrated amplifiers. However, this method is very time consuming considering all the R-peaks as the parameters which should be estimated. The multi-modal approach performs better regarding the time complexity. Natural multi-modality is preferred to partial multi-modality when the two modalities are not completely synchronized, the case which happens in many of the multi-modal data as in the ECG and PCG. This former method gives a good estimation of the fetal R-peaks and the fetal heart rate. Moreover, it provides us with the morphology of the fetal beats. Besides, this method requires one reference signal for any signala which we intend to model. Consequently, it requires one reference for the maternal ECG and one for the fetal ECG, and, along with the observation channel, it needs at least three channels of data. However, the reference modalities can be replaced by 1-bit signals without losing much performance. In this way, the data takes less memory compared to the full-bit signals used nowadays (usually more that 16 bits), and the implementation of the final device would be more practical (considering the integration or power consumption) with cheap sensors or 1-bit ADCs (analog to digital converters).

The thesis considers the signal processing aspects and also some of the experimental ones through the chapters, which are schematically shown in the figure depicted on top of the next page. This schema also shows the type of results used to validate any of the

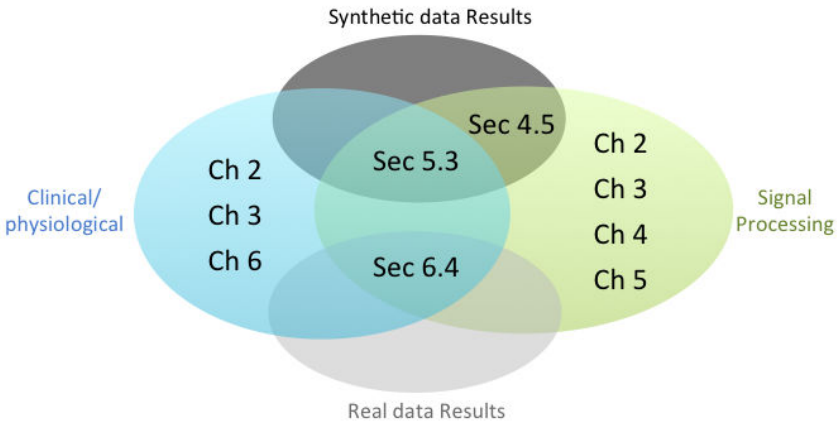

Schema of the chapters regarding their signal processing or clinical/experimental aspects and the results they contain.

mentioned aspects. The results were shown to provide necessary information to the clinical demands (as in fetal heart rate), and this information is proven to be possible to extract from noninvasive ECG data.

Future Work

Further study of the issue would be of interest in several aspects.

Regarding the Gaussian process modeling, as mentioned, one of the limitations is that their direct implementation is computationally demanding, since the size of the covariance functions depends directly on the size of the data, and that makes the prediction computationally complex (to calculate the term $K^{-1}\boldsymbol{x}$ in equation (4.13)). Moreover, the long-term efficient monitoring device requires the online processing of the data. Therefore, one of the future work will involve the implementation of algorithms to reduce the mentioned complexity and equally important online Gaussian process can be developed [Liu et al., 2011, Gao et al., 2014]. Afterwards, the Metropolis-Hasting's algorithm used in this study to estimate the hyperparameters does not use the derivative information available and it may have an inefficient random-walk behavior in the hyperparameter-space, so another solution is to utilize the Hybrid Monte Carlo method [Duane et al., 1987, Williams and Rasmussen, 1996] to sample the posterior.

Moreover, the concept of multi-modality is presented in this study, and its functionality is tested on the GP method. However, multi-modality could be based on any of the state-of-the-art approaches, like ICA or IVA methods, adaptive filter, Kalman filter, etc. As mentioned in Chapter 2 many researches have tried to combine different approaches to achieve better performances. Multi-modality can also be used with several different approaches, since it can provide extra information about the fECG, which might increase

the performance. Or from a clinical aspect, each of the methods might be appropriate for different gestational months regarding the clinical needs or the fetal position. Another aspect, which can be considered, is the employment of other cardiac references, as the second modality. Here the PCG signal is employed while, this modality could be the data coming from other fetal heart monitoring tools described in Chapter 2.

Optimizing the number of sensors, is another aspect which can be taken into account as the future work. In the natural multi-modal method, a single reference signal is said to be required to model the desired signal. In this thesis, the PCG reference is tested in the ninth month when fetus has minimum changes in the position, while this changing can possibly cause some problems in the earlier months. Optimizing the number of reference channels (or even the observation channels) may increase the robustness of the method. As an example, PCG signal (as the reference) may be lost when the fetus moves, or when the fetal heart is very small (in early months of pregnancy). In this case, the simultaneous use of several reference channels might prevent the method to fail or lose its efficiency.

From the experimental aspect, clearly, further research will be required in the data recording. This task can be done on bigger number of subjects, in order that the change of the recording factors could be validated from a clinical aspect and also could be validated with the method.

In a further step, the data recording can be done with synchronization to the fHR from CTG, so that he fHR obtained by this method could be compared to that of the CTG as a ground truth. It would be highly beneficial if the data from the fetal scalp could also be recorded at the labor synchronized with the multi-modal data we need. In this case a better comparison between the morphology obtained by the method and the fetal scalp electrode could be done.

A Time-Varying Covariance Function for ECG

As stated before, this covariance function first models the wave-form of the ECG by modeling each beat separately. Thereby, a possible non-stationary covariance function that suits ECG beats is proposed as follows [Rivet et al., 2012]:

$$k_b(t,t';\boldsymbol{\theta}_1) \quad = \quad \sigma(t)\sigma(t')\sqrt{\frac{2l_d(t)l_d(t')}{l_d(t)^2+l_d(t')^2}} \quad \times \quad \exp\left(-\frac{\left(t-t'\right)^2}{l_d(t)^2+l_d(t')^2}\right), \quad \text{(A.1)}$$

with

$$\sigma(t) = a_m + (a_M - a_m)\exp\left(-\frac{(t-t_0)^2}{2\sigma_T^2}\right), \quad \text{(A.2)}$$

$$l_d(t) = l_M - (l_M - l_m)\exp\left(-\frac{(t-t_0)^2}{2\sigma_l^2}\right), \quad \text{(A.3)}$$

where $\boldsymbol{\theta}_1$ is a set of hyperparameters defined as $\boldsymbol{\theta}_1 = \{a_m, a_M, \sigma_T, l_m, l_M, \sigma_l\}$ and $\sigma(t)$ and $l_d(t)$ allow to have a time-varying amplitude (between a_m and a_M) and a time-varying length scale (between l_m and l_M), respectively.

Figure A.1 shows two functions drawn at random from the zero-mean GP prior with covariance function in (A.1). This figure illustrates the flexibility of such representation, since with the same prior, $\mathcal{GP}(0, k(t,t'))$, it can generate a multitude of different shapes. Finally, in order to model the quasi-periodicity, the full ECG is modeled as the succession of beats and is thus also a Gaussian process, whose covariance function is given by:

$$k_1\big(t,t';\widetilde{\boldsymbol{\theta}}_1\big) = \sum_{n=1}^{N}\sum_{n'=1}^{N} k_b\big(t-\tau_n, t'-\tau_{n'}\big), \quad \text{(A.4)}$$

where $\widetilde{\boldsymbol{\theta}}_{\mathbf{1}} = \big\{\boldsymbol{\theta}_1, \{\tau_n\}\big\}$, and $\{\tau_n\}_{1\leq n\leq N}$ is the set of R-peak instants that has to be detected from the mixture.

Although the proposed method based on the covariance function in (A.4) has been shown to be efficient for ECG denoising and fetal ECG extraction, it suffers from several drawbacks. Indeed, it requires many hyperparameters to fit well the characteristics of an

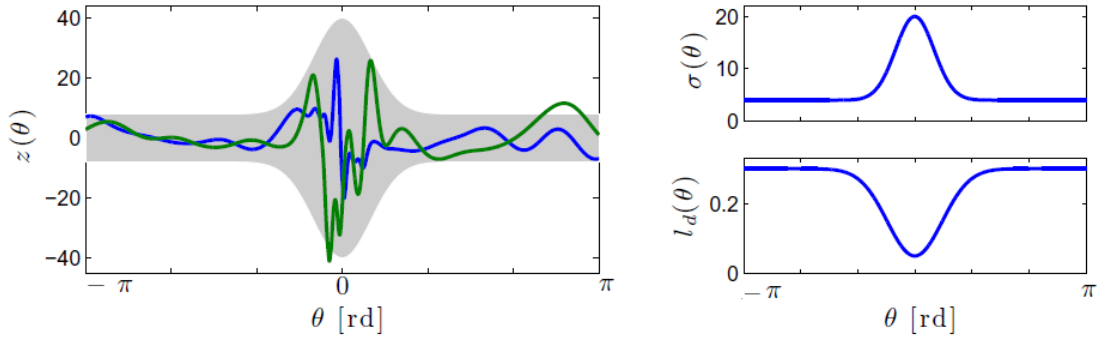

Figure A.1: Two functions drawn at random from a zero-mean GP with time-varying covariance function in equation (A.1). The shaded area represents plus and minus two times the standard deviation of the prior. On the right, the corresponding $\sigma(\theta)$ and $l_d(\theta)$ functions. Figure taken from [Rivet et al., 2012]

ECG beat. For each ECG, a_m, a_M and σ_T form a time-varying amplitude, $\sigma(t)$, and l_m, l_M and σ_l form a time-varying length scale, $l_d(t)$, in (A.2) and (A.3), respectively. This thus leads to a quite complicated model and therefore it is tricky to optimize all the hyperparameters. Moreover, from a computational point of view, the double summation in (A.4) is quite CPU intensive.

B Résumé en Francais

B.1 Introduction

Le bien-être du fœtus doit être soigneusement contrôlé pendant la grossesse et aussi pendant le travail [Meathrel et al., 1995]. En effet, la procédure de surveillance du fœtus permet aux cliniciens d'évaluer la santé du fœtus, de détecter les problèmes fœtaux précocément, et de fournir un traitement approprié [Patterns, 1999, Meathrel et al., 1995]. Une surveillance efficace d'un fœtus nécessite une évaluation continue et est généralement réalisée en utilisant la technologie électronique. Cependant, le nombre de bébés nés avec des malformations cardiaques congénitales a remis en question la validité des techniques de surveillance présentes dans l'identification des fœtus à risque. L'une des principales intentions des soins de santé est de réduire le nombre de bébés nés avec une maladie, et la technologie peut offrir le meilleur à cet égard par le développement d'outils pour la surveillance.

Aujourd'hui, ce qui intéresse les cliniciens est la surveillance précise du rythme cardiaque fœtal (RCF) dit aussi fHR (fetal Heart Rate). La cardiotocographie (CTG), une technique non invasive, est largement utilisée dans les hôpitaux pour mesurer le RCF, et elle est considérée fiable. Toutefois, elle ne convient pas pour la surveillance à long terme, et elle peut aussi entraîner des erreurs dans la détection du RCF ou la perte de ces informations. Pour une patiente avec un foetus à risque, cette perte de signal peut être dangereuse. En outre, la surveillance cardiaque fœtal peut être plus difficile avec la CTG dans certaines catégories de patientes, comme les mères très obèses ou celles avec des arythmies fœtales [Ross and Beall, 2014]. Ces difficultés peuvent exiger des cliniciens d'utiliser un contrôle invasif lorsque la CTG est insatisfaisante chez une patiente pendant le travail. La surveillance ECG invasive utilise une électrode de "scalp" pour donner non seulement une mesure du RCF, mais aussi quelques-unes des caractéristiques relatives à la morphologie de l'ECG foetal (fECG). La surveillance fœtale non invasive est sans danger, et vise à estimer le RCF et la morphologie fECG pendant la grossesse et pendant l'accouchement.

Le traitement de l'ECG non invasif, qui est enregistré à partir de la surface de l'abdomen, a déjà été abordé par un grand nombre de recherches. Le problème principal est que le

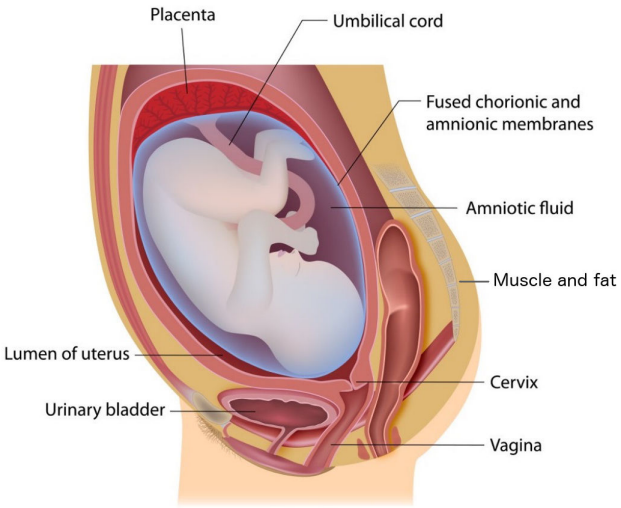

Figure B.1: L'anatomie de l'abdomen d'une femme enceinte.

signal électrique, obtenu grâce aux électrodes de surface abdominales, ne contient pas uniquement les signaux fECG. Le rapport signal sur bruit (RSB) de l'ECG abdominal du fœtus est généralement très faible pour plusieurs raisons:

- l'ECG maternel qui est enregistré à partir d'électrodes de surface abdominales a un amplitude beaucoup plus grande que le fECG.
- Le bruit électrique d'électromyographie (EMG) dû aux activités musculaires maternelles ou fœtales.
- Le cœur du foetus est très petit et le fœtus est entouré par l'amnios et le liquide amniotique qui rend l'examen du foetus très difficile [Greenberg et al., 2004]. Une anatomie simplifiée peut être vue à la figure B.1.
- Le positionnement correct des électrodes abdominaux est l'un des points critiques à cet égard [Vigneron et al., 2005].

Compte tenu de toutes ces contraintes, l'extraction des signaux fECG non invasive est un problème difficile qui nécessite des techniques complexes de traitement de signaux. Des études antérieures ont utilisé différentes approches qui sont basées sur des techniques uni-modales. Cependant, jusqu'à maintenant, il n'y a pas de solution fiable à ce problème.

Dans cette thèse, le traitement du signal et les aspects expérimentaux de l'extraction de fECG non invasive sont étudiés. La contribution principale de l'aspect de traitement du signal, utilise un cadre multi-modal dans ce contexte. La multi-modalité est employée pour bénéficier de l'information complémentaire et redondante que deux modalités de signaux peuvent fournir. Ces deux modalités, qui seront utilisés dans cette étude, sont l'électrocardiogramme (ECG) et le phonocardiogramme (PCG). La multi-modalité est proposée non seulement pour augmenter la robustesse de la méthode, mais aussi pour résoudre

le problème de trouver des indices de battement. L'objectif principal est donc de généraliser les méthodes existantes dans un contexte multi-modal. Dans cette étude, la multi-modalité est basée sur la modélisation des processus gaussiens.

Les méthodes sont ensuite testées sur les données synthétiques pour estimer le RCF et aussi la morphologie de fECG. Il est également nécessaire d'appliquer les méthodes sur les données réelles pour que le fonctionnement du procédé soit évalué. L'absence d'une base de données existante de l'ECG et de données synchrones PCG nous oblige à enregistrer notre propre ensemble de données.

Dans ce qui suit, les méthodes précédentes, qui sont étudiées sur le problème de l'extraction de l'ECG foetal, sont présentées et leurs limites sont discutées à la Section B.2. A la Section B.3 les modalités de signaux cardiaques, utilisées dans cette étude, sont présentées. A la Section B.4, la méthode de processus gaussien est présentée et elle est utilisée pour modéliser les signaux quasi-périodiques basées sur des approches uni-modales et multimodales. Ces méthodes sont utilisées pour extraire l'ECG foetal à partir des signaux d'ECG abdominal, et les résultats sur des données simulées et réelles sont enfin illustrées à la Section B.5. A la Section B.6, les conclusions et les travaux futurs finissent le document.

B.2 État de l'art

L'état de l'art pour l'extraction des signaux cardiaques fœtaux peut être étudié sous deux aspects : les outils cliniques existants, et les méthodes de traitement de signaux qui sont développées pour l'analyse numérique des données enregistrées.

Les Outils Cliniques

Le premier dispositif pour examiner l'état de santé de la fonction cardiaque fœtale était le **stéthoscope fœtal (Pinard)** [Steer, 2008]. Cependant, le développement de la technologie a apporté les systèmes électroniques pour surveiller la santé cardiaque fœtal.

La technique clinique le plus largement utilisé pour surveiller le rythme cardiaque fœtal (RCF) est la **cardiotocographie (CTG)** [Alfirevic et al., 2006]. Ce dispositif est non invasif et fonctionne à base d'ultrasons. La CTG est la méthode la plus couramment utilisée aujourd'hui; cependant, elle peut parfois causer une confusion de rythmes cardiaques maternel et fœtal dans la période intra-partum. En outre, elle ne convient pas pour la surveillance à long terme car il est sensible aux mouvements. De plus, l'exposition du fœtus aux ondes échographiques peut être dangereux [Ibrahimy et al., 2003, Kieler et al., 2002, Barnett and Maulik, 2001]. L'**échocardiographie** fœtale est une échographie de diagnostique également basée sur les ultrasons [Fetal et al., 2011]. La **magnétocardio-**

graphie fœtale est un autre outil non invasif qui mesure le champ magnétique provoqué par l'activité électrique du cœur fœtal [Janjarasjitt, 2006]. Une autre méthode non invasive utilise la **phonocardiographie** fœtale qui peut fournir des informations cliniques significatives sur le cœur du fœtus. Ce signal peut être enregistré en plaçant un petit capteur acoustique sur l'abdomen de la mère [Varady et al., 2003, Kovács et al., 2000]. L'**Électrocardiogramme** fœtal (fECG) est un autre signal qui peut être enregistré de deux façons différentes: *invasive*, en plaçant les électrodes à l'intérieur de l'utérus de la mère, ou *non invasive* [Holls and Horner, 1994]. L'ECG invasif est enregistré seulement dans la période intra-partum et généralement pendant l'accouchement [Hasan et al., 2009] quand il y a un risque pendant l'accouchement.

Traitement du Signal

Malgré les améliorations technologiques, l'extraction de l'ECG foetal à partir d'enregistrements abdominaux est encore un problème difficile qui est abordé par un grand nombre d'études. Une recherche des méthodes existantes a été faite par [Sameni and Clifford, 2010]. Ces études sont effectuées soit pour estimer le RCF, soit pour extraire la morphologie du fECG. Ces techniques peuvent être classées en méthodes uni ou multi modales.

Le **filtrage classique** est une approche basique pour gérer ce problème [Van Bemmel and Van der Weide, 1966]. Parce que le fECG est superposé avec le bruit existant dans l'enregistrement abdominal dans les domaines temporel et de fréquence, ces filtres ne peuvent pas être très efficaces. D'autres chercheurs ont utilisé des **filtres spatiaux** basés sur le fait que les sources de l'ECG maternel et fœtal sont séparés dans l'espace [Bergveld and Meijer, 1981, Vanderschoot et al., 1987, Chen et al., 2001]. Ils utilisent un certain nombre d'électrodes, pour trouver une combinaison linéaire entre les observations, et déterminer les meilleurs coefficients pour modéliser une somme pondérée de ces signaux d'observation. Le **filtre adaptatif** a également été appliqué avec succès sur le problème de l'extraction de l'ECG foetal [Widrow et al., 1975]. Ce filtre est basé sur l'adaptation des coefficients d'un filtre linéaire avec plusieurs itérations afin d'estimer l'ECG maternel dans l'abdomen, en utilisant des signaux de référence. Ce signal est supprimé pour obtenir l'ECG foetal [Ferrara and Widraw, 1982, Thakor and Zhu, 1991]. Le schéma de ce filtre est représenté à la Fig. B.2. Les filtres adaptatifs peuvent être sensibles à la forme temporelle du signal de référence particulièrement si seulement une référence est utilisée; par conséquent, il exige normalement des signaux de référence multiples [Sameni, 2008, Widrow et al., 1975].

Les techniques de décomposition sont également populaires parmi les techniques qui sont utilisées. La **décomposition en valeurs singulières** (SVD) est l'une de ces méthodes qui sont utilisées pour extraire les composantes materneles et fœtales dans les enreg-

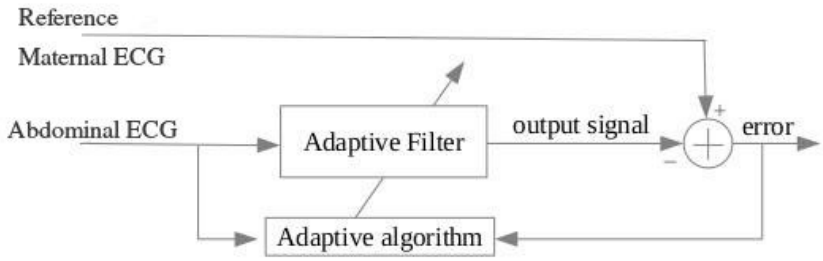

Figure B.2: Schéma de filtrage adaptatif pour l'extraction fECG.

istrements abdominaux [Vanderschoot et al., 1987, Callaerts et al., 1990, Ayat et al., 2008]. En utilisant les techniques qui incluent la décomposition ou la reconstruction de sous-espace, certaines études ont enlevé la composante maternelle [Fatemi et al., 2013, Maier and Dickhaus, 2013]. Dans [Niknazar et al., 2013b], les battements maternels sont identifiés et empilés dans un tenseur tridimensionnel. L'ECG maternel est ensuite reconstruit et soustrait en utilisant une **décomposition tensorielle**. Certaines études ont formulé l'extraction fECG comme un problème de séparation aveugle de sources (SAS) [Comon and Jutten, 2010]. La SAS est basée sur l'hypothèse que les enregistrements d'ECG abdominaux sont constitués de composantes indépendantes. Dans ce cadre, les enregistrements abdominaux sont formulés comme des mélanges instantanés de sources ECG maternelle et fœtale [Zarzoso et al., 1997]. Les deux approches principales qui existent à cet égard sont l'Analyse en Composantes Principales (ACP) [Di Maria et al., 2014, Castells et al., 2007] et l'analyse en composantes indépendantes (ICA) [Cardoso, 1998]. L'ICA est comparée à l'APC et a démontré avoir de meilleures performances [De Lathauwer et al., 1995, Bacharakis et al., 1996]. Cette méthode est aussi comparée aux filtres adaptatifs dans [Zarzoso and Nandi, 2001]. Dans une étude plus récente, une autre version améliorée de l'ICA est utilisée par une méthode d'analyse en composantes périodiques qui bénéficie de la périodicité du signal ECG [Sameni et al., 2008]. Dans ce travail, une mesure de périodicité est définie et maximisée. Afin de traiter l'ECG quasi-périodique comme un signal périodique, ils ont utilisé une fonction pour définir les instants de temps de chaque battement avec une phase comprise entre $[-\pi, \pi]$ fixant les pics R à 0 . Le **transformée en ondelettes** (WT) est une autre approche qui a été proposée pour ce problème. Différentes techniques pour l'élimination et / ou la détection de formes d'ondes fœtales ont été utilisées. Ces techniques impliquent les ondelettes Gabor-8 et la théorie de l'exposant de Lipschitz [Mochimaru et al., 2002], l'ondelette "bi-orthogonal quadratique spline" et la théorie "modulus maxima" [Khamene and Negahdaripour, 2000] et les ondelettes continues complexes [Karvounis et al., 2004]. Le **filtre de Kalman** est un cadre utilisé dans plusieurs applications biomédicales. [Sameni et al., 2005] a utilisé cette technique dans la

première étude pour l'extraction fECG en utilisant un seul canal ECG abdominal. Ceci est basé sur un modèle dynamique qui est obtenu avec le modèle d'électrocardiogramme décrit dans [McSharry et al., 2003]. Il y a d'autres recherches qui ont utilisé la fusion de deux ou plusieurs méthodes pour obtenir de meilleurs résultats de performance [Behar et al., 2014b].

Cependant, malgré le grand nombre d'études à ce sujet, il n'y a pas encore une solution commune à mettre en œuvre comme un outil clinique. Cela peut être dû à plusieurs facteurs:

- Certains des composants fECG sont manquants dans l'extraction,
- La méthode est sensible à la forme temporelle des données et aux emplacements d'électrodes,
- Le manque de précision dans la détection fHR et / ou l'estimation de la forme d'onde du fECG,
- Le coût de calcul des algorithmes,
- L'absence d'une approche commune pour enregistrer les signaux, pour être utilisé dans toutes les méthodes.

D'autre part, toutes les recherches mentionnées sont faites pour étudier le fECG et le fPCG séparément. Chacune de ces modalités a ses propres limites et avantages et la fusion de l'information de ces modalités peut être utilisée dans un contexte multi-modal. La méthode multi-modale qui est présenté dans cette étude est basée sur le modèle de processus gaussien [Rivet et al., 2012, Niknazar et al., 2012]. La méthode est une approche non linéaire et elle est un outil flexible pour modéliser les statistiques du mélange. Ce modèle sera décrit dans les sections suivantes.

B.3 Une étude sur les modalités

Les informations que nous pouvons obtenir sur le cœur peuvent être de différentes natures. Les deux types d'informations qui nous intéressent sont l'ECG et le PCG. Bien que ces deux signaux soient originaires d'un même organe du corps (le cœur), ils transportent des informations différentes. L'ECG montre la propagation de l'impulsion électrique à travers les muscles cardiaques et il est donc une représentation de l'activité électrique du coeur, tandis que le PCG est l'enregistrement des sons émis par le coeur, et il est donc une donnée qui démontre l'activité mécanique du coeur. Afin de clarifier le cadre de la multi-modalité, chacun de ces signaux est d'abord analysé. Après cette brève description, les signaux sont

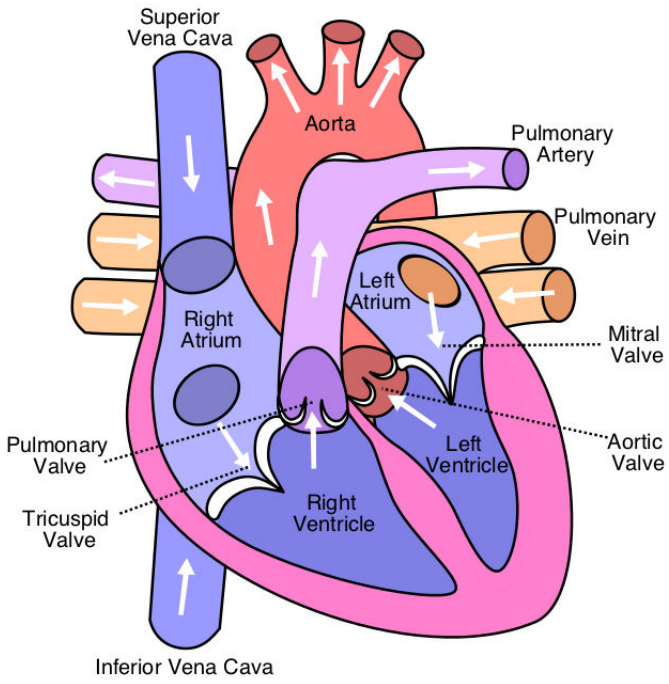

Figure B.3: L'anatomie du cœur. Les éclairs blancs indiquent les directions de la circulation sanguine.

analysés mathématiquement et leurs relations sont abordées du point de vue du traitement du signal.

La Partie physiologique

Le coeur est en fait un muscle dont la fonction principale est de pomper le sang dans le système circulatoire. Il se compose de quatre chambres (voir Fig. B.3) : 2 oreillettes et 2 ventricules. Le cœur est ainsi divisé en deux systèmes de pompage séparées [Moran, 2015] :

- Le côté droit dans lequel le sang entre en arrivant à l'oreillette droite, puis il traverse le ventricule droit. Le ventricule droit pompe du sang vers les poumons où il devient oxygénée.

- La partie gauche dans laquelle le sang oxygéné est amené dans l'oreillette gauche par les veines pulmonaires. Le sang circule ensuite dans le ventricule gauche après l'oreillette gauche. Le ventricule gauche pompe le sang dans l'aorte qui distribuera le sang oxygéné à toutes les parties du corps.

Un même phénomène peut être capturé par des capteurs différents, et les données qui sont obtenues par chaque capteur sont appelées une modalité. Les modalités peuvent être de différents types et dimensions. La multi-modalité est désignée comme le cadre dans

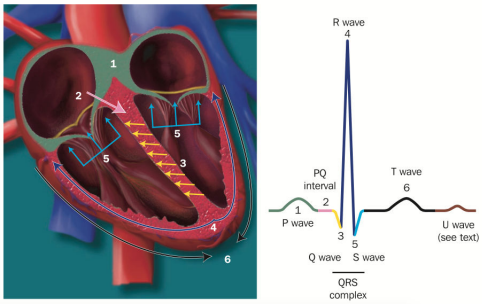

(a) la simulation d'un batement PQRS ([Khan, 2004])

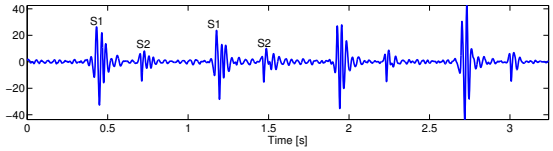

(b) le signal PCG et les deux son S1 et S2

Figure B.4: Les signaux ECG et PCG et leurs origines physiologiques

lequel plusieurs modalités sont utilisées ensemble pour expliquer ou décrire un phénomène, ou pour décrire la relation entre les modalités. Les applications dans lesquelles la multi-modalité est utilisée peut être différente. Par la multi-modalité, nous sommes intéressés à faire une composition dans laquelle certains types d'informations d'un même phénomène sont réunies d'une manière particulière qui illustre le mieux ce que nous voulons décrire. Quelques exemples connus de multi-modalité sont l'utilisation de l'EEG (électroencéphalogramme) et l'IRMf [Laufs, 2012] ou la fusion de différentes données biométriques pour des résultats plus précis [Patil, 2012].

Le PCG et l'ECG sont les deux signaux provenant du même organes physiologique, le coeur, et fournissent des informations complémentaires et redondants à ce sujet. Ces modalités cardiaques sont enregistrées de façon non invasive; l'activité électrique du cœur est enregistrée au moyen d'électrodes comme le signal de l'ECG, et les sons cardiaques, appelées PCG, sont capturés par des microphones. Le signal PCG est d'intérêt parce que le type de bruit qui affecte le PCG est différent de l'ECG. Ce fait rend le signal de PCG plus facile à traiter comme une modalité de référence. La relation physiologique entre l'ECG et le PCG est expliquée ici (Regardez Fig. B.4).

Quand le signal, généré par le nœud SA, se propage à travers le muscle auriculaire, les oreillettes réagissent en se contractant (onde P). À ce moment, les ventricules sont relaxé et les valves auriculo-ventriculaires sont ouvertes et les semilunars sont fermées. Les ventricules se remplissent de sang, et se préparent pour l'éjection. Le nœud AV reçoit le signal et après un délai court, il envoie le signal vers le système de conduction auriculo-ventriculaire et vers les ventricules, en les encourageant à se contracter (complexe QRS). Lorsque les ventricules se contractent, la pression ventriculaire augmente au-dessus de la

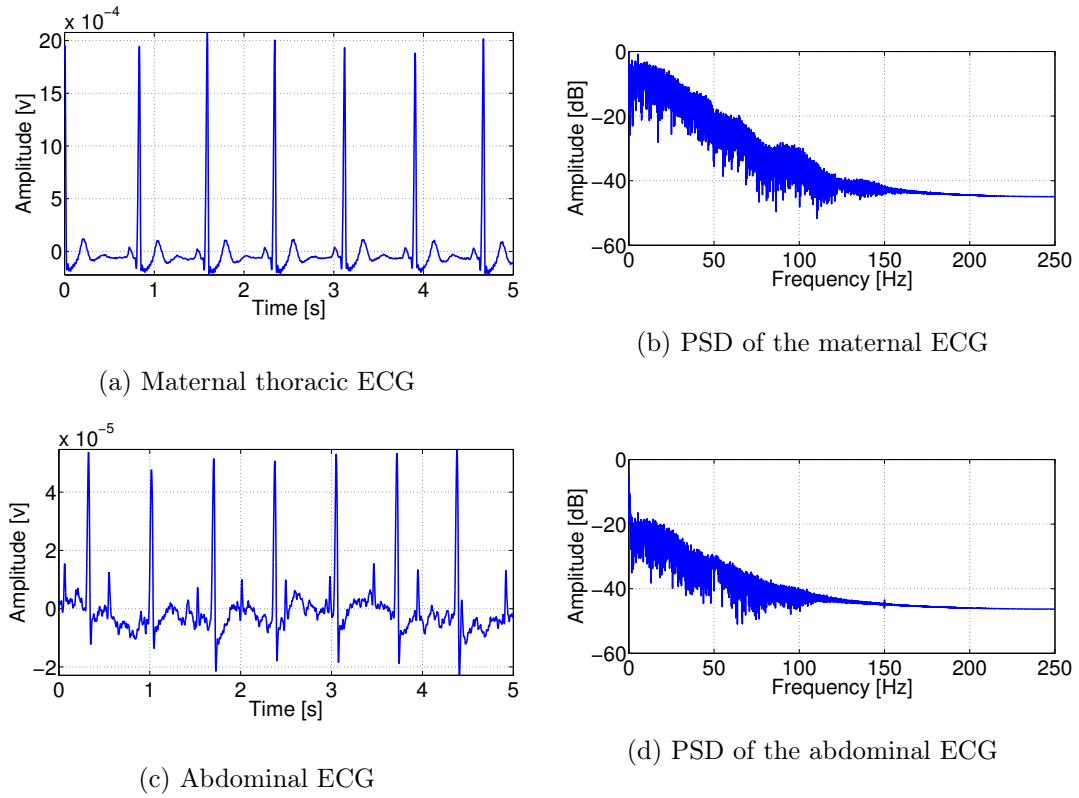

(a) Maternal thoracic ECG

(b) PSD of the maternal ECG

(c) Abdominal ECG

(d) PSD of the abdominal ECG

Figure B.5: A representation of maternal and abdominal ECGs in time and frequency.

pression auriculaire et les valves auriculo-ventriculaires se ferment (son S1). La pression ventriculaire continue d'augmenter, et quand elle dépasse la pression artérielle, les semilunars sont ouvertes et le sang est rapidement éjecté dans l'artère pulmonaire et l'aorte (onde T). Comme les ventricules se détendent, la pression ventriculaire tombe en dessous de la pression artérielle et les valves semi-lunaires se ferment (son S2). Lorsque la pression ventriculaire tombe en dessous de la pression auriculaire, les valves atrioventrcular sont ouvertes et remplissage ventriculaire recommence. À ce moment, les oreillettes et les ventricules sont relaxés et ils attendent la SA pour commencer le prochain cycle cardiaque [Al-Qazzaz et al., 2014].

Traitement du signal

Les signaux l'ECG et du PCG abdominaux et thoraciques sont respectivement présentés à la Fig. B.5 et Fig. B.6 à la fois dans le domaine temporel et fréquentiel.

Le signal ECG est filtré entre $[0.5, 60]$ Hz en utilisant un filtre de Butterworth d'ordre 4 qui est appliqué à la fois directe et inverse pour éviter des distorsions de phase, et la fréquence de 50 Hz est éliminée en utilisant un filtre "notch". Le signal de PCG est filtré dans la gamme de fréquence $[25, 100]$ Hz en utilisant un filtre de 4^{em} ordre. Ici, une bande passante de $[25, 100]$ Hz est choisie pour filtrer le signal PCG [Yang et al.,

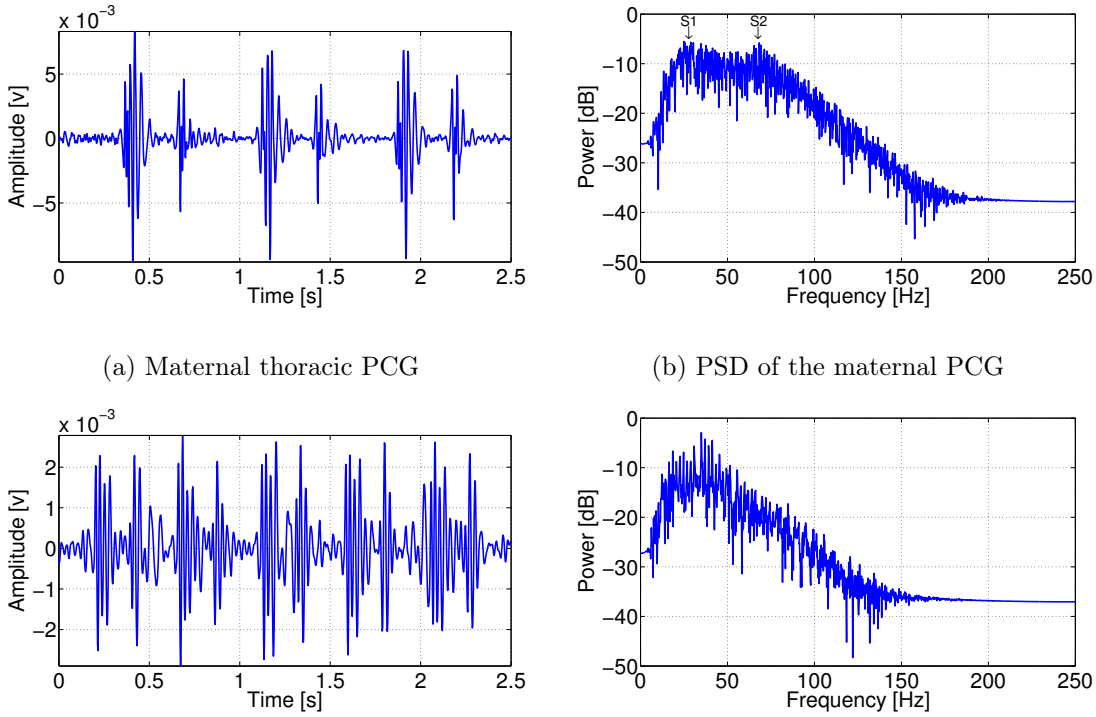

(a) Maternal thoracic PCG

(b) PSD of the maternal PCG

(c) Abdominal PCG (considered as fPCG)

(d) PSD of the abdominal PCG

Figure B.6: A representation of maternal and abdominal PCGs in time and frequency.

2012, Zuckerwar et al., 1993, Varady et al., 2003, Chen et al., 2006]. Clairement, l'ECG abdominal contient deux ECG maternel et fœtal, qui ne peuvent être séparés dans le temps ou les fréquences (Fig. B.5). Cela n'est pas vrai pour le PCG abdominal. L'application d'un filtre passe-bande sur le PCG abdominal peut nous fournir les battements du PCG fœtal dans l'enregistrement abdominal, comme la Fig. B.6. Il est clair que le signal filtré abdominale montre un PCG avec un rythme cardiaque différent et supérieur à celui de la mère. Ce signal correspond donc au PCG fœtal. Les deux pics de fréquence dans le domaine des fréquences du PCG thoracique, marqués dans la figure, montrent les fréquences des deux sons cardiaque : S1, et S2.

Dans l'électrocardiographie, la détection des pics R, et dans la phonocardiographie, la détection des ondes S1 peut fournir une bonne mesure de la fréquence cardiaque. Ceci est illustré à la Fig. B.7, où les pics R de l'ECG, et les sons principaux dans le PCG sont marqués. En outre, en raison de la nature complexe et fortement non-stationnaire des signaux de PCG, l'enveloppe du PCG (ePCG) est largement utilisée à la place du signal [Wu et al., 2012, Haghighi-Mood and Torry, 1995]. Ici, la transformée de Hilbert est utilisée pour extraire l'enveloppe du PCG [Choi and Jiang, 2008].

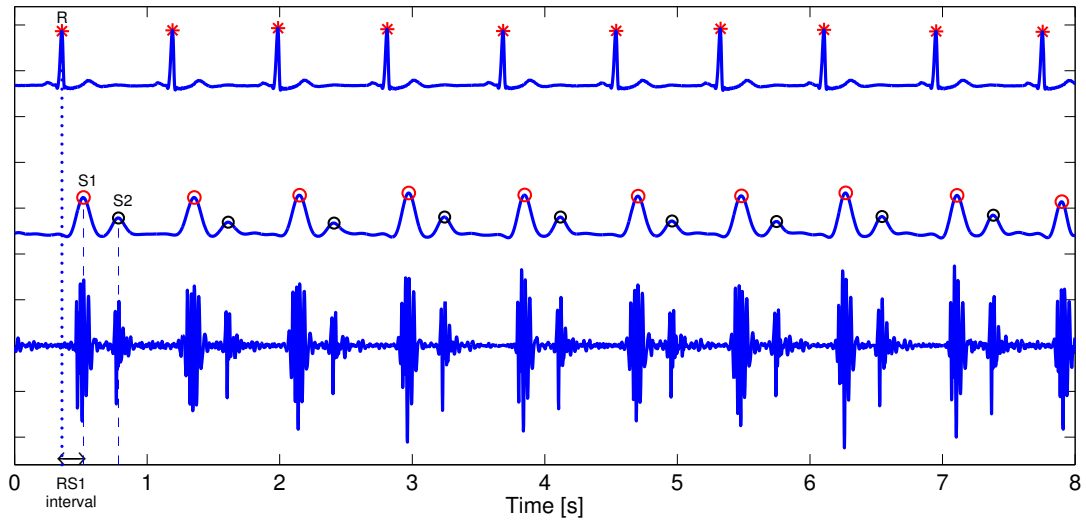

Figure B.7: La détection des ondes de l'ECG et de PCG.

Quasi-synchronicité des signaux ECG et PCG

Ici, un modèle de base des mélanges est présenté afin de mieux comprendre les modalités. Les signaux d'observation ECG peuvent être modélisés comme des mélanges linéaires instantanés: un ensemble de N signaux de source, $s_i(t)$, $1 \leq i \leq N$, qui sont observés par un ensemble de P capteurs, $x_j(t)$, $1 \leq j \leq P$. Notons $\boldsymbol{s}(t) = [s_1(t), \cdots, s_n(t)]^\dagger$ comme les sources de l'ECG († est la notation de la transposition d'une matrice), et $\boldsymbol{x}(t) = [x_1(t), \cdots, x_P(t)]^\dagger$ comme l'ensemble des mélanges observés (Fig. B.8). Ainsi, le mélange instantané des sources cardio-électriques peut être noté comme suit :

$$\boldsymbol{x}(t) = A\boldsymbol{s}(t) + \boldsymbol{e}(t). \tag{B.1}$$

où $\boldsymbol{e}(t)$ est le bruit restant. Le modèle de mélange linéaire instantané suppose qu'aucun retard de propagation des signaux cardio-électrique existe dans le corps humain, et A est la matrice de mélange scalaire. Ce fait n'est cependant pas valable pour le son qui se propage aux microphones placés sur la surface du corps: ceci à cause de la vitesse du son qui est transmis à travers les tissus du corps. Par conséquent, les mesures $\boldsymbol{y}(t) = [y_1(t), \cdots, y_P(t)]^\dagger$ enregistrées par P microphones peuvent être bien représentées par une convolution des sources cardiaques PCG avec le filtre $\boldsymbol{H}(t)$:

$$\boldsymbol{y}(t) = \boldsymbol{H}(t) * \boldsymbol{u}(t) + \boldsymbol{n}(t), \tag{B.2}$$

où $*$ désigne l'opération de convolution, et $\boldsymbol{n}(t)$ désigne le bruit. La voie de transmission entre les capteurs et les sources est donc modélisée comme le filtre $\boldsymbol{H}(t)$, ce qui est une matrice $p \times N$ dont la $(j,i)^{me}$ entrée est le filtre entre la source i pour créer le j^{me} microphone. Les modèles de mélange mentionnés sont représentés à la Fig. B.8. Dans

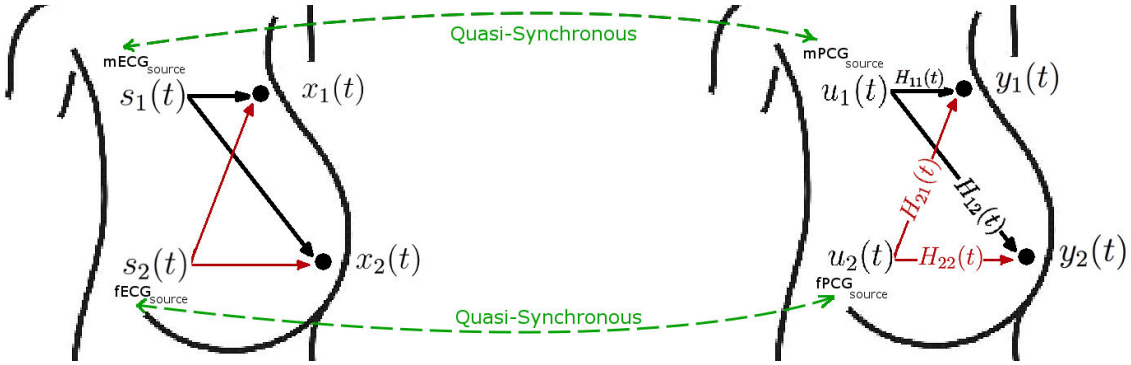

Figure B.8: Les modèles de mélange de l'ECG et du PCG. l'ECG est modélisée comme le mélange linéaire et PCG est modélisée comme le mélange convolutif.

cette application, nous avons deux sources maternelles et foetales ($N = 2$) et ainsi, chacun des signaux cardiaque de source $\boldsymbol{s}(t)$ (sources de l'ECG) et $\boldsymbol{u}(t)$ (sources du PCG) est constituée de deux sources maternelles et fœtales.

En conséquence, le cœur produit deux signaux: $s_i(t)$ et $u_i(t)$. Chacun de ces signaux sont des signaux quasi-périodiques en raison du fonctionnement du cœur. Toutefois, l'ECG est originaire de l'activité électrique du cœur et le PCG est causée par l'activité mécanique du cœur, ceci est la raison pour laquelle les deux signaux ne sont pas totalement synchronisés. En raison de cette quasi-synchronicité, il existe un retard entre les battements correspondant de $s_i(t)$ et $u_i(t)$ qui est différent pour les différents battements. Ce phénomène est illustré à les Figs B.9a et B.9b, où 50 battements ECG sont synchronisés sur la base des pics R. Les battements du PCG sont ensuite reportés sur ces segments de temps de référence et ils sont empilés à la Fig. B.9a. A la Fig. B.9b, les segments de référence sont basés sur les ondes S1 détectés.

Il est clair qu'il y a un retard variable entre l'ECG et les ondes PCG, qui est causé soit par la propagation du signal, soit par l'activité naturelle du cœur. Ce phénomène est largement considéré pour les signaux multi-modaux, puisque les modalités montrent des fonctions différentes d'un même phénomène. Ici, les battement de l'ECG et du PCG peuvent être affectés par différents effets physiologiques et environnementaux comme la respiration. La distribution des variations de cette valeur est indiquée à la Fig B.10 pour un nombre total de 200 battements sur nos données expérimentales. L'histogramme des retards est représenté en gris et la densité de probabilité en bleu est estimée en utilisant un estimateur à noyau de lissage basé sur un noyau gaussien avec une bande passante égale à 6 ms [Wand and Jones, 1994]. Selon cette estimation, les retards entre l'onde R et les ondes S1, appelés les variations RS (Fig. B.7), sont décrits avec une distribution normale de moyenne et d'écart type de 70 ms et 20 ms respectivement:

$$\text{RS} \sim \mathcal{N}(70, 20)[ms] \tag{B.3}$$

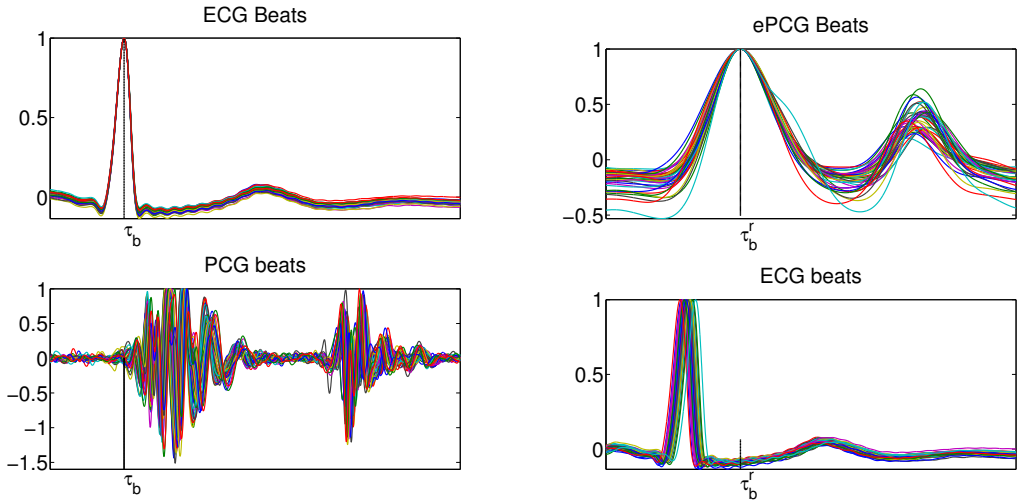

(a) synchronisation de R-Peaks (b) synchronisation de S1

Figure B.9: Illustration des retards entre les battements de l'ECG et du PCG.

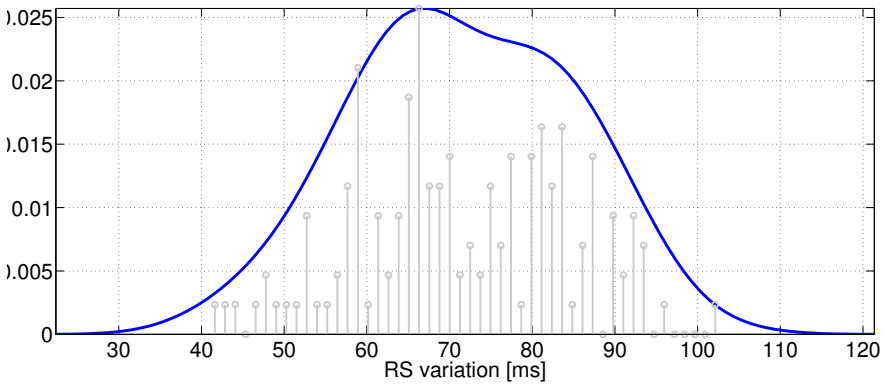

Figure B.10: La fonction de densité de probabilité des variations RS.

B.4 Modélisation des Signaux Quasi-Périodiques

Dans cette section, une méthode à base de processus gaussien (PG) est étudiée comme une méthode générale qui est applicable non seulement sur les signaux ECG ou PCG, mais peut également être utilisée pour modéliser et débruiter toute sorte de paire de signaux qui sont quasi-périodiques , et qui sont (quasi) synchrones.

A la Section B.4.1, le PG est défini et la procédure de débruitage en utilisant le PG est expliquée. Puis à la Section B.4.2, les propriétés des signaux quasi-périodiques sont examinées et les méthodes sont introduites afin de modéliser ces propriétés en utilisant les méthodes précédentes [Rivet et al., 2012, Niknazar et al., 2012]. Par la suite, le prob-

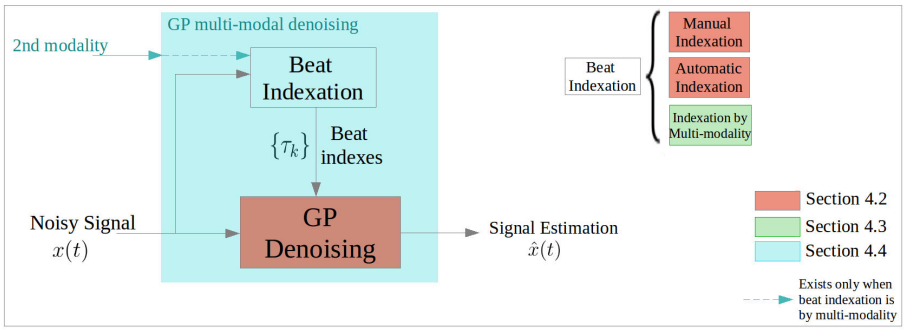

Figure B.11: Le Schème général des techniques présenté dans cette section.

lème de la détection des indices des cycles est présenté. Ces techniques sont en fait unimodales. Cette section est représenté en rouge sur le schéma de la Fig. B.11. Puis à la Section B.4.3.1, représentée en vert dans la Fig. B.11, la première approche multi-modale, appelée multi-modalité partielle, est proposée pour indexer les cycles du signal désiré. A la Section B.4.3.2, une approche multi-modale, appelée multi-modalité naturelle, est proposée afin de modéliser naturellement et extraire le signal souhaité sans une indexation explicite des cycles.

B.4.1 Processus gaussien

B.4.1.1 Définition

Les Processus Gaussiens (PG) sont des outils pratiques qui sont utilisés pour définir une distribution de probabilité sur les fonctions. Le PG est l'extension de la distribution Gaussienne multivariée aux dimensions infinies, cela signifie qu'il contient une collection de variables aléatoires avec une taille infinie. Un PG est complètement déterminé par ses fonctions moyenne et de covariance. Ainsi, une fonction aléatoire, $y(t)$, peut être entièrement décrite au second ordre par sa fonction moyenne, $m(t)$, et sa fonction de covariance, $k(t,t')$ définies comme:

$$\begin{aligned} m(t) &= \mathbb{E}[y(t)], \\ k(t,t') &= \mathbb{E}[\big(y(t)-m(t)\big)\big(y(t')-m(t')\big)]. \end{aligned} \tag{B.4}$$

L'ensemble des fonctions à valeurs réelles, $y(t) \in \mathbb{R}$, peut alors être décrite comme un processus gaussien:

$$y(t) \sim \mathcal{GP}\big(m(t;\boldsymbol{\theta}), k(t,t';\boldsymbol{\theta})\big). \tag{B.5}$$

En choisissant des fonctions particulières de moyenne et de covariance pour le PG, nous pouvons introduire certains hyperparamètres, notés comme l'ensemble $\boldsymbol{\theta}$. Ces hyperparamètres contrôlent le comportement des fonctions sur lesquelles le PG est défini. Main-

tenant, en considérant l'équation (B.5), on peut dire qu'une collection de variables aléatoires $y(t)_{t\in\boldsymbol{t}}$ est tirée d'un PG avec la fonction moyenne, $m(t;\boldsymbol{\theta})$, et la fonction de covariance, $k(t,t';\boldsymbol{\theta})$, si l'ensemble fini de $\{y(t_1),\cdots,y(t_n)\}$ indexé par les entrées $\{t_1,\cdots,t_n\}\in\boldsymbol{t}$ a comme distribution:

$$\begin{bmatrix} y(t_1) \\ \vdots \\ y(t_n) \end{bmatrix} \sim \mathcal{N}\left(\begin{bmatrix} m(t_1) \\ \vdots \\ m(t_n) \end{bmatrix} , \begin{bmatrix} k(t_1,t_1) & \cdots & k(t_1,t_n) \\ \vdots & \ddots & \vdots \\ k(t_n,t_1) & \cdots & k(t_n,t_n) \end{bmatrix} \right). \tag{B.6}$$

Dans ce qui suit, quelques notations, qui seront utilisées plus tard dans ce chapitre, sont définies:

Definition 2 *Given a signal $x(t)$ with M number of samples, and $k.(t,t')$ a covariance function:*

- $\boldsymbol{x}=[x(t_1),\cdots,x(t_M)]^\dagger$ *denotes the column vector indicating signal $x(t)$ with $t\in\boldsymbol{t}=[t_1,\cdots,t_M]^\dagger$,*
- $\boldsymbol{m}=[m(t_1;\boldsymbol{\theta}),\cdots,m(t_M;\boldsymbol{\theta})]^\dagger$ *denotes the mean vector,*
- $\boldsymbol{K}.$ *denotes the covariance matrix where (p,q)-th entry is $k.(t_p,t_q;\boldsymbol{\theta}.)$, where $\boldsymbol{\theta}.$ is the set of hyperparameters defined for $k.$,*
- $\boldsymbol{k}.(t^*)=[k.(t^*,t_1),\cdots,k.(t^*,t_M)]^\dagger$ *denotes a covariance column vector for any t^* time instant.*

Une manière d'estimer les hyperparamètres du modèle, est la maximisation de la fonction log vraisemblance marginale donnée par [Rasmussen, 2006]:

$$\log p\big(\boldsymbol{x}|\boldsymbol{\theta}\big) = -\frac{1}{2}(\boldsymbol{x}-\boldsymbol{m})^\dagger\big(\boldsymbol{K}\big)^{-1}(\boldsymbol{x}-\boldsymbol{m}) - \frac{1}{2}\log\Big|\boldsymbol{K}\Big| - \frac{M}{2}\log(2\pi), \tag{B.7}$$

La maximisation de l'équation (B.7) peut être obtenue par une méthode d'optimisation comme l'algorithme du gradient [Nocedal and Wright, 2006] ou l'algorithme d'optimisation DIRECT [Finkel, 2003].

Le problème de la modélisation d'un signal en utilisant un processus gaussien est de considérer le signal comme une collection de variables aléatoires indexées par les entrées de temps, et de définir un modèle approprié avec des fonctions moyenne et de covariance qui correspondent aux caractéristiques de ce signal. Très souvent, la moyenne du processus gaussien a priori est choisie nulle: $m(t)=0$, ce qui est également le cas dans la présente étude. En conséquence, compte tenu de l'hypothèse de moyenne nulle, le problème de la modélisation est définie comme le problème de trouver une fonction appropriée de covariance du signal à modéliser.

B.4.1.2 Débruitage avec PG

Dans le problème de débruitage d'un signal quasi-périodique souhaité, $s(t)$, contaminé par un bruit additif, $n(t)$, l'observation, $x(t)$, est définie par:

$$x(t) = s(t) + n(t). \tag{B.8}$$

En supposant que le signal $s(t)$, et le bruit $n(t)$, ne sont pas corrélées, nous voulons estimer le signal, $\hat{s}(t)$, qui est modélisé comme un PG. Les signaux $s(t)$ et $n(t)$ sont définis comme:

$$s(t) \sim \mathcal{GP}\big(0, k_s(t, t'; \boldsymbol{\theta}_s)\big), \tag{B.9}$$

$$n(t) \sim \mathcal{GP}\big(0, k_n(t, t'; \boldsymbol{\theta}_n)\big), \tag{B.10}$$

Selon les aprioris définis aux équations (B.9) et (4.8), les valeurs observées de $\boldsymbol{x}$ et $s(t^*)$ ont conjointement une distribution Gaussienne [Rasmussen, 2006]. Pour obtenir la distribution a posteriori, on peut conditionner la distribution a priori gaussienne conjointe sur l'observation:

$$s(t^*) \mid \boldsymbol{x}, \boldsymbol{t}; \boldsymbol{\theta} \sim \mathcal{N}(m^*, K^*), \tag{B.11}$$

$$m^* = \boldsymbol{k}_s(t^*)^\dagger (\boldsymbol{K}_s + \boldsymbol{K}_n)^{-1} \boldsymbol{x}, \tag{B.12}$$

$$K^* = k_s(t^*, t^*) - \boldsymbol{k}_s(t^*)^\dagger (\boldsymbol{K}_s + \boldsymbol{K}_n)^{-1} \boldsymbol{k}_s(t^*). \tag{B.13}$$

Enfin l'estimation que nous considérons pour le signal débruité est la moyenne de la distribution postérieure (4.11) qui est donné par:

$$\forall t^*,\ \hat{s}(t^*) = \boldsymbol{k}_s(t^*)^\dagger (\boldsymbol{K}_s + \boldsymbol{K}_n)^{-1} \boldsymbol{x}. \tag{B.14}$$

Le signal estimé débruité ne se limite pas sur les points de l'observation ($[t_1, ...t_m]$), mais il peut être calculé pour tout ensemble d'échantillons souhaité.

B.4.2 PG Basé sur Uni-Modalité

Un signal quasi-périodique, $s(t)$, peut être considéré comme ayant deux caractéristiques principales qui doivent être prises en compte pour la définition de la fonction de covariance. La première propriété est bien sûr la quasi-périodicité, ce qui signifie que le signal est la concaténation des modèles quasi-similaires aussi appelés pseudo-périodes (ou cycles dans cette étude). Le cycle $c(t)$ est alors répété mais la période du signal est variable dans le temps. Un signal quasi-périodique, avec N cycles , peut donc être écrite comme suit en considérant τ_n le n^{em} indice de cycle de ce signal:

$$s(t) = \sum_{n=1}^{N} c(t - \tau_n), \text{ with} \tag{B.15}$$

$$\Delta_{\tau_n} = \tau_n - \tau_{n-1},$$

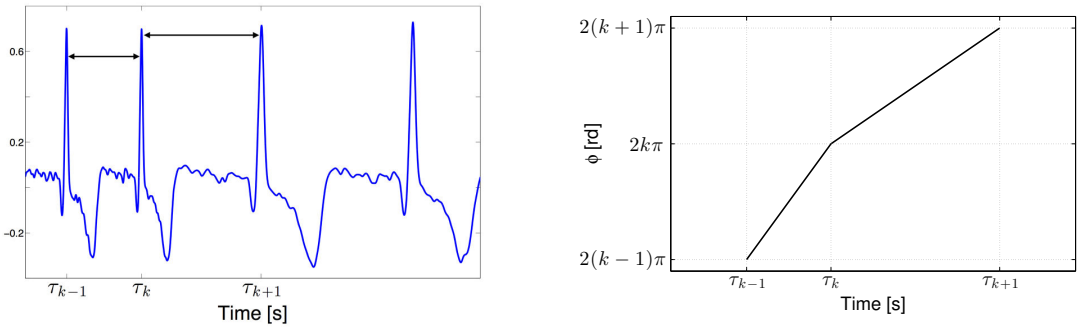

(a) Battements Quasi-periodiques de l'ECG.

(b) Transformation temps-phase

Figure B.12: Transformation temps-phase

où Δ_{τ_n} n'est pas une constante mais varie d'un cycle à l'autre.

La deuxième propriété est la forme du signal, comme l'amplitude, ou les différentes composantes du cycle. Par exemple, dans le cas d'un signal ECG, nous savons qu'il est composé de trois entités principales: l'onde P, le complexe QRS et l'onde T, comme déjà indiqué (voir la Fig. B.4a). Ces entités ont des caractéristiques différentes les unes des autres. Les ondes P et T ont des amplitudes plus faibles que le complexe QRS; en outre, le QRS montre un comportement plus brusque que les ondes P et T.

Ici, la fonction covariance périodique est utilisée pour modéliser le signal ECG. Cette fonction de covariance modélise d'abord la quasi-périodicité en utilisant une déformation temporelle linéaire pour reporter chaque instant des cycles sur une valeur de phase. Ainsi $\phi(t;\{\tau_n\})$, avec $\{\tau_n\}$ comme ses paramètres, est défini de telle sorte que chaque intervalle $[\tau_n, \tau_{n+1})$ est reporté sur l'intervalle $[2(n-1)\pi, 2n\pi)$ (Figure B.12) [Sameni et al., 2005].

Dans ce cas, le signal quasi-périodique, $s(t)$, est un signal périodique dans le domaine de phase, $s(\phi)$. Ensuite, une fonction de covariance périodique est présentée à l'aide des hyperparamètres indépendantes du temps pour modéliser la forme:

$$k(t,t';\widetilde{\boldsymbol{\theta}}) = \sigma^2 \exp\Big(-\frac{(t-t')^2}{2l^2}\Big) \exp\left(-\frac{\sin^2\Big(\frac{\phi(t;\{\tau_n\})-\phi(t';\{\tau_n\})}{2}\Big)}{l_d^2}\right), \tag{B.16}$$

où le terme $\sigma^2 \exp\Big(-\frac{(t-t')^2}{2l^2}\Big)$ modélise la variabilité des amplitudes de différents cycles, et le deuxième terme modélise la quasi-périodicité. $\widetilde{\boldsymbol{\theta}} = \big\{\boldsymbol{\theta}, \{\tau_n\}\big\}$ est l'ensemble des hyperparamètres et $\boldsymbol{\theta} = \big\{\sigma^2, l_d^2\big\}$ où σ^2 et l_d^2 sont l'amplitude, et la longueur de cohérence.

B.4.2.1 Hyperparamètres et indices de cycle

Après avoir introduit les fonctions de covariance qui peuvent décrire les signaux quasi-périodiques, une remarque importante doit être faite en tenant compte des indices des cycles, $\{\tau_n\}$: dans les études précédentes, ces indices ont été soit supposés être des paramètres

connus, soit ils sont détectés manuellement à partir du signal bruité. Cependant, la détection de ces indices peut être une tâche difficile étant donné le signal et l'application. Une solution alternative consiste à inclure ces indices de cycle dans les hyperparamètres de la méthode. Ceux-ci peuvent alors être estimés automatiquement comme les autres hyperparamètres, selon le cadre du maximum de vraisemblance, qui a déjà été présenté dans la Section B.4.1. Pour prendre en compte l'information a priori, il est donc proposé de maximiser la densité de probabilité a posteriori. L'utilisation de l'estimation a posteriori maximale permet d'abord de bénéficier de l'information a priori sur les hyperparamètres pour réduire la complexité de l'estimation. Deuxièmement, elle aborde le problème de la détection des l'indices de cycle en utilisant le modèle de PG. L'estimation maximale d'un posterior est donc une procédure qui intègre une distribution a priori sur les paramètres que nous voulons estimer. Par conséquent, les hyperparamètres sont estimées comme suit:

$$\hat{\widetilde{\boldsymbol{\theta}}} = \arg\max_{\widetilde{\boldsymbol{\theta}}} p(\widetilde{\boldsymbol{\theta}}|\mathbf{x}). \tag{B.17}$$

Selon le schéma bayésien,

$$p(\widetilde{\boldsymbol{\theta}}|\mathbf{x}) \propto p(\mathbf{x}|\widetilde{\boldsymbol{\theta}})p(\widetilde{\boldsymbol{\theta}}), \tag{B.18}$$

Nous pouvons alors bénéficier des fonctions de Densité de probabilité pour les hyperparamètres, $p(\widetilde{\boldsymbol{\theta}}) = p(\sigma^2)p(l^2)p(l_d^2)p(\{\tau_n\}$, selon la connaissance obtenue à partir de la forme du signal et de ces caractéristiques.

B.4.3 PG Basé sur la Multi-Modalité

Les sections précédentes ont expliqué les bases de la modélisation des signaux quasi-périodiques par PG. Les procédés décrits sont basés sur la définition des fonctions de covariance. Il a également été dit que l'une des informations essentielles pour la définition de ces covariances est l'ensemble des indices de cycles, τ_n de l'équation (B.15). Les approches principales pour détecter ces indices sont la détection manuelle ou la maximisation du posterior. La détection manuelle des indices n'est pas toujours possible, si le signal d'observation est très bruité ou trop long. L'estimation a posteriori maximale détecte les indices qui sont définis comme les hyperparamètres du GP, et prends un grand temps de calcul en raison du nombre des hyperparamètres. Les méthodes mentionnées sont des méthodes uni-modales, ce qui signifie que seulement un type de signal est utilisé (par exemple ECG) dans la modélisation; cependant, une autre modalité de données (par exemple, PCG) peut également fournir une information complémentaire qui peut être utile dans l'indexation des cycles.

Supposons que nous ayons deux modalités: $s(t)$, le signal quasi-périodique que nous voulons modéliser, et $r(t)$, la seconde modalité que nous allons utiliser comme référence.

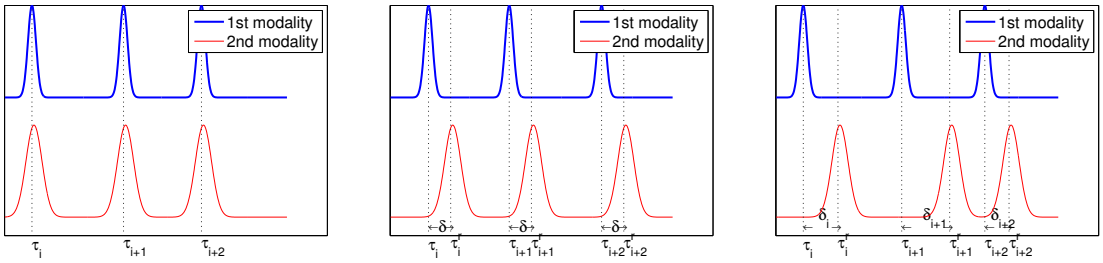

(a) Le premier scénario (b) Le deuxième scénario (c) Le troisième scénario

Figure B.13: Le schéma des 3 scénarios possibles pour la synchronisation des cycles de modalités.

Le signal quasi-périodique, $s(t)$, est déjà défini dans l'équation (B.15). Considérant $\{\tau_n^r\}$ l'ensemble des indices de cycle de la modalité de signal de référence, ce signal est aussi écrit de la même manière:

$$r(t) = \sum_{n=1}^{N} c_r(t - \tau_n^r). \tag{B.19}$$

où c et c_r sont les cycles de $s(t)$ et $r(t)$, respectivement, avec N cycles. Les ensembles d'indices de cycle sont respectivement notés par $\{\tau_n\}$ et $\{\tau_n^r\}$.

B.4.3.1 Multi-Modalité Partielle

Selon ce procédé, trois scénarios différents peuvent se produire. Le premier scénario considère que les deux modalités de signaux sont complètement synchrones, ce qui signifie que les indices se produisent exactement au même instant de temps (Fig. B.13a):

$$\forall n, \quad \tau_n = \tau_n^r. \tag{B.20}$$

Le deuxième scénario considère que les signaux sont synchrones, comme le cas précédent; cependant, il ya un retard constant entre les indices (Fig. B.13b):

$$\tau_n - \tau_n^r = \delta, \quad \text{for all } 1 \leq n \leq N. \tag{B.21}$$

Dans ces deux cas, l'indices de cycle de référence, τ_n^r, peut directement identifier l'indice de cycles, τn, de $s(t)$. Dans le cas du deuxième scénario, la constante de retard δ peut aussi être considérée comme un hyperparamètre supplémentaire de la PG. Le troisième scénario se produit lorsque le retard entre les indices des deux modalités est pas constante:

$$\tau_n - \tau_n^r = \delta_n, \tag{B.22}$$

et δ_n dépend du nombre du cycle, n. Ce délai varie d'un cycle à l'autre. Dans ce scénario, qui est représenté sur la Fig. B.13c, si les indices de cycle de référence sont directement utilisés pour indexer les cycles de signaux, le procédé peut montrer une certaine flexibilité

compte tenu des observations et la quantité de retard, mais il peut aussi causer des conflits dans la modélisation. Cette méthode est appelée multi-modalité partielle parce que la seconde modalité est utilisée seulement dans l'indexation des cycles. Ainsi, les indices de cycles sont détectés en utilisant la modalité de référence. Après, ces indices sont donnés à la fonction covariance. Ensuite, ces méthodes ne considèrent plus la modalité de référence, et le signal désiré est modélisé uniquement sur la base des indices de cycle détecté.

B.4.3.2 Multi-Modalité Naturelle

L'approche qui est introduite ici est multi-modale car elle utilise la modalité de référence naturellement dans le modèle apriori de PG. Dans l'approche uni-modale, la fonction périodique nécessite une connaissance préalable sur les indices de cycle du signal. Ici, une façon plus naturelle de considérer la multi-modalité est présentée. Cela va présenter une nouvelle fonction de covariance qui nécessite un autre canal de données. Revenons d'abord sur la fonction de covariance exponentielle carrée qui est une fonction classique pour décrire les phénomènes naturels. Cette fonction de covariance est définie par l'équation (B.16), pour le processus réel de $s(t)$.

$$k(t,t';\boldsymbol{\theta}) = \exp\big(-\frac{||\vec{u}(t)-\vec{u}(t')||_2^2}{2l^2}\big). \tag{B.23}$$

Ici $||.||_2^2$ désigne la norme L_2 et l est la longueur de cohérence qui est l'hyperparamètre de la fonction de covariance: $\boldsymbol{\theta} = l$. Cette fonction de covariance est définie comme la fonction de l'espace d'entrée, $\vec{u}(t)$. L'espace d'entrée peut être soit les points de temps où $\vec{u}(t) = t$; soit d'autres apports qui peuvent être mappés par une fonction f à la sortie $s(t)$:

$$s(t) = f(\vec{u}(t)) + \epsilon(t), \tag{B.24}$$

Ainsi, la modalité de référence $r(t)$, peut également être utilisé: $\vec{u}(t) = \vec{r}(t)$. Il est important de noter que cette relation entre l'entrée $\vec{u}(t)$ et la sortie de $s(t)$ n'est pas supposée linéaire [Pérez-Cruz et al., 2013]. Maintenant, le PG peut alors être décrit comme:

$$f\big(\vec{\mathbf{u}}_L(t)\big) \sim \mathcal{GP}\bigg(0, k_u\Big(\vec{\mathbf{u}}_L(t), \vec{\mathbf{u}}_L(t')\Big)\bigg), \tag{B.25}$$

ou

$$\vec{\mathbf{u}}_L(t) = [u(t), \cdots, u(t-L+1)]^\dagger.$$

Nous proposerons ensuite la fonction de covariance suivante qui dépend de la fenêtre de la modalité de référence:

$$k(t,t';\boldsymbol{\theta}) = k_u\big(\vec{\mathbf{u}}_L(t), \vec{\mathbf{u}}_L(t')\big) = \sigma^2 \exp\big(-\frac{\big(\vec{\mathbf{u}}_L(t)-\vec{\mathbf{u}}_L(t')\big)^\dagger\big(\vec{\mathbf{u}}_L(t)-\vec{\mathbf{u}}_L(t')\big)}{2l^2}\big), \tag{B.26}$$

où σ est utilisé pour modéliser l'amplitude du signal, et l est la longueur de cohérence. L est la longueur de la fenêtre de l'entrée de la fonction de covariance. Par conséquent, l'ensemble de hyperparamètre est défini comme $\boldsymbol{\theta} = \{\sigma^2, l^2, L\}$.

Nous pouvons utiliser la version 1-bit du signal de référence. En d'autres termes, $u_q(t) = \text{signe}(u_t)$ peut aussi être utilisé comme référence (lorsque la moyenne de $u(t)$ est égale à zéro). Avec la même raison, cette approche ne fonctionne pas seulement avec le signal de référence complète de la modalité, $r(t)$, mais ça fonctionne aussi avec la version 1-bit de cette modalité, $r_q(t)$. L'utilisation du signal de référence de 1-bit est proposé pour un dispositif moins coûteux car il peut être enregistré à l'aide des capteurs bon marché ou un CAN 1-bit. Ce signal est également plus économe en mémoire et il a moins de complexité temporelle à traiter.

B.4.4 L'Extraction du signal ECG foetal

Dans cette section, les méthodes qui ont été expliquées sur la modélisation des signaux quasi-périodique sont appliquées sur l'extraction de l'ECG foetal à partir des canaux abdominaux maternels de l'ECG. Le procédé est utilisé dans la modélisation de deux signaux ECG maternels et fœtaux.

En considérant que le canal ECG abdominal bruité $x(t)$ est un mélange de l'EEG maternel, $s_m(t)$, de l'ECG foetal, $s_f(t)$, et d'autres bruits tels que l'EMG de la mère et/ou du fœtus ou le bruit de l'environnement, $n(t)$, alors

$$x(t) = s_m(t) + s_f(t) + n(t). \tag{B.27}$$

Considérons un canal maternel de référence, $r(t)$, qui peut être l'ECG maternel enregistré à partir de la poitrine de la mère et qui contient principalement l'ECG maternel, $r_m(t)$, et le bruit, $r_n(t)$:

$$r(t) = r_m(t) + r_n(t). \tag{B.28}$$

Les instants de pic-R maternels peuvent être détectés en utilisant la référence $r(t)$. En utilisant ces indices de référence, le premier scénario expliqué dans la section multi-modalité partielle (Section B.4.3.1) est applicable parce que l'ECG thoracique et l'ECG maternel qui apparaît dans l'abdomen sont complètement synchronisés, donc ces indices peuvent être utilisés pour modéliser et extraire l'ECG maternel, $s_m(t)$, à partir du canal abdominale. Si par exemple le signal de référence était choisi comme étant le PCG thoracique, l'indexation des pics R pourrait être faite selon le deuxième scénario de la Section B.4.3.1.

La fonction de covariance expliquée dans l'approche multi-modalité naturelle est également utile ici (Fig. B.14). Les deux signaux $s_m(t)$ et $r_m(t)$, qui sont attribués à l'ECG maternel, sont effectivement fortement corrélés; mais, ils sont décorrélés de l'ECG foetal,

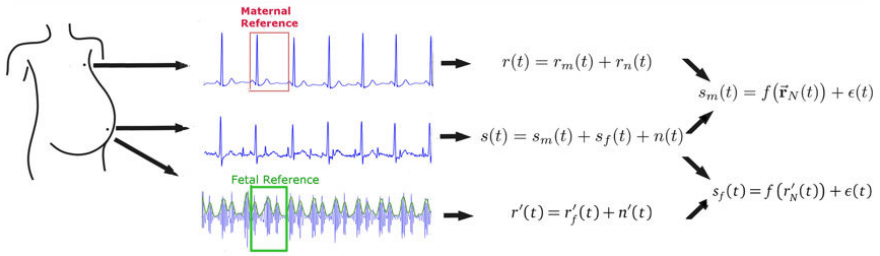

Figure B.14: Un schéma du modèle de covariance qui est basé sur référence pour modéliser l'ECG maternel, $s_m(t)$. la référence, $r(t)$, peut être le signal complet ou le signal 1-bit.

$s_f(t)$, et des bruits $n(t)$ n $r_n(t)$. Maintenant, compte tenu des hypothèses mentionnées, l'ECG maternel, $s_m(t)$, est modélisé comme dépendant d'une fenêtre de l'ECG de référence, $\vec{\mathbf{r}}_N(t)$, par un processus gaussien. Donc, si on a

$$s_m(t) = f\big(\vec{\mathbf{r}}_N(t)\big) + \epsilon_m(t), \tag{B.29}$$

où $\epsilon_m(t)$ est le bruit additif, et le PG est :

$$f\big(\vec{\mathbf{r}}_N(t)\big) \sim \mathcal{GP}\Big(0, k\Big(\vec{\mathbf{r}}_N(t), \vec{\mathbf{r}}_N(t')\Big)\Big), \tag{B.30}$$

où la fonction de covariance est définie comme l'équation (B.26) :

$$k_m(t, t'; \boldsymbol{\theta_m}) = k\Big(\vec{\mathbf{r}}_N(t), \vec{\mathbf{r}}_N(t')\Big), \text{avec} \tag{B.31}$$

$$\boldsymbol{\theta}_m = \{\sigma_m, l_m, N_m\}. \tag{B.32}$$

Le reste du signal abdominal peut alors être modélisé par un PG en utilisant la fonction de covariance

$$k_n(t, t') = \sigma_n^2 \delta(t - t'), \tag{B.33}$$

où $\delta(.)$ est une fonction de Dirac. Puis l'ECG maternel qui est modélisé avec le PG peut être extrait en utilisant l'équation (B.14). Enfin, l'ECG maternel estimé peut être soustrait de l'enregistrement abdominal pour obtenir une estimation de l'ECG foetal: $\hat{s}_f(t) = x(t) - \hat{s}_m(t)$.

Toutefois, la contribution de l'ECG foetal dans l'abdomen, $s_f(t)$, peut également être modélisée en utilisant la covariance basée sur la référence si nous pouvons trouver un signal de référence approprié corrélée à l'ECG foetal (Fig. B.14). La référence utilisée ici pour l'ECG foetal est l'enveloppe d'un signal de PCG qui est enregistré à partir de l'abdomen pour servir de référence au PCG fœtal. Ce signal de référence est noté $p(t)$. Avec un modèle de PG, nous pouvons exprimer que l'ECG foetal est corrélé avec l'enveloppe PCG fœtal :

$$s_f(t) = f\big(\vec{\mathbf{p}}_M(t)\big) + \epsilon_f(t), \tag{B.34}$$

$$f\big(\vec{\mathbf{p}}_M(t)\big) \sim \mathcal{GP}\Big(0, k\Big(\vec{\mathbf{p}}_M(t), \vec{\mathbf{p}}_M(t')\Big)\Big). \tag{B.35}$$

En utilisant la définition de la covariance dans (4.30), la covariance fœtale est écrite comme :

$$k_f(t,t;\boldsymbol{\theta}_f) = k\Big(\vec{\mathbf{p}}_M(t), \vec{\mathbf{p}}_M(t')\Big), \text{ avec} \tag{B.36}$$

$$\boldsymbol{\theta}_f = \{\sigma_f, l_f, N_f\}. \tag{B.37}$$

Afin de résumer la modélisation par PG du signal abdominal et l'extraction de l'ECG foetal, la méthode est décrite ci-après:

1. Définir $k_m(t,t';\boldsymbol{\theta}_m)$, $k_f(t,t';\boldsymbol{\theta}_f)$, et $k_n(t,t';\boldsymbol{\theta}_n)$ avec des paramètres inconnus et définir tous les hyperparamètres $\boldsymbol{\theta} = \boldsymbol{\theta}_m \cup \boldsymbol{\theta}_f \cup \boldsymbol{\theta}_n$.

2. Estimer les hyperparamètres pour créer la matrice de covariance.

3. Créer $\boldsymbol{K}$ pour la covariance de tous les points de l'observation : $\boldsymbol{K} = k_m(t,t';\hat{\boldsymbol{\theta}}_m) + k_f(t,t';\hat{\boldsymbol{\theta}}_f) + k_n(t,t';\hat{\boldsymbol{\theta}}_n)$

4. Créer la covariance entre des instants désirés pour la prédiction, t^*, et les instants de l'observation, i.e, pour la covariance fœtal : $k_f(t^*,t;\hat{\boldsymbol{\theta}}_f)$

5. Estimer la moyenne a posteriori :
   $\hat{s}_f(t^*) = k_f(t^*,t;\hat{\boldsymbol{\theta}}_f)^\dagger \boldsymbol{K}^{-1}\boldsymbol{x}$

B.5 Résultats

Dans cette section, les résultats sont présentés pour évaluer les méthodes qui sont expliquées dans les sections précédentes. Par conséquent, d'abord, les méthodes sont testées pour le débruitage des signaux ECG simulés (Section B.5.1). Ensuite, certains résultats sont illustrés pour valider les méthodes sur l'extraction de l'ECG foetal à partir d'un mélange abdominal stimulé (Section B.5.2). Enfin, l'application de la méthode sur les données réelles est montrée (Section B.5.2).

B.5.1 Résultats du debruitage

Pour synthétiser le signal d'ECG, chaque battement de l'ECG est modélisé comme la somme des 5 fonctions Gaussiennes [Sameni et al., 2007]. Chacune de ces fonctions Gaussiennes modèlise l'une des ondes P, Q, R, S et T (voir la Fig. B.15a) :

$$s(t) = \sum_{i\in\{P,Q,R,S,T\}} a_i \exp\left(-\frac{(t-\mu_i)^2}{2b_i^2}\right), \tag{B.38}$$

où a_i, b_i, et μ_i représente l'amplitude, la largeur et le centre des fonctions Gaussiennes. Dans cette expérience, chaque battement du signal ECG est généré par ce modèle. Afin

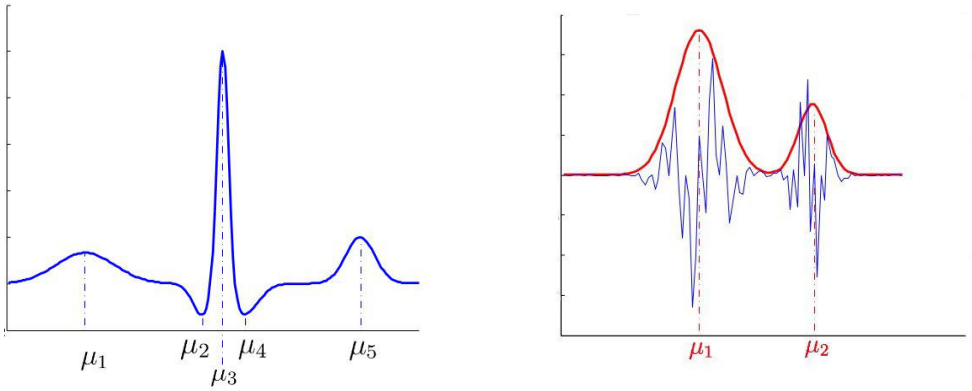

(a) Un battement ECG synthétique

(b) Un battement PCG synthétique

Figure B.15: Les signaux synthétiques.

d'imiter la variabilité présentée dans un ECG réel, les ondes et les amplitudes des intervalles PR et RT sont changées de façon aléatoire autour de leur valeur moyenne. Le signal ECG est alors obtenu sous forme de concaténation de plusieurs battements avec des amplitudes globales aléatoires et les intervalles RR aléatoires, pour modéliser la quasi-périodicité.

Les données PCG synthétiques sont modélisées pour contenir deux fonctions Gaussiennes comme les ondes S1 et S2 dont chacune est multipliée par deux fonctions sinusoïdales avec des fréquences différentes :

$$p(t) = \sum_{i \in \{S1,S2\}} \alpha_i \exp\left(-\frac{(t-u_i)^2}{2\beta_i^2}\right) \sin(2\pi f_i t + \phi_i) \sin(2\pi g_i t + \psi_i), \tag{B.39}$$

Ceci est une méthode simple avec un faible nombre de paramètres qui est inspirée du travail effectué par [Almasi et al., 2011]. Où α_i, β_i, et u_i sont à nouveau l'amplitude, la largeur et le centre des fonctions Gaussiennes, et f_i et g_i sont les fréquences des ondes. Dans cette expérience, les phases initiales ϕ_i, ψ_i sont tirées au hasard à partir d'une distribution uniforme pour permettre à la variabilité entre les battements. Les intervalles S1-S2 et la S2-S1 varient également en fonction de valeurs tirées de Gaussiennes. Le signal de PCG est ensuite généré comme la concaténation de plusieurs battements. Le signal de PCG devrait être quasi-synchrone avec le signal d'ECG. Cela signifie que les sommets S1 sont générés pour être après les pics correspondant R, et la variabilité du délai RS est également pris en considération. La variabilité RS indique que le délai entre R et S1 d'un battement peut être différent des autres battements.

Le pic R détecté à partir des estimations est évalué en utilisant deux mesures. La première est faite en utilisant la différence entre les instants R réels, $\{\tau_i\}_{1 \leq i \leq N}$, et les instants R estimés, $\{\hat{\tau}_i\}_{1 \leq i \leq N}$. L'erreur pour chaque battement est calculée comme :

$$|\tau_i - \hat{\tau}_j|, \tag{B.40}$$

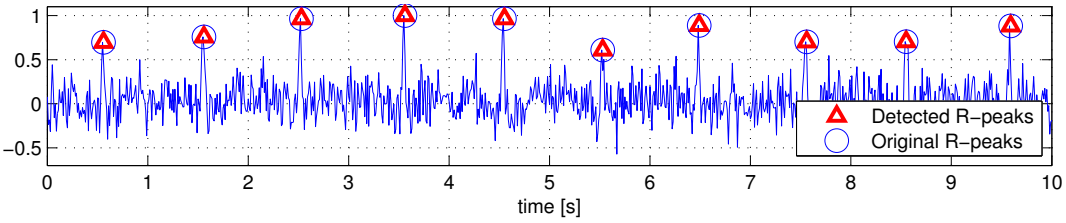

(a) Detection of R-peaks as hyperparameters.

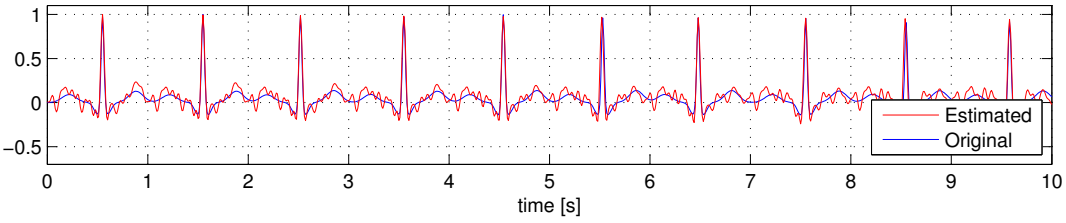

(b) The Estimation of ECG

Figure B.16: The estimation of ECG and R-peaks as hyperparameters, from a synthetic noisy ECG.

et l'erreur moyenne des pics R est

$$\frac{1}{N}\sum_{i=1}^{N}(|\tau_i - \hat{\tau}_i|). \tag{B.41}$$

Un signal d'ECG est généré à la fréquence d'échantillonnage de 100 Hz. Ce signal est ajouté avec un bruit blanc gaussien, $n(t)$, pour former le signal bruité $x(t) = s(t)+n(t)$. Ce signal est ensuite normalisé, ce qui signifie que la moyenne est soustraite et la mise à l'échelle est donnée par la déviation standard; et il est finalement représenté sur la Fig. B.16a. Le signal désiré $s(t)$ est alors modélisé par un PG avec la fonction de covariance périodique présentée dans la Section B.4.2 : $s(t) \sim \mathcal{GP}\big(0, k(t,t';\widetilde{\boldsymbol{\theta}}_s)\big)$, ou $\widetilde{\boldsymbol{\theta}}_s = \{\sigma^2, l^2, l_d^2, \{\tau_n\}\}$. Le bruit est également modélisée par un PG, $n(t) \sim \mathcal{GP}(0, k_n(t,t';\boldsymbol{\theta}_n)$, dont la fonction de covariance est définie par

$$k_n(t,t';\boldsymbol{\theta}_n) = \sigma_n^2\delta(t-t'), \tag{B.42}$$

où $\delta(t)$ est une fonction de Dirac et ainsi les hyperparamètres de bruit sont $\boldsymbol{\theta}_n = \sigma_n$. L'ensemble des hyperparamètres du modèle, $\widetilde{\boldsymbol{\theta}} = \widetilde{\boldsymbol{\theta}}_s \cup \boldsymbol{\theta}_n$, est alors estimé en utilisant l'estimation a posteriori maximale, en utilisant la distribution a priori, $p(\widetilde{\boldsymbol{\theta}})$. Étant donné que les paramètres sont indépendants cette expression est égale à $p(\sigma^2)p(l^2)p(l_d^2)p(\{\tau_n\})p(\sigma_n^2)$. Les hyperparamètres σ, l, l_d et σ_n sont considérés comme des fonctions PDF gamma respectivement définies comme $\Gamma(\alpha_\sigma, \beta_\sigma)$, $\Gamma(\alpha_l, \beta_l)$, $\Gamma(\alpha_{l_d}, \beta_{l_d})$, and $\Gamma(\alpha_{\sigma_n}, \beta_{\sigma_n})$. Parce que l'ensemble des instants R est également supposé être inconnu, il est considéré comme

	ECG Adult
σ^2 [V^2]	$\Gamma(5, .2)$
l_d^2 []	$\Gamma(5, .005)$
l^2 [s^{-2}]	$\Gamma(5, 40)$
intervalle $R-R$ [s]	$\mathcal{N}(1, .002)$
σ_n^2 [V^2]	$\Gamma(5, .2)$

Table B.1: Les valeurs de hyperparamètres de distributions apriori sur $\widetilde{\boldsymbol{\theta}}$ pou l'ECG.

l'hyperparamètre du modèle dont la distribution a priori, $p(\{\tau_n\})$, est dérivée de la distribution des intervalles RR qui sont indépendantes et identiquement distribuées avec une PDF Gaussienne de moyenne μ_R et la variance σ_R^2. Les valeurs qui sont utilisées pour les distributions Gamma et normales antérieures sont présentées dans le tableau B.1. La distribution a posteriori est ensuite échantillonnée par l'algorithme de Metropolis Hasting et les hyperparamètres y compris les pics R sont détectés. Les pics R détectés sont présentés à la Fig. B.16a. Après, l'estimation de l'ECG $\hat{s}(t)$, en utilisant la fonction covariance périodique, est représentée sur la Fig. B.16b. Cette méthode est capable de détecter les pics R. Toutefois, en raison du grand nombre d'hyperparamètres, la complexité des calculs de cette méthode est assez élevée. Par conséquent, les approches multi-modales peuvent être de bonnes solutions pour réduire cette complexité.

Pour appliquer les approches multi-modales, un signal de référence est nécessaire. Le signal de PCG est synthétisé avec l'instants S1 $\{\tau_n^r\}$, qui sont d ms après les instants R, où $d \sim \mathcal{N}(70, 20)[ms]$. L' ePCG est alors calculée et elle est représentée à la Fig. B.17b. Tout d'abord, la méthode multimodalle partielle est utilisée. On imagine que $\{\tau_n\} = \{\tau_n^r\}$, et ensuite, l'approches uni-modale périodique est utilisée et les résultats de l'estimation sont montrés à la Fig. B.17c. Il est clair que compte tenu des retards variant entre le τ et τ^r il y a quelques pics R qui ne sont pas détectés avec précision (montrée en cercle sur la figure).

Ensuite, l'approche multi-modale naturelle est utilisée. Il est rappelé que dans cette approche, l'ensemble ePCG est utilisé comme entrée du PG qui définit l'ECG désiré. Le résultat de l'estimation est représenté à la Fig. B.17d. Ce résultat montre une bonne détection de l'ECG. Le pics R sont également précisément adaptés avec les pics R originaux. Dans la Fig. B.17e, la version 1-bit du signal de PCG, montré dans Fig. B.17b,, est utilisé comme la référence pour le PG. L'estimation est presque la même que lorsque l'ePCG complète est utilisée, tandis que la référence à 1-bit est moins coûteuse à enregistrer et consomme moins de mémoire comme expliqué précédemment.

Par la suite, l'effet de la variabilité du délai entre les indices des modalités est étudié. Le signal PCG est synthétisé avec le variabilité RS qui a une distribution gaussienne de

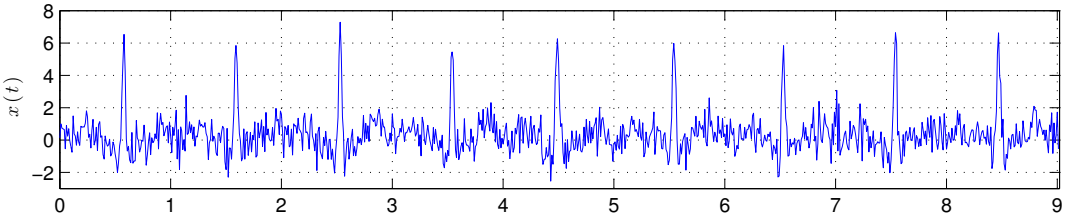

(a) L'ECG bruité.

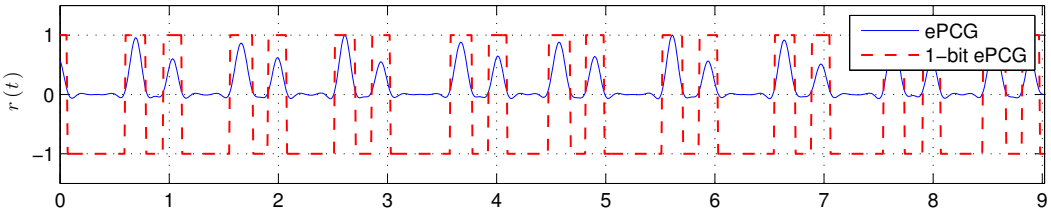

(b) Les signaux références.

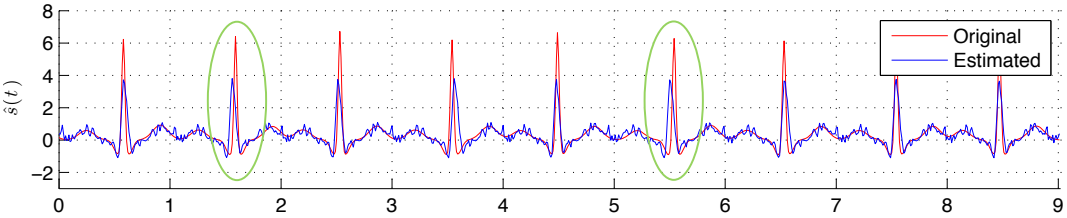

(c) L'estimation de l'ECG avec multi-modalité partielle.

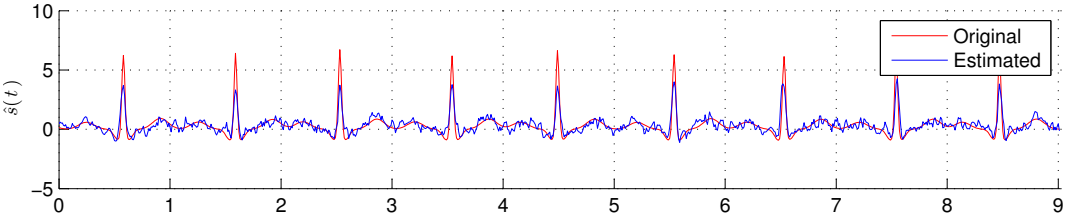

(d) L'estimation de l'ECG avec multi-modalité naturelle avec la référence complet.

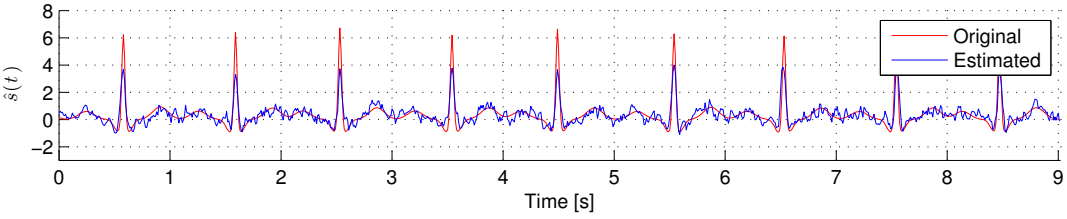

(e) L'estimation de l'ECG avec multi-modalité naturelle avec la référence 1-bit.

Figure B.17: L'estimation de l'ECG avec les méthodes multi-modal à partir de l'ECG bruité synthétique.

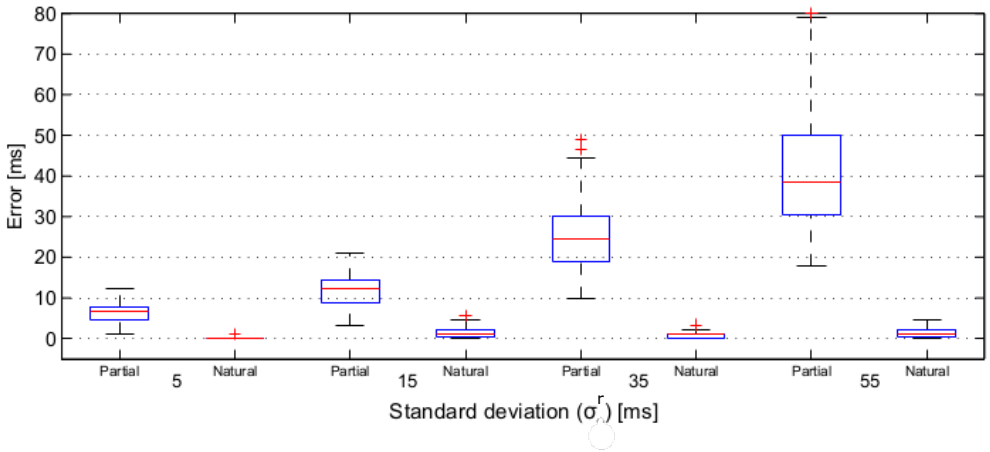

Figure B.18: L'effet de la variation du retard entre les modalités sur l'estimation des pics R.

moyenne $\mu_d = 70$ ms et écart-type σ^r. Le signal ECG est alors modélisé et estimé avec à la fois les méthodes multi-modales partielles et naturelles. Ensuite, les pics R de l'ECG détectés sont calculés et leurs erreurs moyennes sont calculées pour chaque génération du signal avec l'équation (B.40). Ce test est effectué pour 100 générations de différents signaux et les distributions de ces erreurs moyennes sur tous les essais sont représentées à la Fig. B.18. Selon cette figure, les indices de cycle du signal de référence est presque toujours parfaitement détectés en utilisant la méthode naturelle puisque l'erreur est toujours autour de zéro. Cependant, dans le procédé multi-modal partiel, cette erreur augmente avec l'augmentation de la variance de la distribution de délai. Si la variance de l'erreur devient plus grande, la méthode partielle serait incapable d'avoir une bonne estimation, et la méthode naturelle pourra également rencontrer quelques problèmes. Dans ce cas, les retards pourraient être estimés comme des hyperparamètres pour synchroniser les cycles de la modalité de référence.

B.5.2 Résultats de l'extraction du signal ECG fœtal

Les résultats présentés ici sont obtenus par la synthèse des données qui sont générées avec la même procédure que celle expliquée à la SectionB.5.1. L'ECG maternel, $s_m(t)$, l'ECG foetal, $s_f(t)$, et le bruit, $n(t)$, sont synthétisés séparément à 100 Hz et additionnés pour générer l'ECG abdominal synthétique, $x(t)$.

Tout d'abord, la puissance du bruit $n(t)$ est considérée comme suffisamment élevée pour cacher visuellement les pics R de l'ECG fœtal dans l'observation synthétisée $x(t)$. L'observation est montrée à la Fig. B.19. Il est clair que les pics ne peuvent pas être indexés manuellement. Ainsi, la détection automatique des pics R est appliquée, pour les estimer comme les hyperparamètres par la maximisation d'aposteriori (SectionsecB:ch4:aposterior).

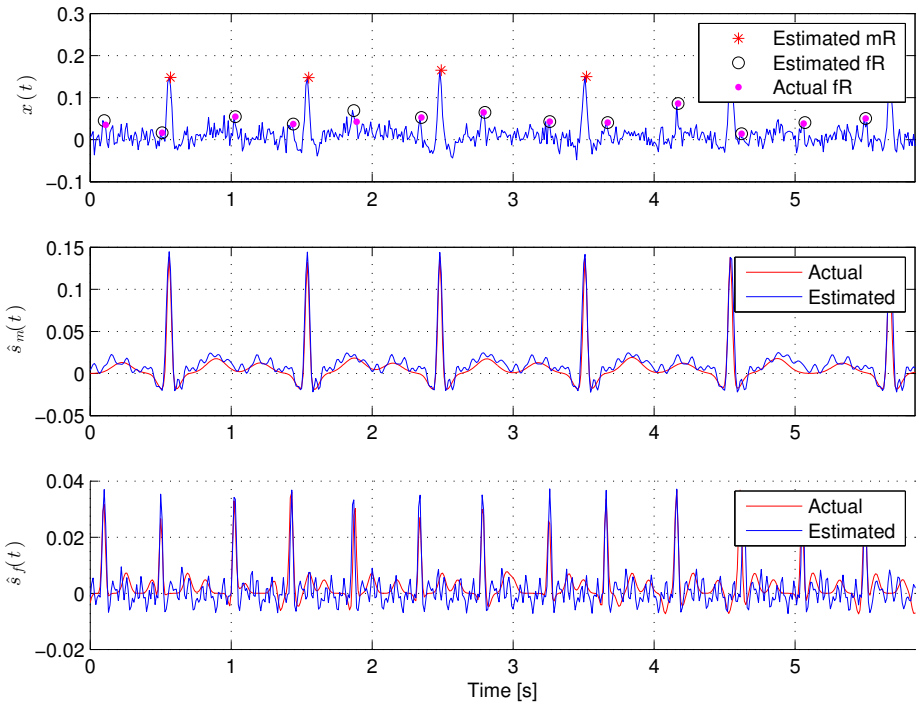

Figure B.19: Détection des pics R fœtales (noté comme fR) et les pics R maternels (notes comme mR) en considérant les pics R comme les hyperparamètres, et l'estimation du mECG et fECG à partir d'un signal synthétique bruyant.

Les distributions a priori qui sont utilisées pour l'ECG maternel (qui est le même que le tableau 4.2) et celles utilisées pour l'ECG foetal et le bruit sont présentées au tableau B.2. Les valeurs indiquées dans ce tableau sont également applicables sur les données réelles La fonction de covariance périodique est utilisée pour modéliser les ECG à la fois maternel et fœtal. Les résultats de la détection des pics R et de l'estimation d'ECG sont ensuite présentés à la Fig. B.19. Les pics R maternels et fœtaux sont presque exactement détectés comme les hyperparamètres; et en utilisant les pics estimés, les signaux ECG sont finalement extraits. On voit que la plupart des pics R sont précisément détectés même lorsque l'amplitude de l'ECG foetal est très faible par rapport à l'ECG maternel et aux autres bruits.

Après, la Fig. B.20 montre un ECG synthétique abdominal et les deux références, $r(t)$ et $p(t)$, générées comme les modalités de référence pour la modélisation des ECG maternels et fœtaux respectivement . $r(t)$ correspond à un ECG thoracique et $p(t)$ correspond à l'enveloppe détectée d'un PCG abdominal comme montré à la figure. Dans la synthèse de l'ECG thoracique, les paramètres sont choisis de façon à être différents des paramètres utilisés pour générer $s_m(t)$ afin de vérifier que le procédé ne dépend pas de la forme temporelle du signal de référence ou des positions d'électrodes. Il n'y a pas de retard entre les pics R de l'abdomen et ceux de référence ECG, et le délai entre les pics R foetals et des ondes S1 sont échantillonnées à partir d'une distribution Gaussienne avec une moyenne

	ECG Maternel	ECG Fœtal	noise
σ^2 [V^2]	$\Gamma(5, .2)$	$\Gamma(5, .001)$	$\Gamma(5, .2)$
l_d^2 []	$\Gamma(5, .005)$	$\Gamma(5, .002)$	
l^2 [s^{-2}]	$\Gamma(5, 40)$	$\Gamma(5, 10)$	
RR intervalle [s]	$\mathcal{N}(1, .002)$	$\mathcal{N}(.5, .004)$	

Table B.2: Les valeurs de hyperparamètres de distributions apriori sur $\widetilde{\boldsymbol{\theta}}_m$, $\widetilde{\boldsymbol{\theta}}_f$, and $\widetilde{\boldsymbol{\theta}}_n$ pour le mECG, le fECG, et la bruits respectivement.

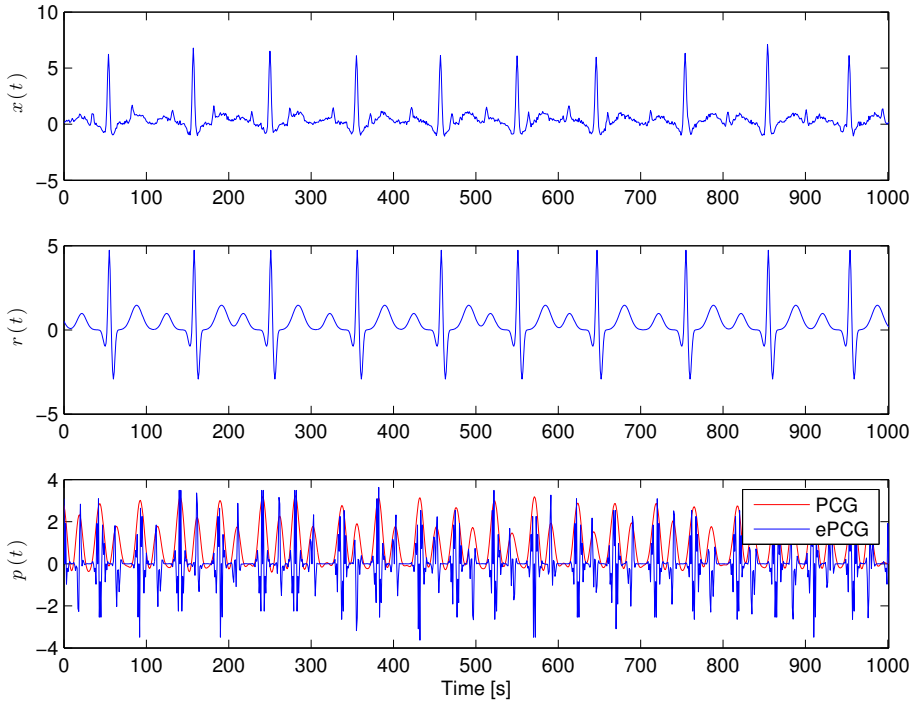

Figure B.20: The synthetic abdominal signal and the maternal and fetal references. $x(t)$ is the abdominal ECG, $r(t)$ is the maternal reference, and $p(t)$ is the fetal reference.

de 70 ms et un écart type de 20 ms, pour correspondre au retard physiologique comme expliqué auparavant dans les sections précédentes.

Considérant le signal d'observation $x(t)$, nous avons l'intention d'estimer l'ECG foetal, $s_f(t)$. Deux façons peuvent être considérées ici: en utilisant un seul signal de référence pour modéliser $s_m(t)$ [Noorzadeh et al., 2015b] et le soustraire du signal abdominal, ou en utilisant deux références pour modéliser les deux signaux $s_m(t)$ et $s_f(t)$ [Noorzadeh et al., 2015c]. Les deux moyens mentionnés sont testés pour extraire l'ECG fœtal. Dans le premier, nous utilisons uniquement le signal $r(t)$ comme la référence pour l'ECG maternel. Dans la seconde approche nous utilisons aussi l'enveloppe du PCG synthétique, pour modéliser l'ECG fœtal.

Les erreurs quadratiques de l'ECG fœtal estimé, $\big(s_f(t) - \hat{s}_f(t)\big)^2$, sont indiquées en rouge

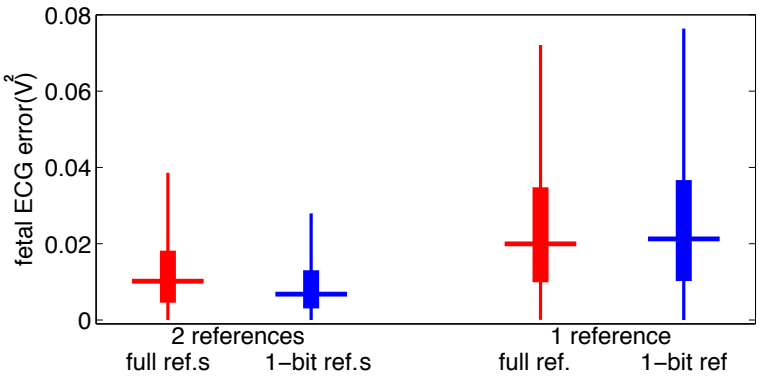

Figure B.21: La comparaison de l'erreur de l'ECG estimée avec un seul modèle de la mère, et avec les deux modèles maternels et fœtaux.

sur la Fig.B.21. En comparant les deux barres rouges, il est clair que deux modèles pour l'ECG maternel et fœtal peuvent améliorer les performances puisque l'erreur de détection est plus petite quand on a deux références. Nous avons alors remplacé les références des deux approches avec des signaux 1-bit, et les résultats d'erreur sont représentés en barres bleues. On voit que l'utilisation des signaux 1-bits pour l'ensemble des deux références donne toujours une meilleure performance. En comparant la performance en utilisant la référence complète et la référence 1-bit (comparant les barres rouges et bleus), on voit qu'en utilisant des signaux de référence 1-bit, la méthode a presque la même erreur que lors de l'utilisation des signaux de référence complets. Les prochains résultats qui sont présentés sont obtenus par la modélisation de deux ECG maternel et fœtal en utilisant leurs références correspondantes.

Les Figs B.22a, et B.22b illustrent l'extraction de mECG et fECG en utilisant la multi-modalité partielle et naturelle. L'estimation parfaite de mECG montre qu'une référence très corrélée peut entraîner une très bonne estimation. Comme précédemment, les pics R fœtaux peuvent être mal estimés en utilisant la méthode partielle en raison du retard entre les signaux fECG et fPCG non-synchronisés. Le battement encerclé à la Fig. B.22a montre un exemple d'une telle erreur. Cependant, dans la méthode naturelle les pics R estimés le sont correctement.

L'erreur des instants des pics R fœtaux détectés pour ces deux méthodes est calculée sur 100 générations de signaux. Ensuite, l'erreur des pics R fœtaux détectée est calculée pour chaque essai de génération avec l'équation (B.41). Les valeurs de tous les essais sont ensuite représentées à la Fig. B.23. L'écart-type de la distribution Gaussienne, dont le retard entre les instants de pic R fœtal et S1 sont échantillonnés, et varie entre 5 ms et 45 ms. Les résultats illustrés pour la méthode partielle montrent que l'erreur augmente avec le retard. Cependant, en regardant les résultats obtenus de la méthode naturelle, nous voyons que la variation des retards entre les deux modalités ne modifie pas les pics

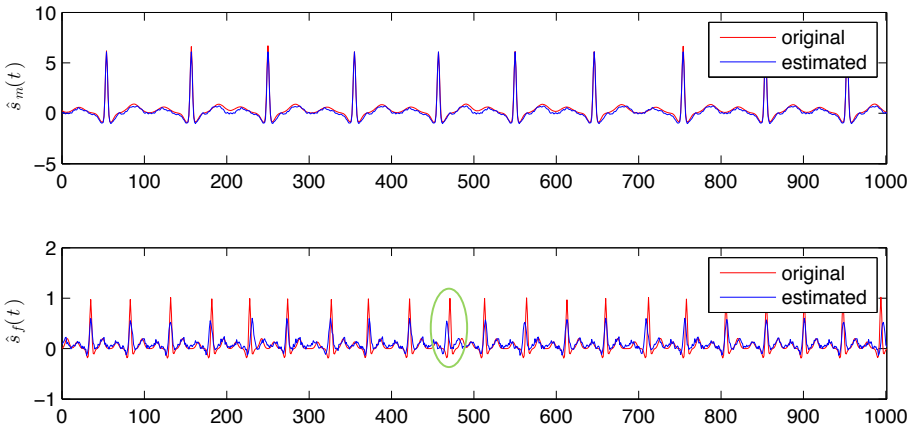

(a) L' extraction avec multi-modalité partielle

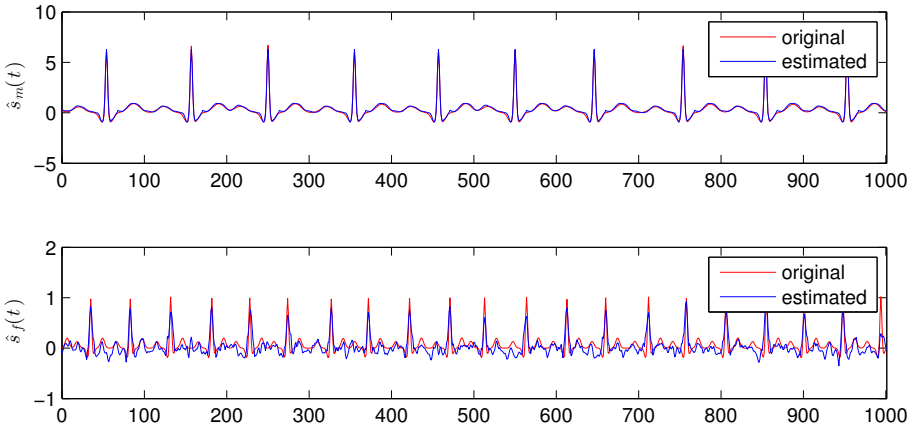

(b) L'extraction avec multi-modalité naturelle

Figure B.22: L'estimation de mECG et fECG avec multi-modalité a partir du signal synthétique.

R fœtaux détectés. L'erreur de ces pics R détectés est presque toujours autour de zéro. Parce que l'information que les cliniciens veulent surveiller est habituellement le rythme cardiaque fœtal, cette information est extraite à partir des données et elle est affichée sur un signal détecté par les deux méthodes multi-modales à la Fig. B.24. La figure montre le fHR original et le fHR détecté par les deux méthodes. Le fHR obtenu par la multi-modalité partielle est considéré comme parfois plus lisse que celui originel. Par exemple, autour de 22 ms, il y a une variation presque rapide du fHR; mais, la méthode partielle estime un fHR lisse. Cela pourrait causer des difficultés à détecter les problèmes cardiaques, et peut causer une erreur de faux positif qui provoque une ignorance de certaines maladies possibles.

L'erreur du fHR détecté par deux méthodes est également calculée pour les deux approches multi-modales. Cette erreur est calculée en fonction de l'erreur de fréquence car-

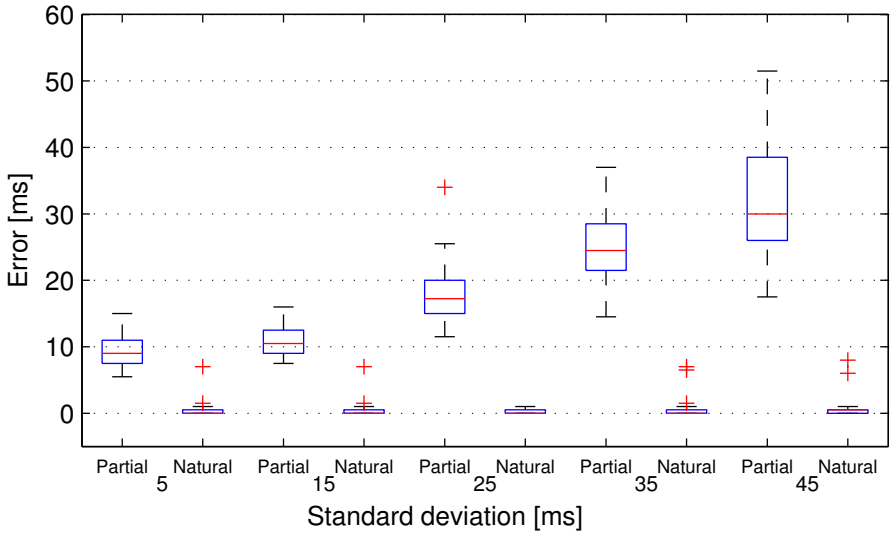

Figure B.23: L'erreur des pics R fœtus détectés en utilisant la multi-modalité.

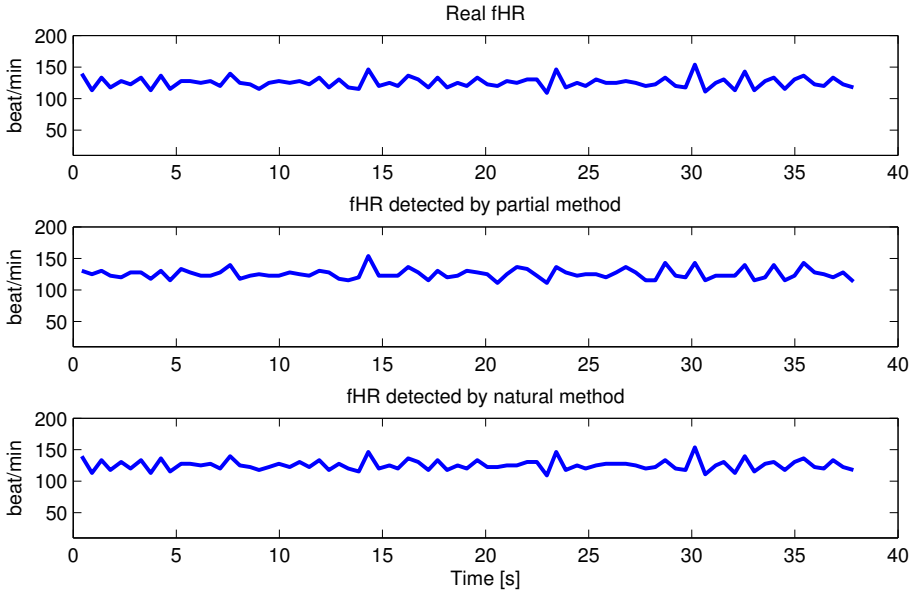

Figure B.24: Le fHR détecté par des approches multimodales.

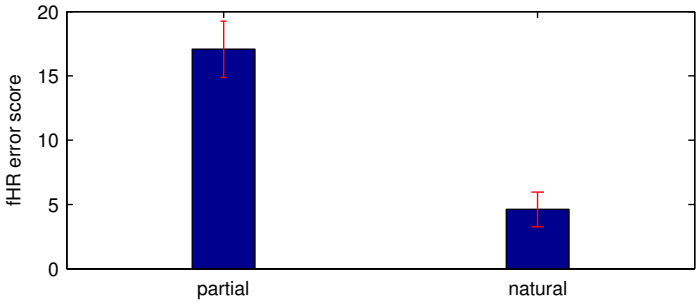

Figure B.25: L'erreur du fHR détecté par des approches multimodales.

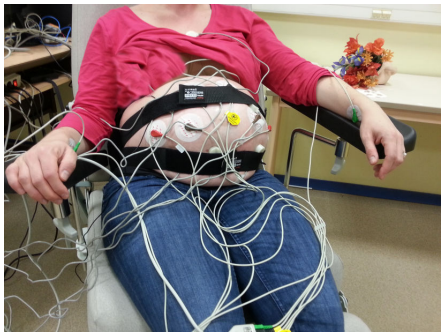

Figure B.26: Une femme enceinte lors d'une session d'enregistrement de données.

diaque décrite dans [Andreotti et al., 2014] :

$$Error_{fHR} = \sqrt{\frac{1}{I}\sum_{i=1}^{I}(RR_i - RR_i^d)^2}, \tag{B.43}$$

où i est l'indice de détection, RR_i et RR_i^d sont les intervalles RR réels et détectés du i^{me} battement $\tau_i - \tau_{i-1}$. Les scores obtenus pour 100 essais de signaux sont représentés à la Fig. B.25. Cette figure montre que la multi-modalité naturelle pourrait être une méthode plus fiable pour la détection du fHR.

B.5.3 Résultats sur les donnée réels

Les données ont été enregistrées chez des femmes enceintes à différents mois de la grossesse avec un canal de mPCG et un canal de mECG (Fig. B.26). Les données abdominalles, cependant, sont enregistrées par un certain nombre de canaux dont l'optimisation du placement n'est pas dans le cadre de cette étude. Les expériences nous fournissent des signaux à partir d'un sujet au le neuvième mois de grossesse et la méthode proposée donne de bons résultats à partir de ces données.

Les premiers résultats présentés à la Fig. B.28a sont obtenus en utilisant une seule référence maternelle pour estimer $\hat{s}_m(t)$ et la soustraire à l'observation pour obtenir une

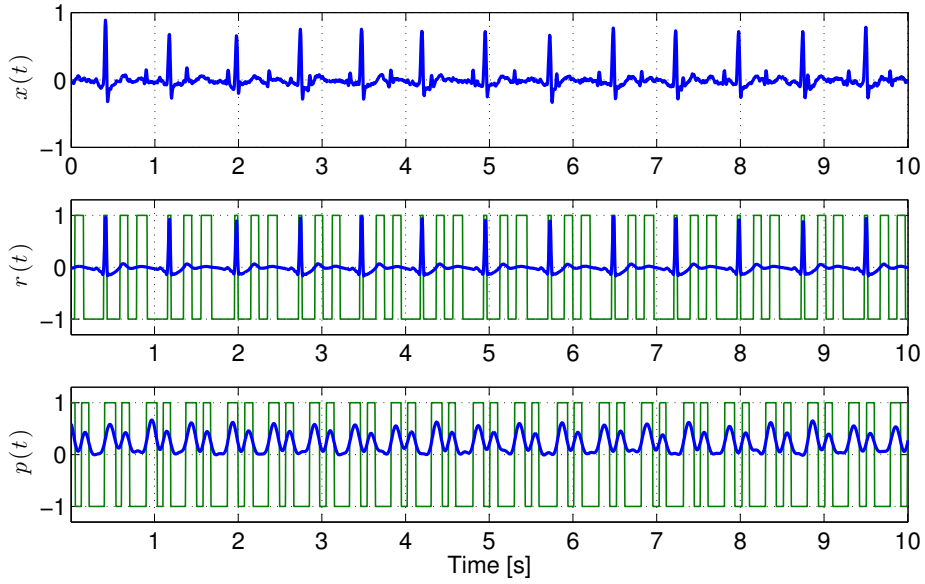

Figure B.27: L'ECG d'observation abdominale et les deux références. $x(t)$ est l'ECG abdominal , $r(t)$ est la référence pour modéliser le mECG, et $p(t)$ est la référence pour modéliser le fECG.

estimation du fECG, $\hat{s}_f(t)$. Le signal maternel est ainsi modélisé en utilisant l'ECG thoracique comme la modalité de référence. Ceci est fait pour comparer les résultats obtenus avec ceux du filtrage adaptatif. Cette figure montre que le filtre adaptatif donne presque le même résultat que le processus Gaussien. Or, dans la figure ci-après les signaux des deux méthodes de référence sont remplacés par le signaux 1-bit. La Fig. B.28b montre ce point; bien que le PG soit capable de détecter les ECG maternels et fœtaux, le filtre adaptatif ne l'est pas. La raison est que la version 1-bit de la référence ne peut pas être transformé linéairement pour ressembler à la contribution de l'ECG maternelle abdominalle. Cependant, le PG peut fournir les estimations non-linéaires. Maintenant, la multi-modalité naturelle est appliquée en utilisant les deux signaux maternels et fœtaux référence qui ont été montrés à la Fig. B.27. Ce résultat est présenté à la Fig. B.29. En comparant cette figure à la colonne de gauche de la Fig. B.28, il est clair que l'estimation en utilisant 2 références (une pour la mère et l'autre pour le fœtus) est moins bruitée que lorsqu'un seul signal maternel est modélisé. Ce résultat contient également moins d'erreurs. Par exemple, à la Fig. B.28b, multi-modalité naturelle a détecté deux pics autour de l'instant de 3.5s dans l'estimation de $\hat{s}_f(t)$, tandis que cette erreur a été corrigée à la Fig. B.29 par l'utilisation du modèle de l'ECG foetal.

Ensuite, le fHR obtenu d'un signal d'une minute est calculé. Ici, l'estimation de fECG, $\hat{s}_f(t)$, est basée sur l'approche naturelle multi-modale conjointe avec 2 références: l'ECG maternel thoracique 1-bit et l'ePCG fœtale 1-bit. Les pics R fœtaux sont ensuite extraits

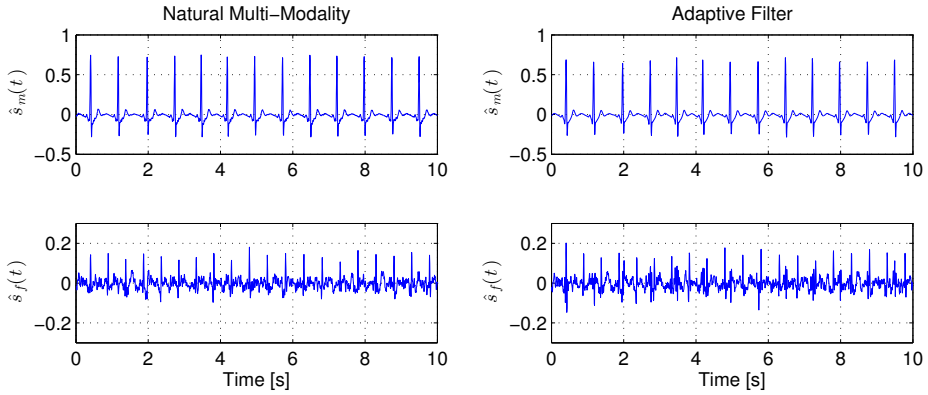

(a) L'extraction du mECG et fECG en utilisant uniquement la référence maternelle thoracique complète.

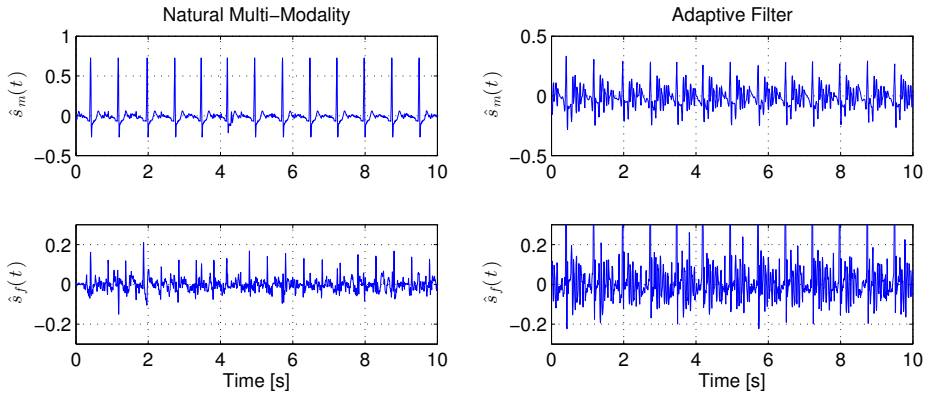

(b) L'extraction du mECG et fECG en utilisant uniquement la référence 1-bit thoracique complète.

Figure B.28: Comparaison de l'extraction avec PG et le filtre adaptatif.

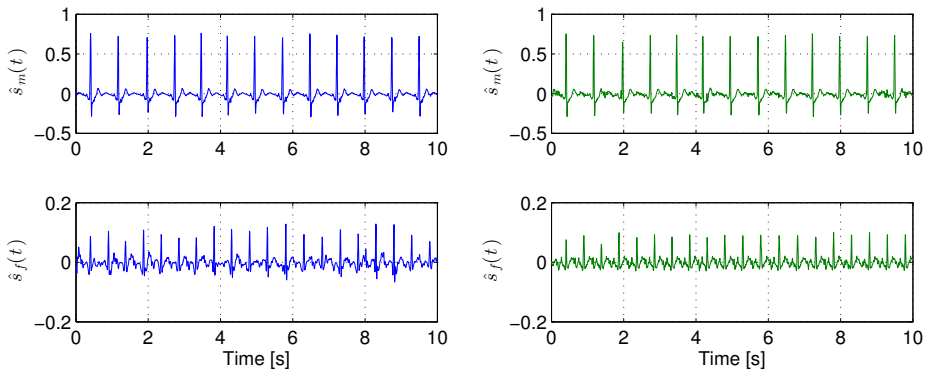

Figure B.29: L'estimation du mECG et fECG à partir des données réelles en utilisant des références complètes et 1-bit par multi-modalité naturelle. Les signaux en bleu sont des estimations en utilisant les références complètes et celles en vert sont l'estimation en utilisant des références de 1-bit.

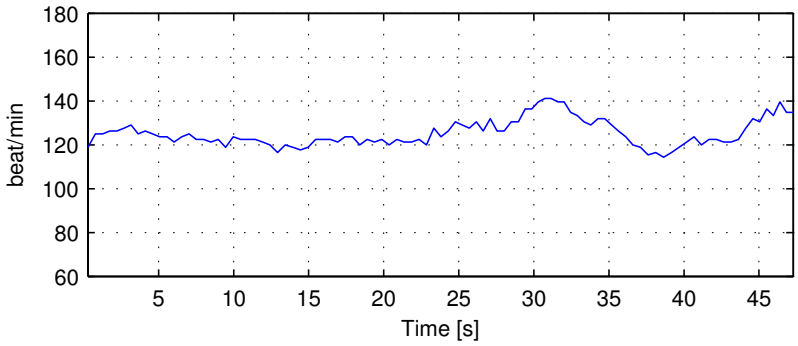

Figure B.30: Calcul de fHR de la fECG détecté à partir des données réelles avec multi-modalité naturelle.

de $\hat{s}_f(t)$ et le fHR est ensuite calculé en battements par minute comme (en considérant que R pics fœtaux sont détectés):

$$\frac{60}{\tau_i^f - \tau_{i-1}^f}, \ 2 \leq i \leq R, \tag{B.44}$$

où τ_i^f est le i^{em} pic R fœtal détecté. Le fHR détecté est ensuite représenté à la Fig. B.30. Le fHR détecté à partir de l'ECG non invasif pourrait être validé avec les données enregistrées avec la CTG.

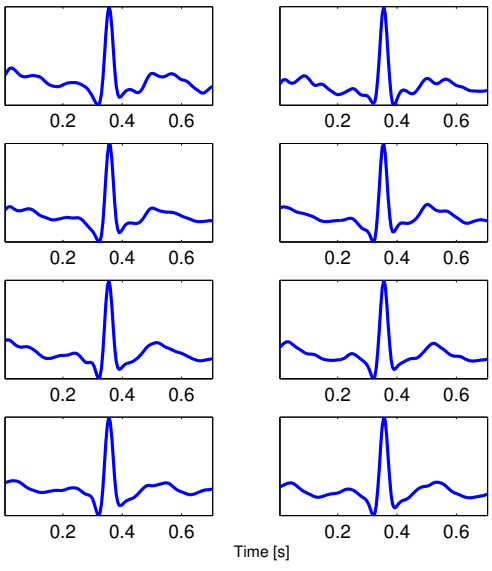

Figure B.31: L'estimation des battements d'ECG fœtal par multi-modalité naturelle: la moyenne tous les 4 battements.

Un mot doit aussi être dit concernant la morphologie détectée à partir du signal. Cela

n'a jamais encore été analysé par les spécialistes de la santé car ils n'avaient pas accès à ce genre de l'information pendant la grossesse. Ici, bien que les battements fœtaux détectés peuvent être bruités, leur moyenne sur plusieurs battements montre la forme d'un battement d'ECG dont l'exactitude et la précision doit être validée selon une référence, comme l'ECG invasif fœtal, ou par les cliniciens. La moyenne tous les 4 battements est assez pour avoir une forme lisse des battements. Ceci est illustré à la Fig. B.31.

B.6 Conclusion et Perspectives

Cette recherche a étudié l'extraction d'un signal fECG, grâce à des enregistrements qui sont enregistrés de façon non invasive sur l'abdomen de la mère. En ce qui concerne les limites des technologies conventionnelles, comme la CTG ou le fECG *invasive*, le fECG *non invasive* peut être approprié pour détecter le rythme cardiaque fœtal, et peut également apporter des informations aux spécialistes au sujet de la morphologie du fECG. Cependant, l'extraction non invasive du fECG est toujours un défi pour la recherche. Cette étude a introduit une approche multi-modale en utilisant deux signaux cardiaques: l'ECG (l'activité électrique du cœur) et le PCG (le activité mécanique du cœur). La multi-modalité bénéficie alors de l'information complémentaire que ces signaux fournissent sur la fonction cardiaque. Ici, la multi-modalité est utilisée sur la base de modèle de processus gaussien, et elle peut être appliquée à n'importe quel procédé existant. Un processus gaussien est une méthode d'estimation non linéaire avec peu hypothèses et peu d'informations a priori sur le signal désiré.

Un des principaux enjeux de cette recherche est la connaissance a priori sur les pics R d'ECG maternel et / ou d'ECG foetal nécessaire aux méthodes existantes alors que cette information est essentielle à extraire pour les cliniciens. A cet effet, une solution automatique a été présentée à la Section B.4.2.1 qui a estimé les pics R en modélisant les signaux souhaités que des processus Gaussiens dans un cadre uni-modal, et détecté les pics R en utilisant le maximum a posteriori. Deuxièmement, le concept de multi-modalité a été présenté, dont l'intention est de faire usage d'une autre modalité pour compléter l'information qui peut être obtenue à partir du signal ECG. Le PCG, le signal audio produit par les valvules cardiaques, est considéré comme la modalité de référence, car elle a une nature différente de l'ECG, et est contaminé par d'autres types de bruit.

Deux approches appelées multi-modalité partielle (Section B.4.3.1) et multi-modalité naturelle (Section B.4.3.2) ont été introduites. La première est une solution pour détecter les pics, suivi d'un procédé uni-modal pour débruiter les signaux ECG. La seconde méthode est un moyen plus naturel de considérer la seconde modalité comme l'entrée du processus Gaussien. Il est à noter que les méthodes ne sont pas applicables uniquement sur l'ECG,

mais elles peuvent être utilisées pour modéliser tout signal quasi-périodique, puisque cette classe de signaux a des propriétés communes qui ont été discutées. Les méthodes peuvent également être appliquées à d'autres types de signaux dans la mesure où il existe une modalité de référence. Par exemple, dans [Noorzadeh et al., 2015a], l'artefact du mouvement de l'oeil est modélisé et retiré de l'EEG, en considérant le signal Gaze comme modalité de référence.

La performance réalisée par les méthodes proposées a été évaluée par des expériences de simulation. Ensuite, le procédé a été appliqué sur les données réelles qui ont été enregistrées au cours de cette thèse. Bien que les expériences soient préliminaires, elles nous ont permis d'obtenir certains signaux de haute qualité dans le dernier mois de la grossesse. Cela peut être un bon modèle pour la période intrapartum de la grossesse sur le fait que la position de fœtus est presque stabilisée.

Les résultats obtenus ont montré que la maximisation de la densité de probabilité a posteriori donne une détection précise des pics R. Ainsi, en utilisant cette méthode, il n'y a pas besoin de connaître les pics R à l'avance. Comme les résultats l'ont montré, cette méthode peut être utile dans les applications où le signal d'observation est très bruité. Cependant, cette méthode est très coûteuse en temps de calcul compte tenu de tous les pics R qui doivent être détectés. L'approche multi-modale a de meilleures performances en ce qui concerne la complexité calculatoire. La multi-modalité naturelle est préférable à la multi-modalité partielle lorsque les deux modalités ne sont pas complètement synchronisées: ce qui se passe dans la plupart des données multi-modales et aussi dans le cas de l'ECG et du PCG. Cette méthode donne une bonne estimation des pics R fœtaux et du rythme cardiaque fœtal. En outre, elle nous fournit la morphologie des battements du fœtus. Cette méthode nécessite un signal de référence pour tous les signaux que nous désirons modéliser. Par conséquent, elle nécessite une référence pour l'ECG maternel et une pour l'ECG foetal, et, en même temps le canal d'observation, il faut au moins trois canaux de données. Cependant, les modalités de référence peuvent être remplacés par des signaux à 1-bit sans perte de performance. De cette façon, les données prennent moins de mémoire par rapport aux signaux sur plusieurs bits (habituellement plus de 16 bits), et la mise en œuvre du dispositif final est plus pratique (compte tenu de l'intégration ou de la consommation d'énergie) avec des capteurs bon marché ou un CAN (convertisseurs analogique-numérique) 1-bit.

Perspectives

Une étude plus approfondie serait intéressante pour plusieurs aspects.

En ce qui concerne la modélisation par processus Gaussien, comme mentionné, une

des limitations est que leur mise en œuvre directe est le temps de calcul, puisque la taille des fonctions de covariance dépend directement de la taille des données, et qui fait la prédiction de calcul complexe (pour calculer la durée $K^{-1}\boldsymbol{x}$ dans l'équation (4.13)). En outre, le dispositif de surveillance efficace à long terme exige le traitement en ligne des données. Par conséquent, un futur travail impliquera la mise en œuvre d'algorithmes pour réduire la complexité calculatoire mentionnée et aussi des processus Gaussien en ligne peuvent être développés [Liu et al., 2011, Gao et al., 2014].

En outre, le concept de multi-modalité est présenté dans cette étude, et sa fonctionnalité est testée sur la méthode PG. Cependant, la multi-modalité pourrait être basée sur l'une des approches de l'état de l'art, comme l'ICA ou IVA, le filtre adaptatif, le filtre de Kalman, etc. Comme mentionné dans la Section B.2 de nombreuses recherches ont essayé de combiner différentes approches pour atteindre de meilleures performances. La multi-modalité peut également être utilisée avec plusieurs approches différentes, car elle peut fournir des informations supplémentaires concernant le fECG, ce qui pourrait augmenter les performances. Ou d'un aspect clinique, chacune des méthodes pourrait être appropriée pour un différent mois de gestation concernant les besoins cliniques ou la position fœtale. Un autre aspect qui peut être considéré, est l'emploi d'autres références cardiaques, comme la seconde modalité. Ici le signal PCG est employé; mais, cette modalité pourrait être les données obtenues par d'autres outils de surveillance du cœur fœtal comme la CTG.

L'optimisation du nombre de capteurs est un autre aspect qui peut être pris en compte comme futurs travaux. Dans le procédé multi-modal, un signal de référence unique est nécessaire pour modéliser le signal désiré. Dans cette thèse, la référence PCG est testée pendant le neuvième mois lorsque le fœtus a un minimum de changements de position, tandis que ce changement peut éventuellement causer des problèmes dans les mois précédents. L'optimisation du nombre de canaux de référence (ou même les canaux d'observation) peut augmenter la robustesse de la méthode. A titre d'exemple, le signal PCG (comme référence) peut être perdu lorsque le fœtus se déplace, ou lorsque le cœur du fœtus est très petit. Dans ce cas, l'utilisation simultanée de plusieurs canaux de référence pourrait améliorer la méthode et son efficacité.

Dans une étape ultérieure, l'enregistrement de données peut être fait de façon synchrone au fHR obtenu par la CTG, et le fHR obtenu par cette méthode. Il serait très utile si les données du fECG invasif peuvent être enregistrées. Dans ce cas, une meilleure comparaison entre la morphologie obtenue par notre méthode et l'électrode invasive fœtale pourrait être faite.

Bibliography

[Adam, 2012] Adam, J. (2012). The future of fetal monitoring. *Reviews in Obstetrics and Gynecology*, 5(3-4):e132.

[Ahlström, 2006] Ahlström, C. (2006). Processing of the phonocardiographic signal: methods for the intelligent stethoscope.

[Al-Qazzaz et al., 2014] Al-Qazzaz, N., Abdulazez, I. F., and Ridha, S. A. (2014). Simulation recording of an ECG, PCG, and PPG for feature extractions. *Al-Khwarizmi Engineering Journal*, 10(4):81–91.

[Alfirevic et al., 2006] Alfirevic, Z., Devane, D., and Gyte, G. M. (2006). Continuous cardiotocography (CTG) as a form of electronic fetal monitoring (EFM) for fetal assessment during labour. *Cochrane Database Syst Rev*, 3(3):CD006066.

[Almasi et al., 2011] Almasi, A., Shamsollahi, M. B., and Senhadji, L. (2011). A dynamical model for generating synthetic phonocardiogram signals. In *Engineering in Medicine and Biology Society, EMBC, 2011 Annual International Conference of the IEEE*, pages 5686–5689. IEEE.

[AmericanHeartAssociation, 2015] AmericanHeartAssociation (Accessed: Aug-2015). Fetal circulation. *http://www.heart.org/HEARTORG/Conditions/CongenitalHeartDefects/SymptomsDiagnosisofCongenitalHeartDefects/Fetal-Circulation_UCM_315674_Article.jsp*.

[Andreotti et al., 2014] Andreotti, F., Riedl, M., Himmelsbach, T., Wedekind, D., Wessel, N., Stepan, H., Schmieder, C., Jank, A., Malberg, H., and Zaunseder, S. (2014). Robust fetal ECG extraction and detection from abdominal leads. *Physiological measurement*, 35(8):1551.

[Ayat et al., 2008] Ayat, M., Assaleh, K., and Nashash, H. (2008). Fetal ECG extraction from a single abdominal ECG signal using svd and polynomial classifiers. In *Machine Learning for Signal Processing, 2008. MLSP 2008. IEEE Workshop on*, pages 250–254. IEEE.

[Bacharakis et al., 1996] Bacharakis, E., Nandi, A. K., and Zarzoso, V. (1996). Foetal ECG extraction using blind source separation methods. *Signal Processing Division. University of Srathclyde*.

[Bakker et al., 2004] Bakker, P. C. A. M., Colenbrander, G. J., Verstraeten, A. A., and Van Geijn, H. P. (2004). The quality of intrapartum fetal heart rate monitoring. *European Journal of Obstetrics & Gynecology and Reproductive Biology*, 116(1):22–27.

[Barnett and Maulik, 2001] Barnett, S. B. and Maulik, D. (2001). Guidelines and recommendations for safe use of doppler ultrasound in perinatal applications. *Journal of Maternal-Fetal and Neonatal Medicine*, 10(2):75–84.

[Behar et al., 2014a] Behar, J., Andreotti, F., Zaunseder, S., Li, Q., Oster, J., and Clifford, G. D. (2014a). An ECG simulator for generating maternal-foetal activity mixtures on abdominal ECG recordings. *Physiological measurement*, 35(8):1537.

[Behar et al., 2013] Behar, J., Oster, J., and Clifford, G. D. (2013). Non-invasive FECG extraction from a set of abdominal sensors. In *Computing in Cardiology Conference (CinC), 2013*, pages 297–300. IEEE.

[Behar et al., 2014b] Behar, J., Oster, J., and Clifford, G. D. (2014b). Combining and benchmarking methods of foetal ECG extraction without maternal or scalp electrode data. *Physiological measurement*, 35(8):1569.

[Bergveld and Meijer, 1981] Bergveld, P. and Meijer, W. J. H. (1981). A new technique for the suppression of the MECG. *Biomedical Engineering, IEEE Transactions on*, 28(4):348–354.

[Callaerts et al., 1990] Callaerts, D., De Moor, B., Vandewalle, J., Sansen, W., Vantrappen, G., and Janssens, J. (1990). Comparison of svd methods to extract the foetal electrocardiogram from cutaneous electrode signals. *Medical and Biological Engineering and Computing*, 28(3):217–224.

[Cardoso, 1998] Cardoso, J. F. (1998). Multidimensional independent component analysis. In *Acoustics, Speech and Signal Processing, 1998. Proceedings of the 1998 IEEE International Conference on*, volume 4, pages 1941–1944. IEEE.

[Castells et al., 2007] Castells, F., Laguna, P., Sörnmo, L., Bollmann, A., and Roig, J. M. (2007). Principal component analysis in ECG signal processing. *EURASIP Journal on Applied Signal Processing*, 2007(1):98–98.

[Cerutti et al., 1986] Cerutti, S., Baselli, G., Civardi, S., Ferrazzi, E., Marconi, A. M., Pagani, M., and Pardi, G. (1986). Variability analysis of fetal heart rate signals as obtained

from abdominal electrocardiographic recordings. *Journal of Perinatal Medicine-Official Journal of the WAPM*, 14(6):445–452.

[Chen et al., 2006] Chen, J., Phua, K., Song, Y., and Shue, L. (2006). A portable phonocardiographic fetal heart rate monitor. In *Circuits and Systems, 2006. ISCAS 2006. Proceedings. 2006 IEEE International Symposium on*, pages 4–pp. IEEE.

[Chen et al., 2001] Chen, M., Wakai, R. T., and Van Veen, B. (2001). Eigenvector based spatial filtering of fetal biomagnetic signals. *Journal of perinatal medicine*, 29(6):486–496.

[Choi and Jiang, 2008] Choi, S. and Jiang, Z. (2008). Comparison of envelope extraction algorithms for cardiac sound signal segmentation. *Expert Systems with Applications*, 34(2):1056–1069.

[Clifford et al., 2011] Clifford, G., Sameni, R., Ward, J., Robinson, J., and Wolfberg, A. J. (2011). Clinically accurate fetal ECG parameters acquired from maternal abdominal sensors. *American journal of obstetrics and gynecology*, 205(1):47–e1.

[Clifford et al., 2014] Clifford, G. D., Silva, I., Behar, J., and Moody, G. B. (2014). Non-invasive fetal ECG analysis. *Physiological measurement*, 35(8):1521.

[Comani et al., 2004] Comani, S., Mantini, D., Lagatta, A., Esposito, F., Di Luzio, S., and Romani, G. L. (2004). Time course reconstruction of fetal cardiac signals from fmcg: independent component analysis versus adaptive maternal beat subtraction. *Physiological measurement*, 25(5):1305.

[Comon and Jutten, 2010] Comon, P. and Jutten, C. (2010). *Handbook of Blind Source Separation: Independent component analysis and applications*. Academic press.

[Cremer, 1906] Cremer, M. (1906). *Über die Ursache der elektromotorischen Eigenschaften der Gewebe, zugleich ein Beitrag zur Lehre von den polyphasischen Elektrolytketten*. R. Oldenbourg.

[De Lathauwer et al., 1995] De Lathauwer, L., De Moor, B., and Vandewalle, J. (1995). Fetal electrocardiogram extraction by source subspace separation. In *IEEE SP/Athos Workshop on Higher-Order Statistics*, page 134.

[De Lathauwer et al., 2000] De Lathauwer, L., De Moor, B., and Vandewalle, J. (2000). Fetal electrocardiogram extraction by blind source subspace separation. *IEEE transactions on biomedical engineering*, 47(5):567–572.

[de Talhouet and Webster, 1996] de Talhouet, H. and Webster, J. G. (1996). The origin of skin-stretch-caused motion artifacts under electrodes. *Physiological Measurement*, 17(2):81.

[Di Maria et al., 2014] Di Maria, C., Liu, C., Zheng, D., Murray, A., and Langley, P. (2014). Extracting fetal heart beats from maternal abdominal recordings: selection of the optimal principal components. *Physiological measurement*, 35(8):1649.

[Duane et al., 1987] Duane, S., Kennedy, A. D., Pendleton, B. J., and Roweth, D. (1987). Hybrid monte carlo. *Physics letters B*, 195(2):216–222.

[Durand and Pibarot, 1995] Durand, L. G. and Pibarot, P. (1995). Digital signal processing of the phonocardiogram: review of the most recent advancements. *Critical Reviews in Biomedical Engineering*, 23(3-4).

[Einthoven, 1895] Einthoven, W. (1895). Ueber die form des menschlichen electrocardiogramms. *Pflügers Archiv European Journal of Physiology*, 60(3):101–123.

[Fatemi et al., 2013] Fatemi, M., Niknazar, M., and Sameni, R. (2013). A robust framework for noninvasive extraction of fetal electrocardiogram signals. In *Computing in Cardiology Conference (CinC), 2013*, pages 201–204. IEEE.

[Fatemian et al., 2010] Fatemian, S. Z., Agrafioti, F., and Hatzinakos, D. (2010). Heartid: Cardiac biometric recognition. In *Biometrics: Theory Applications and Systems (BTAS), 2010 Fourth IEEE International Conference on*, pages 1–5. IEEE.

[Ferrara and Widraw, 1982] Ferrara, E. R. and Widraw, B. (1982). Fetal electrocardiogram enhancement by time-sequenced adaptive filtering. *Biomedical Engineering, IEEE Transactions on*, 29(6):458–460.

[Fetal et al., 2011] Fetal, E. T. F., of Ultrasound in Medicine Clinical Standards Committee, A. I., et al. (2011). AIUM practice guideline for the performance of fetal echocardiography. *Journal of ultrasound in medicine: official journal of the American Institute of Ultrasound in Medicine*, 30(1):127.

[Finkel, 2003] Finkel, D. E. (2003). Direct optimization algorithm user guide. *Center for Research in Scientific Computation, North Carolina State University*, 2.

[Freeman et al., 2012] Freeman, R. K., Garite, T. J., Nageotte, M. P., and Miller, L. A. (2012). *Fetal heart rate monitoring*. Lippincott Williams & Wilkins.

[Gamerman and Lopes, 2006] Gamerman, D. and Lopes, H. F. (2006). *Markov Chain Monte Carlo*. Chapman & Hall/CRC.

[Gao et al., 2003] Gao, P., Chang, E., and Wyse, L. (2003). Blind separation of fetal ECG from single mixture using svd and ica. In *Information, Communications and Signal Processing, 2003 and Fourth Pacific Rim Conference on Multimedia. Proceedings of the 2003 Joint Conference of the Fourth International Conference on*, volume 3, pages 1418–1422. IEEE.

[Gao et al., 2014] Gao, W., Richard, C., Bermudez, J.-C. M., and Huang, J. (2014). Convex combinations of kernel adaptive filters. In *Machine Learning for Signal Processing (MLSP), 2014 IEEE International Workshop on*, pages 1–5. IEEE.

[Gentner and Hammacher, 1967] Gentner, O. and Hammacher, K. (1967). An improved method for the determination of the instantaneous fetal heart frequency from the fetal phonocardiogram. In *Proc. 7th Int. Conf. Med. Biol. Eng*, number 140.

[Gill et al., 2005] Gill, D., Gavrieli, N., and Intrator, N. (2005). Detection and identification of heart sounds using homomorphic envelogram and self-organizing probabilistic model. In *Computers in Cardiology, 2005*, pages 957–960. IEEE.

[Godinez et al., 2003] Godinez, M., Ortiz, R., and Peña, M. (2003). On-line fetal heart rate monitor by phonocardiography. In *Engineering in Medicine and Biology Society, 2003. Proceedings of the 25th Annual International Conference of the IEEE*, volume 4, pages 3141–3144. IEEE.

[Graatsma et al., 2009] Graatsma, E. M., Jacod, B. C., Van Egmond, L. A. J., Mulder, E. J. H., and Visser, G. H. A. (2009). Fetal electrocardiography: feasibility of long-term fetal heart rate recordings. *BJOG: An International Journal of Obstetrics & Gynaecology*, 116(2):334–338.

[Graczyk et al., 1995] Graczyk, S., Jeżewski, J., Wróbel, J., and Gacek, A. (1995). Abdominal electrohysterogram data acquisition problems and their source of origin. In *Engineering in Medicine and Biology Society, 1995 and 14th Conference of the Biomedical Engineering Society of India. An International Meeting, Proceedings of the First Regional Conference., IEEE*, pages PS13–PS14. IEEE.

[Greenberg et al., 2004] Greenberg, R., Christion, J. A., Moses, E. J., and Sternberger, W. I. (2004). Apparatus and method for non-invasive, passive fetal heart monitoring. US Patent 6,751,498.

[Haghighi-Mood and Torry, 1995] Haghighi-Mood, A. and Torry, J. (1995). A sub-band energy tracking algorithm for heart sound segmentation. In *Computers in Cardiology 1995*, pages 501–504. IEEE.

[Hasan et al., 2009] Hasan, M. A., Reaz, M. B. I., Ibrahimy, M. I., Hussain, M. S., and Uddin, J. (2009). Detection and processing techniques of FECG signal for fetal monitoring. *Biological procedures online*, 11(1):263–295.

[Holls and Horner, 1994] Holls, W. M. and Horner, S. L. (1994). Method for suppressing a maternal electrocardiogram signal from a fetal electrocardiogram signal obtained with invasive and non-invasive techniques using an almost pure maternal electrocardiogram signal as a trigger. US Patent 5,372,139.

[Hurst, 1998] Hurst, J. W. (1998). Naming of the waves in the ECG, with a brief account of their genesis. *Circulation*, 98(18):1937–1942.

[Ibrahimy et al., 2003] Ibrahimy, M., Ahmed, F., Ali, M., Zahedi, E., et al. (2003). Real-time signal processing for fetal heart rate monitoring. *Biomedical Engineering, IEEE Transactions on*, 50(2):258–261.

[Jafari and Chambers, 2005] Jafari, M. G. and Chambers, J. (2005). Fetal electrocardiogram extraction by sequential source separation in the wavelet domain. *Biomedical Engineering, IEEE Transactions on*, 52(3):390–400.

[Janjarasjitt, 2006] Janjarasjitt, S. (2006). *A new QRS detection and ECG signal extraction technique for fetal monitoring*. PhD thesis, Case Western Reserve University.

[Jezewski et al., 2011] Jezewski, J., Roj, D., Wrobel, J., and Horoba, K. (2011). A novel technique for fetal heart rate estimation from doppler ultrasound signal. *Biomed Eng Online*, 10(92):10–1186.

[Jimenez-Gonzalez and James, 2008] Jimenez-Gonzalez, A. and James, C. J. (2008). Blind source separation to extract foetal heart sounds from noisy abdominal phonograms: A single channel method.

[Jin and Sattar, 2013] Jin, F. and Sattar, F. (2013). A multiscale mean shift localization approach for robust extraction of heart sounds in respiratory signals. In *Acoustics, Speech and Signal Processing (ICASSP), 2013 IEEE International Conference on*, pages 1291–1295. IEEE.

[Kanjilal et al., 1997] Kanjilal, P. P., Palit, S., and Saha, G. (1997). Fetal ECG extraction from single-channel maternal ECG using singular value decomposition. *Biomedical Engineering, IEEE Transactions on*, 44(1):51–59.

[Kariniemi et al., 1974] Kariniemi, V., Ahopelto, J., Karp, P. J., and Katila, T. E. (1974). The fetal magnetocardiogram. *J Perinat Med*, 2(3):214–216.

[Karvounis et al., 2004] Karvounis, E. C., Papaloukas, C., Fotiadis, D., and Michalis, L. K. (2004). Fetal heart rate extraction from composite maternal ECG using complex continuous wavelet transform. In *Computers in Cardiology, 2004*, pages 737–740. IEEE.

[Khamene and Negahdaripour, 2000] Khamene, A. and Negahdaripour, S. (2000). A new method for the extraction of fetal ECG from the composite abdominal signal. *Biomedical Engineering, IEEE Transactions on*, 47(4):507–516.

[Khan, 2004] Khan, E. (2004). Clinical skills: the physiological basis and interpretation of the ecg. *British journal of nursing*, 13(8):440–447.

[Kieler et al., 2002] Kieler, H., Cnattingius, S., Haglund, B., Palmgren, J., and Axelsson, O. (2002). Ultrasound and adverse effects. *Ultrasound in Obstetrics & Gynecology*, 20(1):102–103.

[Kimber et al., 1996] Kimber, S., Downar, E., Masse, S., Sevaptsidis, E., Chen, T., Mickleborough, L., and Parsons, I. (1996). A comparison of unipolar and bipolar electrodes during cardiac mapping studies. *Pacing and clinical electrophysiology*, 19(8):1196–1204.

[Kovács et al., 2011] Kovács, F., Horváth, C., Balogh, Á. T., and Hosszú, G. (2011). Fetal phonocardiography—past and future possibilities. *Computer methods and programs in biomedicine*, 104(1):19–25.

[Kovács et al., 2000] Kovács, F., Torok, M., and Habermajer, I. (2000). A rule-based phonocardiographic method for long-term fetal heart rate monitoring. *Biomedical Engineering, IEEE Transactions on*, 47(1):124–130.

[Künzi et al., 2013] Künzi, H. P., Krelle, W., and von Randow, R. (2013). *Nichtlineare programmierung*. Springer-Verlag.

[Kuss and Rasmussen, 2005] Kuss, M. and Rasmussen, C. E. (2005). Assessing approximate inference for binary gaussian process classification. *The Journal of Machine Learning Research*, 6:1679–1704.

[Lahat et al., 2014] Lahat, D., Adaly, T., and Jutten, C. (2014). Challenges in multimodal data fusion. In *Signal Processing Conference (EUSIPCO), 2013 Proceedings of the 22nd European*, pages 101–105. IEEE.

[Laufs, 2012] Laufs, H. (2012). A personalized history of EEG–fMRI integration. *Neuroimage*, 62(2):1056–1067.

[Lawrence, 2005] Lawrence, N. (2005). Probabilistic non-linear principal component analysis with gaussian process latent variable models. *The Journal of Machine Learning Research*, 6:1783–1816.

[Lawrence et al., 2009] Lawrence, N. D., Rattray, M., and Titsias, M. K. (2009). Efficient sampling for gaussian process inference using control variables. In *Advances in Neural Information Processing Systems*, pages 1681–1688.

[Liu et al., 2011] Liu, W., Principe, J. C., and Haykin, S. (2011). *Kernel adaptive filtering: a comprehensive introduction*, volume 57. John Wiley & Sons.

[Maeda, 1965] Maeda, K. (1965). Studies on the cardiotachography during labor. In *Proc. VI Intern Conf Med Elect Biol Eng*, pages 514–515.

[Maeda et al., 1980] Maeda, K., Arima, T., Tatsumura, M., and Nagasawa, T. (1980). Computer-aided fetal heart rate analysis and automatic fetal distress diagnosis during labor and pregnancy utilizing external technique in fetal monitoring. *Medinfo*, 80:1214–1219.

[Maier and Dickhaus, 2013] Maier, C. and Dickhaus, H. (2013). Fetal QRS detection and rr interval measurement in noninvasively registered abdominal ECGs. In *Computing in Cardiology Conference (CinC), 2013*, pages 165–168. IEEE.

[Mäntyjärvi et al., 2005] Mäntyjärvi, J., Lindholm, M., Vildjiounaite, E., Mäkelä, S., and Ailisto, H. A. (2005). Identifying users of portable devices from gait pattern with accelerometers. In *Acoustics, Speech, and Signal Processing, 2005. Proceedings.(ICASSP'05). IEEE International Conference on*, volume 2. IEEE.

[Martens et al., 2007] Martens, S. M. M., Rabotti, C., Mischi, M., and Sluijter, R. (2007). A robust fetal ECG detection method for abdominal recordings. *Physiological measurement*, 28(4):373.

[McSharry et al., 2003] McSharry, P. E., Clifford, G. D., Tarassenko, L., Smith, L., et al. (2003). A dynamical model for generating synthetic electrocardiogram signals. *Biomedical Engineering, IEEE Transactions on*, 50(3):289–294.

[Meathrel et al., 1995] Meathrel, W., Saleem, M., and Binks, S. A. (1995). Non-invasive fetal probe. US Patent 5,474,065.

[Miaou and Chen, 2001] Miaou, S. and Chen, K. (2001). Improving storage efficiency of vector quantization codebook for physiological quasi-periodic signals. *Medical engineering & physics*, 23(6):401–410.

[Mittra et al., 2008] Mittra, A. K., Choudhary, N. K., and Zadgaonkar, A. S. (2008). Development of an artificial womb for acoustical simulation of mother's abdomen. *International Journal of Biomedical Engineering and Technology*, 1(3):315–328.

[Miyashiro and Mintz-Hittner, 1999] Miyashiro, M. J. and Mintz-Hittner, H. A. (1999). Penetrating ocular injury with a fetal scalp monitoring spiral electrode. *American journal of ophthalmology*, 128(4):526–528.

[Mochimaru et al., 2002] Mochimaru, F., Fujimoto, Y., and Ishikawa, Y. (2002). Detecting the fetal electrocardiogram by wavelet theory-based methods. *Progress in Biomedical Research*, 7:185–193.

[Moghavvemi et al., 2003] Moghavvemi, M., Tan, B. H., and Tan, S. Y. (2003). A non-invasive pc-based measurement of fetal phonocardiography. *Sensors and Actuators A: Physical*, 107(1):96–103.

[Moran, 2015] Moran, G. (Accessed: Aug-2015). Cardiology teaching package. *http://www.nottingham.ac.uk/nursing/practice/resources/cardiology/index.php*.

[Niknazar et al., 2012] Niknazar, M., Rivet, B., and Jutten, C. (2012). Fetal ecg extraction from a single sensor by a non-parametric modeling. In *Signal Processing Conference (EUSIPCO), 2012 Proceedings of the 20th European*, pages 949–953. IEEE.

[Niknazar et al., 2013a] Niknazar, M., Rivet, B., and Jutten, C. (2013a). Fetal ECG extraction by extended state kalman filtering based on single-channel recordings. *Biomedical Engineering, IEEE Transactions on*, 60(5):1345–1352.

[Niknazar et al., 2013b] Niknazar, M., Rivet, B., and Jutten, C. (2013b). Fetal QRS complex detection based on three-way tensor decomposition. In *Computing in Cardiology Conference (CinC), 2013*, pages 185–188. IEEE.

[Nocedal and Wright, 2006] Nocedal, J. and Wright, S. (2006). *Numerical optimization*. Springer Science & Business Media.

[Noorzadeh et al., 2015a] Noorzadeh, S., Rivet, B., and Gumery, P. Y. (2015a). An application of gaussian processes on ocular artifact removal from eeg. In *Engineering in Medicine and Biology Society (EMBC)*. IEEE.

[Noorzadeh et al., 2015b] Noorzadeh, S., Rivet, B., and Guméry, P.-Y. (2015b). Enhancing fetal ecg using gaussian process. In *International Conference on Mathematics in Signal Processing IMA*.

[Noorzadeh et al., 2015c] Noorzadeh, S., Rivet, B., and Guméry, P.-Y. (2015c). A multimodal approach using a non-parametric model to extract fetal ecg. In *IEEE Int. Conf. Acoustics, Speech, and Signal Processing (ICASSP)*. IEEE.

[Ortiz et al., 1999] Ortiz, M. R., Pena, M. A., Charleston, S., Aljama, A. T., and González, R. (1999). The use of wavelet packets to improve the detection of cardiac sounds from the fetal phonocardiogram. In *Computers in Cardiology, 1999*, pages 463–466. IEEE.

[Osei and Faulkner, 1999] Osei, E. K. and Faulkner, K. (1999). Fetal position and size data for dose estimation. *The British journal of radiology*, 72(856):363–370.

[Patil, 2012] Patil, S. B. (2012). A study of biometric, multimodal biometric systems: Fusion techniques, applications and challenges. *IJCST*, 3(1):524–526.

[Patterns, 1999] Patterns, I. (1999). Interpretation of the electronic fetal heart rate during labor. *Am. Fam. Physician*, 59:2487–500.

[Pérez-Cruz et al., 2013] Pérez-Cruz, F., Van Vaerenbergh, S., Murillo-Fuentes, J. J., Lázaro-Gredilla, M., and Santamaria, I. (2013). Gaussian processes for nonlinear signal processing: An overview of recent advances. *Signal Processing Magazine, IEEE*, 30(4):40–50.

[Phanphaisarn et al., 2011] Phanphaisarn, W., Roeksabutr, A., Wardkein, P., Koseeyaporn, J., and Yupapin, P. P. (2011). heart detection and diagnosis based on Ecg and EPcg relationships. *Medical devices (Auckland, NZ)*, 4:133.

[Rabotti et al., 2010] Rabotti, C., Mischi, M., Oei, S., and Bergmans, J. W. M. (2010). Noninvasive estimation of the electrohysterographic action-potential conduction velocity. *Biomedical Engineering, IEEE Transactions on*, 57(9):2178–2187.

[Randall et al., 1988] Randall, N. J., Steer, P. J., and Sutherland, I. A. (1988). Detection of the fetal ECG during labour by an intrauterine probe. *Journal of biomedical engineering*, 10(2):159–164.

[Rasmussen, 2006] Rasmussen, C. E. (2006). Gaussian processes for machine learning.

[Rawther and Cheriyan,] Rawther, N. N. and Cheriyan, J. Detection and classification of cardiac arrhythmias based on ECG and PCG using temporal and wavelet features.

[Rivet et al., 2012] Rivet, B., Niknazar, M., and Jutten, C. (2012). Nonparametric modelling of ecg: applications to denoising and to single sensor fetal ecg extraction. In *Latent Variable Analysis and Signal Separation*, pages 470–477. Springer.

[Rooijakkers et al., 2014] Rooijakkers, M. J., Song, S., Rabotti, C., Oei, S. G., Bergmans, J. W. M., Cantatore, E., and Mischi, M. (2014). Influence of electrode placement on signal quality for ambulatory pregnancy monitoring. *Computational and mathematical methods in medicine*, 2014.

[Ross and Beall, 2014] Ross, M. G. and Beall, M. H. (2014). Scalp lead placement periprocedural care. *http://emedicine.medscape.com/article/1998111-periprocedure*.

[Ruffo et al., 2010] Ruffo, M., Cesarelli, M., Romano, M., Bifulco, P., and Fratini, A. (2010). An algorithm for fhr estimation from foetal phonocardiographic signals. *Biomedical Signal Processing and Control*, 5(2):131–141.

[Ruffo et al., 2011] Ruffo, M., McEwan, A., van Schaik, A., Sullivan, C., Jin, C., Gargiulo, G., Romano, M., Cesarelli, M., Bifulco, P., and Shephard, R. W. (2011). *Non Invasive Foetal Monitoring with a Combined ECG-PCG System*. INTECH Open Access Publisher.

[Sameni, 2008] Sameni, R. (2008). *Extraction of fetal cardiac signals from an array of maternal abdominal recordings*. PhD thesis, Sharif University of Technology, Tehran, Iran.

[Sameni and Clifford, 2010] Sameni, R. and Clifford, G. D. (2010). A review of fetal ECG signal processing; issues and promising directions. *The open pacing, electrophysiology & therapy journal*, 3:4.

[Sameni et al., 2007] Sameni, R., Clifford, G. D., Jutten, C., and Shamsollahi, M. B. (2007). Multichannel ecg and noise modeling: application to maternal and fetal ecg signals. *EURASIP Journal on Applied Signal Processing*, 2007(1):94–94.

[Sameni et al., 2008] Sameni, R., Jutten, C., and Shamsollahi, M. B. (2008). Multichannel electrocardiogram decomposition using periodic component analysis. *Biomedical Engineering, IEEE Transactions on*, 55(8):1935–1940.

[Sameni et al., 2005] Sameni, R., Shamsollahi, M. B., Jutten, C., and Babaie-Zadeh, M. (2005). Filtering noisy ECG signals using the extended kalman filter based on a modified dynamic ECG model. In *Computers in Cardiology, 2005*, pages 1017–1020. IEEE.

[Schamroth and Schamroth, 1990] Schamroth, L. and Schamroth, C. (1990). An introduction to electrocardiology.

[Snelson, 2007] Snelson, E. L. (2007). *Flexible and efficient Gaussian process models for machine learning*. PhD thesis, Citeseer.

[Steer, 2008] Steer, P. J. (2008). Has electronic fetal heart rate monitoring made a difference? In *Seminars in Fetal and Neonatal Medicine*, volume 13, pages 2–7. Elsevier.

[Stinstra, 2001] Stinstra, J. G. (2001). *The reliability of the fetal magnetocardiogram*. Universiteit Twente.

[Strobach et al., 1994] Strobach, P., Abraham-Fuchs, K., and Harer, W. (1994). Event-synchronous cancellation of the heart interference in biomedical signals. *Biomedical Engineering, IEEE Transactions on*, 41(4):343–350.

[Sykes, 1987] Sykes, A. H. (1987). Ad waller and the electrocardiogram, 1887. *BMJ*, 294(6584):1396–1398.

[Tan and Moghavvemi, 2000] Tan, B. H. and Moghavvemi, M. (2000). Real time analysis of fetal phonocardiography. In *TENCON 2000. Proceedings*, volume 2, pages 135–140. IEEE.

[Taylor et al., 2005] Taylor, M. J., Thomas, M. J., Smith, M. J., Oseku-Afful, S., Fisk, N. M., Green, A. R., Paterson-Brown, S., and Gardiner, H. M. (2005). Non-invasive intrapartum fetal ECG: preliminary report. *BJOG: An International Journal of Obstetrics & Gynaecology*, 112(8):1016–1021.

[Thakor and Zhu, 1991] Thakor, N. V. and Zhu, Y. (1991). Applications of adaptive filtering to ecg analysis: noise cancellation and arrhythmia detection. *Biomedical Engineering, IEEE Transactions on*, 38(8):785–794.

[Ungureanu et al., 2007] Ungureanu, M., Bergmans, J. W. M., Oei, S. G., and Strungaru, R. (2007). Fetal ECG extraction during labor using an adaptive maternal beat subtraction technique. *Biomedizinische Technik*, 52(1):56–60.

[Ungureanu and Wolf, 2006] Ungureanu, M. and Wolf, W. M. (2006). Basic aspects concerning the event-synchronous interference canceller. *Biomedical Engineering, IEEE Transactions on*, 53(11):2240–2247.

[Vaisman et al., 2012] Vaisman, S.and Salem, S. Y., Holcberg, G., and Geva, A. B. (2012). Passive fetal monitoring by adaptive wavelet denoising method. *Computers in biology and medicine*, 42(2):171–179.

[Van Bemmel and Van der Weide, 1966] Van Bemmel, J. H. and Van der Weide, H. (1966). Detection procedure to represent the foetal heart rate and electrocardiogram. *Biomedical Engineering, IEEE Transactions on*, 13(4):175–182.

[Van Eck et al., 2003] Van Eck, H. J. R., Kors, J. A., and van Herpen, G. (2003). The elusive U wave: a simple explanation of its genesis. *Journal of electrocardiology*, 36:133–137.

[van Oosterom, 1986] van Oosterom, A. (1986). Spatial filtering of the fetal electrocardiogram. *Journal of Perinatal Medicine-Official Journal of the WAPM*, 14(6):411–419.

[Vanderschoot et al., 1987] Vanderschoot, J., Callaerts, D., Sansen, W., Vandewalle, J., Vantrappen, G., and Janssens, J. (1987). Two methods for optimal MECG elimination and FECG detection from skin electrode signals. *Biomedical Engineering, IEEE Transactions on*, 34(3):233–243.

[Varady, 2001] Varady, P. (2001). Wavelet-based adaptive denoising of phonocardiographic records. In *Engineering in Medicine and Biology Society, 2001. Proceedings of the 23rd Annual International Conference of the IEEE*, volume 2, pages 1846–1849. IEEE.

[Varady et al., 2003] Varady, P., Wildt, L., Benyó, Z., and Hein, A. (2003). An advanced method in fetal phonocardiography. *Computer Methods and programs in Biomedicine*, 71(3):283–296.

[Varanini et al., 2013] Varanini, M., Tartarisco, G., Billeci, L., Macerata, A., Pioggia, G., and Balocchi, R. (2013). A multi-step approach for non-invasive fetal ecg analysis. In *Computing in Cardiology Conference (CinC), 2013*, pages 281–284. IEEE.

[Vigneron et al., 2005] Vigneron, V., Azancot, A., Herail, C., Schmidt, M., Sibony, O., and Jutten, C. (2005). Sensor array for fetal ECG. part 2: Sensor selections. In *2nd IEEE International Conference on Computational Intelligence in Medical and Healthcare*, pages 434–442.

[Vigneron et al., 2003] Vigneron, V., Paraschiv-Ionescu, A., Azancot, A., Sibony, O., and Jutten, C. (2003). Fetal electrocardiogram extraction based on non-stationary ica and wavelet denoising. In *Signal Processing and Its Applications, 2003. Proceedings. Seventh International Symposium on*, volume 2, pages 69–72. IEEE.

[Vullings et al., 2009] Vullings, R., Peters, C. H. L., Sluijter, R. J., Mischi, M., Oei, S. G., and Bergmans, J. W. M. (2009). Dynamic segmentation and linear prediction for maternal ecg removal in antenatal abdominal recordings. *Physiological measurement*, 30(3):291.

[Waldo and Wit, 1993] Waldo, A. L. and Wit, A. L. (1993). Mechanisms of cardiac arrhythmias. *The Lancet*, 341(8854):1189–1193.

[Wand and Jones, 1994] Wand, M. P. and Jones, M. C. (1994). *Kernel smoothing*. Crc Press.

[Warrick et al., 2010] Warrick, P., Hamilton, E. F., Precup, D., and K., R. E. (2010). Classification of normal and hypoxic fetuses from systems modeling of intrapartum cardiotocography. *Biomedical Engineering, IEEE Transactions on*, 57(4):771–779.

[Welin et al., 2007] Welin, A. K., Norén, H., Odeback, A., Andersson, M., Andersson, G., and Rosén, K. G. (2007). Stan, a clinical audit: the outcome of 2 years of regular use in the city of varberg, sweden. *Acta obstetricia et gynecologica Scandinavica*, 86(7):827–832.

[Widrow et al., 1975] Widrow, B., Glover Jr, J. R., McCool, J. M., Kaunitz, J., Williams, C. S., Hearn, R. H., Zeidler, J. R., Dong Jr, E., and Goodlin, R. C. (1975). Adaptive noise cancelling: Principles and applications. *Proceedings of the IEEE*, 63(12):1692–1716.

[Williams and Rasmussen, 1996] Williams, C. K. and Rasmussen, C. E. (1996). Gaussian processes for regression.

[Wong et al., 2006] Wong, M. Y. M., Poon, C. C. Y., and Zhang, Y. T. (2006). Can the timing-characteristics of phonocardiographic signal be used for cuffless systolic blood pressure estimation? In *Engineering in Medicine and Biology Society, 2006. EMBS'06. 28th Annual International Conference of the IEEE*, pages 2878–2879. IEEE.

[Wu et al., 2012] Wu, J.-b., Zhou, S., Wu, Z., and Wu, X.-m. (2012). Research on the method of characteristic extraction and classification of phonocardiogram. In *Systems and Informatics (ICSAI), 2012 International Conference on*, pages 1732–1735. IEEE.

[Yang et al., 2012] Yang, K., Jiang, H., Dong, J., Zhang, C., and Wang, Z. (2012). An adaptive real-time method for fetal heart rate extraction based on phonocardiography. In *Biomedical Circuits and Systems Conference (BioCAS), 2012 IEEE*, pages 356–359. IEEE.

[Zarzoso and Nandi, 2001] Zarzoso, V. and Nandi, A. K. (2001). Noninvasive fetal electrocardiogram extraction: blind separation versus adaptive noise cancellation. *Biomedical Engineering, IEEE Transactions on*, 48(1):12–18.

[Zarzoso et al., 1997] Zarzoso, V., Nandi, A. K., and Bacharakis, E. (1997). Maternal and foetal ECG separation using blind source separation methods. *Mathematical Medicine and Biology*, 14(3):207–225.

[Zaunseder et al., 2012] Zaunseder, S., Andreotti, F., Cruz, M., Stepan, H., Schmieder, C., Malberg, H., Jank, A., and Wessel, N. (2012). Fetal QRS detection by means of kalman filtering and using the event synchronous canceller. In *7th int workshop on Biosig Interpretation Como*.

[Zuckerwar et al., 1993] Zuckerwar, A. J., Pretlow, R., Stoughton, J. W., and Baker, D. (1993). Development of a piezopolymer pressure sensor for a portable fetal heart rate monitor. *Biomedical Engineering, IEEE Transactions on*, 40(9):963–969.